



Messinger, Anette (2021) *The quantum optics of metamaterials*. PhD thesis.

<https://theses.gla.ac.uk/82364/>

Copyright and moral rights for this work are retained by the author

A copy can be downloaded for personal non-commercial research or study,  
without prior permission or charge

This work cannot be reproduced or quoted extensively from without first  
obtaining permission in writing from the author

The content must not be changed in any way or sold commercially in any  
format or medium without the formal permission of the author

When referring to this work, full bibliographic details including the author,  
title, awarding institution and date of the thesis must be given

Enlighten: Theses

<https://theses.gla.ac.uk/>  
[research-enlighten@glasgow.ac.uk](mailto:research-enlighten@glasgow.ac.uk)

# The Quantum Optics of Metamaterials

Anette Messinger

Submitted in fulfilment of the requirements for the  
Degree of Doctor of Philosophy

School of Physics and Astronomy  
College of Science and Engineering  
University of Glasgow



University  
of Glasgow

July 2021

# Abstract

The interaction of light and matter is a widely studied field in physics: Both quantum mechanical and classical effects have been treated to a large extent in theoretical studies but also in a wide range of experiments. One particularly interesting manifestation of such interactions are macroscopic materials with a linear response to the light field. This can be either a response due to the electric or due to the magnetic field, depending on the internal structure of the medium. However, the magnetic response is typically much weaker than the electric response and magnetic effects have been neglected in the majority of theoretical considerations.

The recently emerging field of metamaterials brings new possibilities of tailoring the electromagnetic properties of a medium, which gives rise to a class of materials with both electric and magnetic responses that have not been observed in naturally occurring materials - hence the name metamaterial.

For such materials the theories developed for purely dielectric media, materials with no magnetic response, do not hold anymore. The main goal of this thesis is to generalize electromagnetic theory, especially for the interaction of the light field with electric and magnetic dipoles, to arbitrary magneto-dielectric media. In particular, this includes lossy

magnetic materials and biaxial anisotropic media, but also a general investigation of the nature of light-matter interactions from the magnetic point of view. Magnetic and electric effects are often treated very differently. It is my aim to show the similarities, and immense symmetry between them, and therefore always treat electric and magnetic effects side by side whenever possible, and wherever a theory is only properly derived for the electric quantities, I shall complement the magnetic analogies to fill these gaps.

The second part of this thesis covers another important aspect of light-matter interaction, the transfer of coherence between atoms and the electromagnetic field inside a cavity, which is of particular importance in the context of quantum thermodynamics and the resource theory of coherence. This work is not directly linked to the main body of the thesis, but builds on the same theoretical framework of light-matter interaction in the Jaynes-Cummings model. We examine the catalytic nature of quantum optical coherence, in particular, the degradation of a coherent state in the cavity as coherence is transferred to a sequence of atoms through a Jaynes-Cummings interaction. In comparison with an earlier, rather artificial proposal of the catalytic creation of coherence, we investigate the role of correlations and the robustness of this more natural protocol of coherence transfer.

# Contents

<b>I</b>	<b>Macroscopic QED</b>	<b>1</b>
<b>1</b>	<b>Introduction</b>	<b>2</b>
1.1	Fundamentals of electromagnetism . . . . .	2
1.1.1	Electromagnetic waves . . . . .	3
1.1.2	Scalar and vector potential . . . . .	4
1.2	The dipole . . . . .	5
1.2.1	Electric dipole moment . . . . .	6
1.2.2	Magnetic dipole moment . . . . .	10
1.3	Electromagnetic waves in macroscopic media . . . . .	12
1.4	Electromagnetic field quantization . . . . .	16
1.5	Atom-photon interactions: Dipole radiation . . . . .	19
1.5.1	Generalized considerations . . . . .	22
1.5.2	Example: Magnetodielectrics . . . . .	24
1.6	Method of Green's functions . . . . .	25
1.6.1	Mathematical definition . . . . .	25
1.6.2	Green's Functions in quantum physics: Kubo Formula . . . . .	27
1.6.3	Example: Green's function of the vector potential . . . . .	28
1.6.4	Application to spontaneous emission rates . . . . .	29

1.7	Local fields . . . . .	31
1.8	(Meta)materials . . . . .	35
1.8.1	Magnetodielectric media . . . . .	36
1.8.2	Anisotropic media . . . . .	39
<b>2</b>	<b>The B vs. H debate</b>	<b>43</b>
2.1	What is the “fundamental” field? . . . . .	44
2.1.1	Duality arguments . . . . .	45
2.1.2	Experimental accessibility . . . . .	46
2.1.3	No magnetic monopoles . . . . .	46
2.1.4	Lorentz transformation . . . . .	49
2.2	Which field does a dipole interact with? . . . . .	50
2.2.1	Derivation of the local magnetic field . . . . .	51
2.2.2	Weak-permeability approximation . . . . .	53
<b>3</b>	<b>Dipole emission in anisotropic media</b>	<b>54</b>
3.1	Quantization of the electromagnetic field . . . . .	55
3.2	Spontaneous emission of electric dipoles . . . . .	60
3.2.1	Uniaxial dielectrics . . . . .	61
3.2.2	Biaxial dielectrics . . . . .	67
3.2.3	Local Field effects . . . . .	71
3.3	Magnetic generalization . . . . .	72
3.3.1	Waves in general anisotropic magnetodielectrics . . . . .	72
3.3.2	Solutions in uniaxial magnetodielectrics . . . . .	75
3.3.3	Electric dipole radiation . . . . .	76
3.3.4	Magnetic dipole radiation . . . . .	76

<b>4</b>	<b>Dipole emission in absorbing magnetodielectrics</b>	<b>79</b>
4.1	Electric Dipoles . . . . .	80
4.2	Magnetic Dipoles . . . . .	85
4.3	Local field effects . . . . .	86
<b>5</b>	<b>Conclusion and outlook</b>	<b>90</b>
<b>II</b>	<b>Coherence and catalysis in the Jaynes-Cummings model</b>	
	<b>92</b>	
<b>6</b>	<b>Introduction</b>	<b>93</b>
6.1	Coherence as a resource . . . . .	94
6.2	Catalytic Coherence: Åberg's proposal . . . . .	98
6.3	Correlations . . . . .	100
6.4	Variations to the initial protocol . . . . .	103
6.4.1	Coherent states . . . . .	103
6.4.2	The Jaynes Cummings Model . . . . .	106
<b>7</b>	<b>Coherence catalysis in the Jaynes-Cummings model</b>	<b>109</b>
7.1	Successive interactions with the same cavity . . . . .	110
7.2	Evolution of the cavity field . . . . .	113
7.3	Catalyticity and Robustness . . . . .	117
7.3.1	The effect of squeezing . . . . .	118
7.3.2	Correlations . . . . .	120
7.4	Discussion . . . . .	122
<b>8</b>	<b>Conclusion</b>	<b>125</b>

*CONTENTS*

vi

**A Green's functions from vector potential 127**

**B Approximation of success probabilities 131**

# List of Tables

7.1	Probability amplitudes after two rounds for $ \alpha  = 10$ with adjustment of interaction times after the first cycle. Bold ciphers show the deviation from the corresponding single-atom probabilities for easier comparison. . . . .	121
7.2	Comparison of probabilities and joint probabilities obtained from using coherent states in a Jaynes-Cummings interaction and using Ladder states in the scheme proposed by Åberg. . . . .	122

# List of Figures

1.1	A slab of dielectric in which a polarization $\mathbf{P}$ has been induced by an electric field. . . . .	9
1.2	“Macroscopic” local field model: The field at the dipole position is the sum of the average macroscopic field $\mathbf{E}_{\text{avg}}$ , the field due to the surface charges induced by the macroscopic medium at the boundary to the cavity $\mathbf{E}_S$ , and the contributions from the dipoles inside the cavity taken into account microscopically. . . . .	32
1.3	“Microscopic” local field model: The field at the dipole position is equal to the externally applied electric field $E_{\text{ext}}$ . The macroscopic field $E_{\text{avg}}$ inside the medium is the sum of the external field and the average of the fields from the induced dipoles $E_{\text{dip}}$ . This average can be calculated from the surface charges of a spherical cavity, i.e. the charges due to dipoles <i>inside</i> the cavity. The local field can hence be calculated from the average field $E_{\text{avg}}$ by <i>subtracting</i> the dipole contribution $E_{\text{dip}}$ . . . . .	35
1.4	Light beams entering a negative refractive index material.	38

1.5 Electric and displacement field polarization vectors of a wave with wave vector  $\mathbf{k}$  in an anisotropic medium. Both  $\mathbf{D}_1$  and  $\mathbf{D}_2$  are orthogonal to  $\mathbf{k}$ , but not orthogonal to each other. Instead,  $\mathbf{D}_1 \perp \mathbf{E}_2$  and  $\mathbf{D}_2 \perp \mathbf{E}_1$ . The blue plane depicts the plane orthogonal to  $\mathbf{k}$ , or equivalently the plane formed by  $\mathbf{D}_1$  and  $\mathbf{D}_2$ . . . . . 40

2.1 Maxwell's equations, written in terms of either possible pair of electric and magnetic fields, with and being the free charges and currents. . . . . 47

3.1 Angular distribution  $f(\theta)$  of the spontaneous emission rate (in units of the vacuum emission rate) to a fixed polar angle  $\varphi$ , for various configurations  $\varepsilon_{o,e} \in \{1, 7\}$  of a uniaxial medium with fixed  $\varepsilon_o$  (left) and fixed  $\varepsilon_e$  (right). A change in  $\varepsilon_o$  only changes the sides of the distribution, leaving the emission to an angle  $\theta = \pi/2$  constant, while a change in  $\varepsilon_e$  impacts on the relative distribution, leaving the total rate (integrated over all angles) constant. . . . . 64

3.2 Dependency of the spontaneous emission rate in units of the vacuum emission rate on the relative permittivity  $\varepsilon_y/\varepsilon_0$  with fixed values of  $\varepsilon_x = 1.5\varepsilon_0$  and  $\varepsilon_z = 5\varepsilon_0$  for a dipole aligned with the  $\varepsilon_z$ -axis. Analytical models obtained from linear interpolation with  $\varepsilon_x$ , linear interpolation with  $\varepsilon_y$  and an average of both (solid lines) are compared to numerical results (crosses). . . . . 69

3.3	Comparison of the averaged model (solid lines) with numerical results (crosses) for various different configurations of $\varepsilon_x/\varepsilon_0 = 6, 3, 1$ (blue, red, green group of graphs) and $\varepsilon_z/\varepsilon_0 = 4, 2, 1.2$ (light, medium, dark graph from each group) for a dipole aligned with $\varepsilon_z$ . The corresponding values for $\varepsilon_x$ and $\varepsilon_z$ are also indicated by arrows where they match the value of $\varepsilon_y$ for each curve. . . . .	70
6.1	Possible energy transfer protocol between two identical reservoirs using coherence. . . . .	96
6.2	Phase space representation of a coherent state (left) and a squeezed state (right). The center of the coherent state distribution is at the phase-space coordinate $p = 0, q = 3$ , corresponding to a state $ \alpha\rangle$ with $\alpha = 3$ . The squeezed state has the same average quadratures, but a reduced variance in $q$ at the cost of a higher variance in $p$ . . . . .	105
7.1	Photon number distribution of the cavity field after one successful (blue) or failed (orange) interaction. . . . .	114
7.2	Evolution of the number and phase uncertainties of the cavity state after several iterations. . . . .	116
7.3	Q-function of the cavity state before the interactions and after 3,6 and 9 rounds of interactions in the case of all atoms being found in the intended state. . . . .	116
7.6	Q-function of the (mixed) cavity state before the interactions and after 3,6 and 9 rounds of interactions without knowledge of the atomic state. . . . .	117

7.4 Q-function of the cavity state before the interactions and after 3,6 and 9 rounds of interactions in the case of all atoms being found in the undesired state. . . . . 117

7.5 Q-function of the cavity state after 1,3,6 and 9 rounds of interactions in a mixed sequence with the first atom being found in the undesired state but all following rounds being successful. . . . . 117

7.7 Left: Probability for the last ( $r$ -th) qubit to be found in the  $|+\rangle$  state after all previous were measured in  $|+\rangle$  with (orange) or without (blue) adjustment of interaction times according to an increase of half a photon in the cavity per round. The dashed line shows the probability for obtaining the state  $|+\rangle$  when the cavity field starts in a new coherent state with an increased photon number of  $1/2$  per each step. Right: Probability for the  $r$ -th qubit to end up in the state  $|+\rangle$  after all previous were measured in  $|-\rangle$ . . . . . 118

7.8 Probability of measuring the qubit in the state  $|+\rangle$  after one round with the cavity initially being in a q-quadrature squeezed state with mean photon number  $\bar{n} = 100.5$ , as a function of the squeezing parameter  $\zeta$ . The dashed line shows the probability without squeezing. . . . . 119

- 7.9 Double-logarithmic plot of the probability for all atoms to end up in the state  $|-\rangle$  during one to five rounds as a function of  $\alpha$ . The graphs were obtained from numeric calculations with adjustment of interaction times. The dotted lines show power series  $0.3667\alpha^{-1.954}$ ,  $0.2693\alpha^{-3.899}$ ,  $0.3064\alpha^{-5.847}$ ,  $0.4884\alpha^{-7.805}$  and  $1.0225\alpha^{-9.772}$  (top to bottom) obtained from fitting the numerical data for  $\alpha > 3$ . . 123

# Acknowledgements

I owe the biggest gratitude to my supervisors, Prof. Stephen Barnett and Dr. Sarah Croke for their continuing support and guidance during the last few years, and for all the things they have taught me. Not only were they fully dedicated to the progress of my work, but also always concerned with the personal well-being of their students in these times that were hard for everyone. I also want to thank all members and honorary members of the quantum theory group, for great companionship and also for sharing their professional expertise with me. I especially want to thank Niclas Westerberg, for helping me gain a broader insight into the peculiarities of quantum electromagnetism and being a driving force whenever my own motivation was lacking, and Scarlett Gao for her moral support and friendship from the very beginning.

Special Thanks goes to Prof. Giovanna Morigi and her group at Saarland University for offering me a place to work during my pandemic escape to Germany. It makes a big difference if one works at home on a small laptop, or in a university office with access to scientific publications, a fully equipped library and like-minded physicists to discuss with.

Last but not least, I want to thank those who endured me during all my ups and downs, my Friends, my Family, and of course my Fiancé,

Aleksei Konovalov.

I am grateful for the EPSRC scholarship program to fund my PhD and also to the Graduate School of the University of Glasgow, especially Heather Lambie for her great support of the PhD community and professional development opportunities.

# Declaration

With the exception of the introductory chapters, all work in this thesis was carried out by the author unless otherwise explicitly stated.

Part I

Macroscopic QED

# Chapter 1

## Introduction

### 1.1 Fundamentals of electromagnetism

The basis of all studies of electromagnetism, and with that, the one thing we postulate without proof, are Maxwell's equations. They tell us how electric and magnetic fields influence each other, and how they are both influenced by electric charges and currents as the fundamental sources of the fields. The differential form of Maxwell's equations is

$$\nabla \cdot \mathbf{E} = \frac{\rho}{\epsilon_0} \quad (1.1)$$

$$\nabla \cdot \mathbf{B} = 0 \quad (1.2)$$

$$\nabla \times \mathbf{E} = -\frac{\partial \mathbf{B}}{\partial t} \quad (1.3)$$

$$\nabla \times \mathbf{B} = \epsilon_0 \mu_0 \frac{\partial \mathbf{E}}{\partial t} + \mu_0 \mathbf{J}, \quad (1.4)$$

where  $\rho$  is the charge density and  $\mathbf{J}$  the current density satisfying

$$\frac{\partial \rho}{\partial t} + \nabla \cdot \mathbf{J} = 0. \quad (1.5)$$

This continuity equation describing the conservation of charge is not an additional condition but can be deduced from Maxwell's equations alone: If we apply the di-

vergence on both sides of equation 1.4, we get

$$0 = \varepsilon_0 \mu_0 \nabla \cdot \frac{\partial \mathbf{E}}{\partial t} + \mu_0 \nabla \cdot \mathbf{J} \quad (1.6)$$

which, using equation 1.1 reduces to the continuity equation. In principle we could also require charge conservation as a basic principle and the first of Maxwell's equations then follows as a consequence. Similarly, equation 1.2 is equivalent to the statement that there are no direct sources of the magnetic field, i.e. no magnetic monopoles.

We can obtain the charge and current density from discrete particles of charge  $q_i$ , position  $\mathbf{r}_i$  and velocity  $\mathbf{v}_i$  as

$$\begin{aligned} \rho(\mathbf{r}, t) &= \sum_i q_i \delta(\mathbf{r} - \mathbf{r}_i(t)) \\ \mathbf{J}(\mathbf{r}, t) &= \sum_i q_i \mathbf{v}_i(t) \delta(\mathbf{r} - \mathbf{r}_i(t)), \end{aligned}$$

which gives the connection from the field equations to the equations of motion of charged particles. This connection builds the foundation of all light-matter interaction and shows the codependency of mechanical variables with the electromagnetic field variables.

### 1.1.1 Electromagnetic waves

In the absence of any charges or currents, the solution to equations 1.1 to 1.4 can be easily found: Taking the curl of equation 1.3, in combination with equation 1.4 gives

$$\begin{aligned} \nabla \times (\nabla \times \mathbf{E}) &= -\frac{\partial}{\partial t} \nabla \times \mathbf{B} \\ &= -\varepsilon_0 \mu_0 \frac{\partial^2 \mathbf{E}}{\partial t^2}. \end{aligned} \quad (1.7)$$

In free space we also have  $\nabla \cdot \mathbf{E} = 0$  so that the left side of equation 1.7 reduces to

$$\begin{aligned} \nabla \times (\nabla \times \mathbf{E}) &= \nabla(\nabla \cdot \mathbf{E}) - \nabla^2 \mathbf{E} \\ &= -\nabla^2 \mathbf{E}, \end{aligned} \quad (1.8)$$

and we arrive at the Helmholtz equation

$$\nabla^2 \mathbf{E} + \frac{1}{c^2} \frac{\partial^2 \mathbf{E}}{\partial t^2} = 0 \quad (1.9)$$

with  $c$  being the speed of light,  $c = \frac{1}{\sqrt{\epsilon_0 \mu_0}}$ . Similarly, we can derive the equivalent equation for the magnetic field,

$$\nabla^2 \mathbf{B} + \frac{1}{c^2} \frac{\partial^2 \mathbf{B}}{\partial t^2} = 0 \quad (1.10)$$

from the curl of equation 1.4. Both the electric and the magnetic fields can thus be written in terms of plane waves,

$$\mathbf{E}(\mathbf{k}, \omega) = \mathbf{E}_{\mathbf{k}} e^{i(\mathbf{k}\mathbf{r} - \omega t)} + \mathbf{E}_{\mathbf{k}}^* e^{-i(\mathbf{k}\mathbf{r} - \omega t)} \quad (1.11)$$

$$\mathbf{B}(\mathbf{k}, \omega) = \mathbf{B}_{\mathbf{k}} e^{i(\mathbf{k}\mathbf{r} - \omega t)} + \mathbf{B}_{\mathbf{k}}^* e^{-i(\mathbf{k}\mathbf{r} - \omega t)} \quad (1.12)$$

where any linear combination of such waves is a solution as well. Plugging a specific solution into the Helmholtz equation, we see that the frequency  $\omega$  and the wave vector  $\mathbf{k}$  must fulfil the relation

$$k^2 - \frac{\omega^2}{c^2} = 0, \quad (1.13)$$

so for a fixed  $\mathbf{k}$ , the frequency  $\omega$  is determined by  $\omega = kc$ .

### 1.1.2 Scalar and vector potential

Instead of describing the electromagnetic field by six degrees of freedom, i.e. the three spatial components of both  $\mathbf{E}$  and  $\mathbf{B}$ , we can reduce some of the redundancy in Maxwell's equations by introducing a scalar potential  $\phi$  and a vector potential  $\mathbf{A}$  and thereby reducing the problem to four unknowns. From  $\nabla \cdot \mathbf{B} = 0$  we know that the magnetic field must be completely transverse, and we therefore can express it as the curl of another field,

$$\mathbf{B} \equiv \nabla \times \mathbf{A}. \quad (1.14)$$

To be consistent with Maxwell's equations, we must now write the electric field as

$$\mathbf{E} = -\frac{\partial \mathbf{A}}{\partial t} - \nabla \phi. \quad (1.15)$$

The first part is to satisfy equation 1.3, where an additional gradient field  $\nabla \phi$  has to be added to simultaneously satisfy equation 1.1 in the existence of charges. Now  $\mathbf{A}$  and  $\phi$  are not uniquely defined, as different choices can lead to the same electric and magnetic fields. The choice that we will be using in this work is the Coulomb gauge, which is defined by the additional constraint that  $\nabla \cdot \mathbf{A} = 0$ . In this gauge, Maxwell's equations reduce to the two field equations

$$-\nabla^2 \mathbf{A} + \frac{1}{c^2} \frac{\partial^2}{\partial t^2} \mathbf{A} = \mu_0 \mathbf{J}^T \quad (1.16)$$

$$\frac{1}{c^2} \frac{\partial}{\partial t} \nabla \phi = \mu_0 \mathbf{J}^L \quad (1.17)$$

where the superscripts L and T denote the longitudinal and transverse parts of the current density (note that  $\nabla \cdot \mathbf{J}^L = -\frac{\partial \rho}{\partial t}$ ). This is particularly helpful in electro- and magneto-statics to deduce the fields caused by charge or current distributions. The electric field can then be calculated from the scalar potential,

$$\phi(\mathbf{r}) = \int \frac{\rho(\mathbf{r}')}{4\pi\epsilon_0|\mathbf{r} - \mathbf{r}'|} dV \quad (1.18)$$

and the magnetic field from the vector potential

$$\mathbf{A}(\mathbf{r}) = \int \frac{\mu_0 \mathbf{J}^T(\mathbf{r}')}{4\pi|\mathbf{r} - \mathbf{r}'|} dV. \quad (1.19)$$

## 1.2 The dipole

As we have seen, the only necessary ingredients to describe the sources of the electromagnetic fields are charges and currents. In principle, even charged particles alone, like for example electrons or protons are sufficient, as we can describe currents as moving (or rotating) charges. Here, we now want to introduce the concept of dipoles as an additional and extremely helpful way to describe charge distributions and their effect on the electromagnetic field.

### 1.2.1 Electric dipole moment

An electric dipole describes the set of two charges,  $+q$  and  $-q$  which are located at a small distance  $l$ . If we are interested in fields sufficiently far from the dipole, or with sufficiently large wavelength, it is helpful to take the limit of infinitesimally small separation between the charges,  $l \rightarrow 0$  while keeping the product  $d = ql$  constant. The vector quantity

$$\mathbf{d} = ql = ql\hat{\mathbf{e}} \quad (1.20)$$

is called the dipole moment, where  $\hat{\mathbf{e}}$  is the unit vector pointing from the negative to the positive charge. The dipole moment of any continuous charge distribution is defined by the integral

$$\mathbf{d} = \int \rho(\mathbf{r})\mathbf{r} d^3\mathbf{r} \quad (1.21)$$

which, for a distribution made by two discrete point charges, simplifies to equation 1.20 again.

The dipole moment has a particularly important role: Together with the total charge  $Q = \int \rho(\mathbf{r})d^3\mathbf{r}$ , knowing the dipole moment is often sufficient to describe the effect of any arbitrary charge distribution on the electric field at a point far from the distribution. Let us have a look at the general expression for the potential at a point  $\mathbf{r}$  given a (static) charge distribution  $\rho(\mathbf{r}')$  around the origin:

$$\phi(\mathbf{r}) = \frac{1}{4\pi\epsilon_0} \int \frac{\rho(\mathbf{r}')}{|\mathbf{r} - \mathbf{r}'|} d^3\mathbf{r}' \quad (1.22)$$

For arbitrary charge distributions this may be a rather messy integral. If the charge distribution is confined within a region small compared to the distance to the point of interest  $\mathbf{r}$ , we can make the approximation  $r' \ll r$  to simplify the situation. We first pull out the constant distance  $r$ ,

$$\frac{1}{|\mathbf{r} - \mathbf{r}'|} = \frac{1}{r} \left( 1 - 2\frac{\mathbf{r} \cdot \mathbf{r}'}{r^2} + \left(\frac{r'}{r}\right)^2 \right)^{-\frac{1}{2}} \quad (1.23)$$

and now expand the square root in terms of  $\Delta = -2\frac{\mathbf{r} \cdot \mathbf{r}'}{r^2} + \left(\frac{r'}{r}\right)^2$  which we know is

small whenever  $r' \ll r$ :

$$(1 + \Delta)^{-\frac{1}{2}} = 1 - \frac{1}{2}\Delta + \mathcal{O}(\Delta^2) \quad (1.24)$$

Hence, we have

$$\frac{1}{|\mathbf{r} - \mathbf{r}'|} \approx \frac{1}{r} \left[ 1 + \frac{\mathbf{r} \cdot \mathbf{r}'}{r^2} - \frac{1}{2} \left( \frac{r'}{r} \right)^2 + \dots \right] \quad (1.25)$$

and inserting this back into the integral, equation 1.22, gives

$$\phi(\mathbf{r}) \approx \frac{1}{4\pi\epsilon_0} \left[ \frac{1}{r} \underbrace{\int \rho(\mathbf{r}') d^3\mathbf{r}'}_Q + \frac{1}{r^2} \hat{\mathbf{r}} \cdot \underbrace{\int \rho(\mathbf{r}') \mathbf{r}' d^3\mathbf{r}'}_{\mathbf{d}} - \frac{1}{r^3} \int \dots \right] \quad (1.26)$$

where we have introduced the normalized vector  $\hat{\mathbf{r}} = \mathbf{r}/|\mathbf{r}|$ . Now we can see that the first term, the most dominant one at far distances, is the potential due to the total charge  $Q$ . The second term, which becomes dominant for electrically neutral distributions, is exactly the potential due to a dipole, i.e.

$$\phi_{\text{dip}}(\mathbf{r}) = \frac{1}{4\pi\epsilon_0} \frac{\hat{\mathbf{r}} \cdot \mathbf{d}}{r^2} \quad (1.27)$$

with  $\mathbf{d}$  being the dipole moment of the distribution. Hence, the total charge and dipole moment are sufficient to describe the field caused by any localized charge distribution up to second order in the inverse distance to the object. The corresponding electric field of such a dipole follows as

$$\mathbf{E}(\mathbf{r}) = \frac{3\hat{\mathbf{r}}(\hat{\mathbf{r}} \cdot \mathbf{d}) - \mathbf{d}}{4\pi\epsilon_0 r^3}. \quad (1.28)$$

In fact, for a simple point dipole this is exactly its electric field, as all other terms in the expansion vanish<sup>1</sup>.

If there is a large number of dipoles in a medium, we can define a polarization

---

<sup>1</sup>Two things should be mentioned at this point. First, this expression is not valid at  $\mathbf{r} = 0$ , in fact it diverges. Second, for oscillating dipoles the electric field has an additional term proportional to  $\frac{1}{r^2}$ . In general, the given expression can be used whenever  $l \ll r \ll \lambda$  for  $l$  being the size of the charge distribution,  $r$  the distance from it and  $\lambda$  the wavelength of interest. This is the regime we will need in this work. For a generalization to other situations, see for example Chapter 9 in [1].

$\mathbf{P}$  as the sum of all electric dipole moments per unit volume, i.e. a dipole moment density,

$$\mathbf{P} = \sum \frac{\mathbf{d}}{V} \quad (1.29)$$

so that the total dipole moment of a macroscopic object is

$$\mathbf{d} = \int \mathbf{P} dV. \quad (1.30)$$

In dielectrics, external electric fields can displace the average positions of electrons relative to their nuclei and thereby invoke such polarizations, even where no dipole was present before. This is why the polarization is often directly proportional to the electric field, but we will come to that later. Now let us consider a polarization which is homogeneous over a certain volume, for example within a dielectric slab in a constant electric field. One might wonder what the corresponding charge distribution looks like. If the material was electrically neutral before, the total charge should still be zero. Furthermore, inside the material, the number of electrons and protons is still the same, so the average charge density inside the material should also be zero. Only on the surface can we expect to see a difference, as on one side there will be a higher electron density, while on the other side the nuclei will be slightly closer to the surface. In fact, one can easily verify that the charge density per surface element is exactly equal to the polarization induced in the material,

$$\sigma = \sum \frac{q}{A} = \sum \frac{ql}{V} = \sum \frac{d}{V}. \quad (1.31)$$

From this, we can calculate the (volume) charge density induced by the polarization: The total charge that is displaced out of the material over a surface  $S$  is

$$Q = - \int_S \mathbf{P} \cdot \mathbf{n} dA \quad (1.32)$$

with  $\mathbf{n}$  being the outward normal of the surface. Hence, the volume charge density, which is defined via  $Q = \int \rho dV$  can be related to the polarization as

$$\rho_{\text{dip}} = -\nabla \cdot \mathbf{P}. \quad (1.33)$$

Now a few remarks are in order. First, we must not forget that in a general situation there can be single charges that are not part of any dipoles, and therefore the total charge distribution should rather be

$$\rho = \rho_{\text{dip}} + \rho_{\text{free}}. \quad (1.34)$$

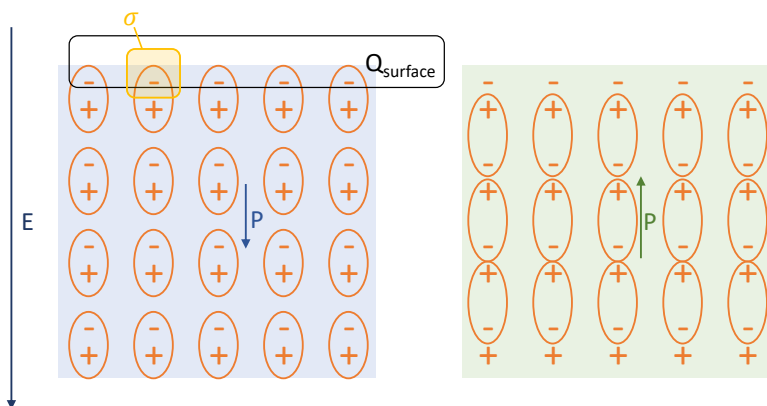


Figure 1.1: A slab of dielectric in which a polarization  $\mathbf{P}$  has been induced by an electric field. The surface charge density  $\sigma$  is the total charge which is displaced from the dielectric divided by the surface area of the unit volume, i.e. it can be understood as the charge of exactly one dipole divided by its area. The right hand side depicts the same situation, when the medium charges are paired up to a different set of dipoles. This in fact leads to an opposite polarization, but together with the now unbound charges at the sides, describes the same physical situation when looked at from a distance. It also makes the intuition of surface charges easier as inside the medium all charges can be paired up, making it electrically neutral, while the surface charges remain unpaired.

Second, the polarization, or in general the dipole distribution is not uniquely defined. Consider the situation of figure 1.1 for example. If we have a distribution of positive charges mixed with another distribution of negative charges, it is up to us to decide which charges to pair up to a dipole (as long as the distances between the charges remains sufficiently small). The resulting physical situation is not changed, as changing the declaration of dipoles thereby also changes which charges remain free, and where surface charges will build up. However, in most situations occurring in nature, the displacements of electrons with respect to their nuclei will be small compared to the interatomic distance and the choice of dipoles therefore always clear.

## 1.2.2 Magnetic dipole moment

The magnetic dipole is a bit less straightforward as we cannot simply construct it from two magnetic monopoles<sup>2</sup>. If we want to describe a magnetic dipole in terms of electric quantities, we can do so by introducing an infinitesimally small current loop. As we will see, this produces the same magnetic (far) field as the electric field from the electric dipole. Naturally, such a dipole could be formed for example by the spin or orbital angular momentum of an electron.

The magnetic dipole moment, or just magnetic moment, is then defined as the product of the current  $\mathbf{I}$  in the loop and the area  $S$  it surrounds. The direction of the moment points orthogonal to the surrounded surface, consistent with the right hand rule with respect to the current direction:

$$\mathbf{m} = I S \mathbf{n} \quad (1.35)$$

For an arbitrary current distribution, confined to a relatively small object around the origin, we can get the magnetic moment through

$$\mathbf{m} = \int \mathbf{r} \times \mathbf{J}(\mathbf{r}) dV \quad (1.36)$$

which reduces to equation 1.35 for a discrete current loop. For an arbitrary but dense distribution of magnetic dipoles we can again introduce a macroscopic quantity, the magnetization  $\mathbf{M}$  as the magnetic moment per unit volume,

$$\mathbf{M} = \sum \frac{\mathbf{m}}{V}. \quad (1.37)$$

We now expand the vector potential<sup>3</sup>

$$\mathbf{A}(\mathbf{r}) = \frac{\mu_0}{4\pi} \int \frac{\mathbf{J}(\mathbf{r}')}{|\mathbf{r} - \mathbf{r}'|} d^3\mathbf{r}' \quad (1.38)$$

---

<sup>2</sup>We could, but we are assuming a world without magnetic monopoles so this construction would be pointless.

<sup>3</sup>We are not troubling ourselves with time-varying fields yet and thus simply write the total current in the following, noting that the longitudinal part is zero in magnetostatics.

in the same manner as in the previous section, leading to

$$\mathbf{A}(\mathbf{r}) \approx \frac{\mu_0}{4\pi} \left[ \frac{1}{r} \int \mathbf{J}(\mathbf{r}') d^3\mathbf{r}' + \frac{1}{r^2} \int (\hat{\mathbf{r}} \cdot \mathbf{r}') \mathbf{J}(\mathbf{r}') d^3\mathbf{r}' - \frac{1}{r^3} \int \dots \right]. \quad (1.39)$$

The first term vanishes in the case of a closed current loop, or in general whenever there is no net current flowing through the volume of interest. The second term can be rewritten using Stokes's theorem, for a single current loop this gives

$$\begin{aligned} \int (\hat{\mathbf{r}} \cdot \mathbf{r}') \mathbf{J}(\mathbf{r}') d^3\mathbf{r}' &= \oint (\hat{\mathbf{r}} \cdot \mathbf{r}') I d\mathbf{l}' \\ &= -\hat{\mathbf{r}} \times \int I d\mathbf{A} \\ &= \mathbf{m} \times \hat{\mathbf{r}} \end{aligned} \quad (1.40)$$

Hence, we can write the vector potential of a magnetic dipole as

$$\mathbf{A}(\mathbf{r}) = \frac{\mu_0}{4\pi} \frac{1}{r} \mathbf{m} \times \mathbf{r} \quad (1.41)$$

and the magnetic field follows as<sup>4</sup>

$$\mathbf{B}(\mathbf{r}) = \mu_0 \frac{3\hat{\mathbf{r}}(\hat{\mathbf{r}} \cdot \mathbf{m}) - \mathbf{m}}{4\pi r^3}. \quad (1.42)$$

For a distribution of magnetic dipoles we can write the vector potential as

$$\begin{aligned} \mathbf{A}(\mathbf{r}) &= \frac{\mu_0}{4\pi} \int \mathbf{M}(\mathbf{r}') \times \frac{(\mathbf{r} - \mathbf{r}')}{|\mathbf{r} - \mathbf{r}'|} d^3\mathbf{r}' \\ &= \frac{\mu_0}{4\pi} \int \mathbf{M}(\mathbf{r}') \times \nabla' \frac{1}{|\mathbf{r} - \mathbf{r}'|} d^3\mathbf{r}' \\ &= \frac{\mu_0}{4\pi} \int \frac{(\nabla' \times \mathbf{M}(\mathbf{r}'))}{|\mathbf{r} - \mathbf{r}'|} d^3\mathbf{r}' \end{aligned} \quad (1.43)$$

where in the last step we used the vector identity  $\nabla \times (\phi \mathbf{F}) = \nabla \phi \times \mathbf{F} + \phi \nabla \times \mathbf{F}$  and the fact that

$$\int \nabla' \times \frac{\mathbf{M}(\mathbf{r}')}{|\mathbf{r} - \mathbf{r}'|} d^3\mathbf{r}' = \int \frac{\mathbf{n} \times \mathbf{M}(\mathbf{r}')}{|\mathbf{r} - \mathbf{r}'|} dS' \quad (1.44)$$

---

<sup>4</sup>The same limitations to the validity as in the electric case apply.

vanishes for finitely localized magnetization distributions. Hence, we can identify the effective current which causes the vector potential of a magnetic dipole distribution  $\mathbf{M}$  as

$$\mathbf{J}_M = \nabla \times \mathbf{M}. \quad (1.45)$$

We now have a similar situation with currents as we had with charges before. Inside a bulk medium with a constant, homogeneous magnetization, there will be no net currents present as the currents from two neighbouring parallel dipoles will be opposite to each other and cancel out. Again, only the edge contributions matter, in this case this is an effective surface current around the whole medium<sup>5</sup>.

Finally, we need to make a quick detour to electrodynamics to include the effect of oscillating electric dipoles on the vector potential. We noted earlier that the first term in equation 1.39 vanishes in electrostatics. This is no longer the case if we allow time-varying charge distributions. Using partial integration we can rewrite the term as

$$\int \mathbf{J}(\mathbf{r}') d^3 \mathbf{r}' = - \int \mathbf{r}' (\nabla' \cdot \mathbf{J}(\mathbf{r}')) d^3 \mathbf{r}' \quad (1.46)$$

which, using the continuity equation  $\nabla \cdot \mathbf{J} = -\frac{\partial \rho}{\partial t}$  turns out to be simply the derivative of the dipole moment of the charge distribution

$$\int \mathbf{r}' \frac{\partial \rho}{\partial t} d^3 \mathbf{r}' = \frac{\partial \mathbf{d}}{\partial t}. \quad (1.47)$$

We can thus identify a further contribution to the effective current from the electric dipoles,

$$\mathbf{J}_P = \frac{\partial \mathbf{P}}{\partial t}. \quad (1.48)$$

### 1.3 Electromagnetic waves in macroscopic media

Let us now come to a more macroscopic treatment of matter. With the use of the relations derived in the previous section, Maxwell's equations can be adapted to include the averaged effect of electric and magnetic dipole densities in media

---

<sup>5</sup>One should not imagine this as electrons actually travelling all around the material, but more like a conveyor system made out of many small wheels or rollers, each of which moves in the same direction at the surface, without necessarily moving as a whole.

without explicitly having to account for every charge in the medium separately. We first express all charge and current densities that are attributed to dipoles in terms of the corresponding polarization and magnetization,

$$\nabla \cdot \mathbf{P} = -\rho_{\text{dip}} \quad (1.49)$$

$$\nabla \times \mathbf{M} + \frac{\partial \mathbf{P}}{\partial t} = \mathbf{J}_{\text{dip}}. \quad (1.50)$$

The total charge and current densities thus are split up into the contributions from the medium dipoles and additional free, unbound charges or currents:

$$\rho = \rho_{\text{free}} + \rho_{\text{dip}} \quad (1.51)$$

$$\mathbf{J} = \mathbf{J}_{\text{free}} + \mathbf{J}_{\text{dip}} \quad (1.52)$$

With this, we can rewrite Maxwell's equations 1.1 to 1.4 in terms of polarization and magnetization so that only free charges and currents remain explicitly in the equations,

$$\nabla \cdot (\varepsilon_0 \mathbf{E} + \mathbf{P}) = \rho_{\text{free}} \quad (1.53)$$

$$\nabla \cdot \mathbf{B} = 0 \quad (1.54)$$

$$\nabla \times \mathbf{E} = -\frac{\partial \mathbf{B}}{\partial t} \quad (1.55)$$

$$\nabla \times (\mu_0^{-1} \mathbf{B} - \mathbf{M}) = \frac{\partial}{\partial t} (\varepsilon_0 \mathbf{E} + \mathbf{P}) + \mathbf{J}_{\text{free}}. \quad (1.56)$$

This suggests a new definition of macroscopic fields  $\mathbf{D} = \varepsilon_0 \mathbf{E} + \mathbf{P}$  and  $\mathbf{H} = \mu_0^{-1} \mathbf{B} - \mathbf{M}$  with which the equations take their original form again, but with different field variables:

$$\nabla \cdot \mathbf{D} = \rho_{\text{free}} \quad (1.57)$$

$$\nabla \cdot \mathbf{B} = 0 \quad (1.58)$$

$$\nabla \times \mathbf{E} = -\frac{\partial \mathbf{B}}{\partial t} \quad (1.59)$$

$$\nabla \times \mathbf{H} = \frac{\partial \mathbf{D}}{\partial t} + \mathbf{J}_{\text{free}}. \quad (1.60)$$

In linear and isotropic media the polarization and magnetization depend linearly on the corresponding fields,  $\mathbf{P} = \chi_e \mathbf{E}$  and  $\mathbf{M} = \chi_m \mathbf{H}$ , with  $\chi_e = \varepsilon_r - 1$  and  $\chi_m = \mu_r - 1$  being the electric and magnetic susceptibility. The relationships between the new and the old fields are therefore also linear,

$$\mathbf{D} = \varepsilon_0 \varepsilon_r \mathbf{E} = \varepsilon \mathbf{E} \quad (1.61)$$

and

$$\mathbf{B} = \mu_0 \mu_r \mathbf{H} = \mu \mathbf{H} \quad (1.62)$$

where  $\varepsilon_{(r)}$  and  $\mu_{(r)}$  are called the (relative) permittivity and permeability, respectively. To be more exact, this linear relationship is valid only for a certain frequency component of the fields, i.e.

$$\mathbf{D} = \int \mathbf{D}_\omega e^{i\omega t} d\omega = \int \varepsilon_\omega \mathbf{E}_\omega e^{i\omega t} d\omega \quad (1.63)$$

and

$$\mathbf{B} = \int \mathbf{B}_\omega e^{i\omega t} d\omega = \int \mu_\omega \mathbf{H}_\omega e^{i\omega t} d\omega. \quad (1.64)$$

In a medium without any excitable dipoles present,  $\chi = 0$  and  $\varepsilon_r = 1 = \mu_r$  for all frequencies. In that case the fields are related by the (constant) vacuum permittivity and permeability  $\varepsilon_0$  and  $\mu_0$ .

We have thus introduced new fields which intrinsically contain the effect of the dipoles but still satisfy a set of equations in the same structure. In the absence of free charges and currents, we can derive in analogy to the first section, the new Helmholtz equations in a linear medium:

$$\nabla^2 \mathbf{E}_\omega - \frac{n^2}{c^2} \omega^2 \mathbf{E}_\omega = 0 \quad (1.65)$$

$$\nabla^2 \mathbf{B}_\omega - \frac{n^2}{c^2} \omega^2 \mathbf{B}_\omega = 0. \quad (1.66)$$

The refractive index  $n$  is defined as

$$n = \sqrt{\mu_r \varepsilon_r} \quad (1.67)$$

and describes how the wave vector of a plane wave solution of equations 1.57-1.60 is altered compared to a wave in vacuum of the same frequency<sup>6</sup>,  $k = nk_0$ . All the medium does here is introduce the additional factor of  $n$  in the wave equation, and we could incorporate this effect by replacing  $c$  with the new speed of light in the medium,

$$v = \frac{c}{n} = \frac{1}{\sqrt{\epsilon_0\mu_0}} \frac{1}{\sqrt{\epsilon_r\mu_r}} = \frac{1}{\sqrt{\epsilon\mu}}. \quad (1.68)$$

This is called the phase velocity, as it describes the speed with which points of constant phase move in a propagating wave.

Most common media have a refractive index bigger than or equal to 1, which means light usually doesn't travel faster than  $c$ <sup>7</sup>. However, values below 1 or even negative values are possible in special cases. Furthermore, since the response of a medium usually depends on the frequency of the wave, the refractive index is also in general a function of frequency. Free space without any dipoles can be interpreted in the same framework as a medium of refractive index 1.

Complex refractive indices describe lossy media, where part of the electromagnetic field is absorbed by some of the dipoles which do not decay into the electromagnetic field again but rather into other, mechanical degrees of freedom. Consider a plane wave<sup>8</sup>  $\mathbf{E} = \mathbf{E}_0 e^{i(k_0x - \omega t)}$  entering a medium with complex refractive index  $n = n_R + in_I$ . The wave in the medium will have the form

$$\mathbf{E} = \mathbf{E}_0 e^{i(nk_0x - \omega t)} = \mathbf{E}_0 e^{i(n_R k_0x - \omega t)} e^{-n_I k_0x}. \quad (1.69)$$

Thus, the real part of the refractive index  $n_R$  changes the effective wavelength and wavevector, whereas the imaginary part leads to an exponential decay of the amplitude. The first effect is called dispersion, the second describes absorption.

Special care needs to be taken for so-called negative index materials. In most materials, the ratio between the wave vectors in vacuum and in the medium is the

---

<sup>6</sup>Actually, the refractive index just alters the relation between  $k$  and  $\omega$ , but when a wave enters the medium, the energy needs to be preserved, so  $\omega$  stays constant and  $k$  will change accordingly.

<sup>7</sup>The term "travel" should be interpreted carefully here, as the refractive index describes the travelling speed of individual nodes and antinodes of a light wave, and not that of photons or wave envelopes.

<sup>8</sup>One should not be confused by the complex conjugate missing, as we can in principle describe the fields as complex quantities. However, as measurements always reveal the real part of such a complex field one often writes the real part directly. Here we have simply left it out for simplicity.

positive solution of the square root in equation 1.67 and by convention, the refractive index is therefore defined to be positive as well. However, whenever both  $\varepsilon$  and  $\mu$  have negative real parts, the refractive index needs to be chosen to be the negative solution so that  $\mathbf{E} = \mathbf{E}_0 e^{i(nk_0 x - \omega t)}$  is still a solution of the wave equations. More details about negative refractive indices will follow in section 1.8.1.

## 1.4 Electromagnetic field quantization

A quantized description of the electromagnetic field can be obtained by expressing the energy of the field in terms of harmonic oscillators and introducing the usual bosonic field operators by comparison with a quantum harmonic oscillator. This is a rather credulous method, trusting that the operators obtained by such a replacement indeed represent the correct quantum behaviour. Most importantly, the correct form of the energy in terms of canonical variables must be known. We skip the derivation of the Hamiltonian here as it is well known and not relevant to our problems, but the interested reader can find a proper Lagrangian derivation for example in Ref. [2] or [3].

In this shorter quantization procedure, we already anticipate that the electromagnetic field can be described as a harmonic oscillator. We thus first write the field operators as plane wave solutions and derive the field energy in terms of the wave amplitudes. We will then compare this expression to the Hamiltonian of the quantum harmonic oscillator and make the corresponding replacements of the wave amplitudes to bosonic creation and annihilation operators so that the Hamiltonian of the electromagnetic field takes the expected form.

We first attempt to find solutions to Maxwell's equations by solving the wave equation in free space, equation 1.9. We write the solutions in the form [4]

$$\mathbf{E}(\mathbf{r}, t) = \sum_{\mathbf{k}, \lambda} \mathbf{e}_{\mathbf{k}\lambda} (A_{\mathbf{k}\lambda} e^{i(\mathbf{k}\mathbf{r} - \omega_k t)} + A_{\mathbf{k}\lambda}^* e^{-i(\mathbf{k}\mathbf{r} - \omega_k t)}) \quad (1.70)$$

$$\mathbf{B}(\mathbf{r}, t) = \sum_{\mathbf{k}, \lambda} -\frac{1}{\omega_k} (\mathbf{k} \times \mathbf{e}_{\mathbf{k}\lambda}) (A_{\mathbf{k}\lambda} e^{i(\mathbf{k}\mathbf{r} - \omega_k t)} + A_{\mathbf{k}\lambda}^* e^{-i(\mathbf{k}\mathbf{r} - \omega_k t)}) \quad (1.71)$$

with  $\omega_k = c|\mathbf{k}|$  and orthonormal unit vectors  $\mathbf{e}_{\mathbf{k}\lambda} \cdot \mathbf{e}_{\mathbf{k}\lambda'} = \delta_{\lambda\lambda'}$  that satisfy  $\mathbf{e}_{\mathbf{k}\lambda} \cdot \mathbf{k} = 0$  for polarizations  $\lambda = 1, 2$ . This is the most general solution fulfilling the wave equations.

In principal we could have an arbitrary polarization vector  $\mathbf{e}_{\mathbf{k}}$ . However, the first Maxwell equation restricts the allowed polarizations to the plane orthogonal to  $\mathbf{k}$ , so we only need a basis of two orthogonal vectors (which we can choose arbitrarily) to represent all allowed polarizations.

The allowed wavevectors  $\mathbf{k}$  depend on the boundary conditions: For a box of dimensions  $V = L \times L \times L$  with periodic boundaries we must have  $k_i = n_i \frac{2\pi}{L}$  for  $i = x, y, z$  and integer numbers  $n_i = 0, \pm 1, \pm 2, \dots$ . With that, we can calculate the energy stored in the electromagnetic field within the box,

$$\begin{aligned} H &= \frac{1}{2} \int (\varepsilon_0 \mathbf{E}^2 + \frac{1}{\mu_0} \mathbf{B}^2) dV \\ &= \sum_{\mathbf{k}, \lambda} \varepsilon_0 V (A_{\mathbf{k}\lambda} A_{\mathbf{k}\lambda}^* + A_{\mathbf{k}\lambda}^* A_{\mathbf{k}\lambda}), \end{aligned} \quad (1.72)$$

where we have made use of the identities

$$\int_L e^{i \frac{2\pi}{L} (n-n')r} dr = L \delta_{nn'} \quad (1.73)$$

for  $n, n' \in \mathbb{Z}$  and

$$(\mathbf{k} \times \mathbf{e}_{\mathbf{k}\lambda}) \cdot (\mathbf{k} \times \mathbf{e}_{\mathbf{k}\lambda'}) = k^2 \mathbf{e}_{\mathbf{k}\tilde{\lambda}} \cdot \mathbf{e}_{\mathbf{k}\tilde{\lambda}'} = k^2 \delta_{\lambda\lambda'} \quad (1.74)$$

(with  $\tilde{\lambda} = \lambda + 1 \pmod{2}$ ).

We now compare our Hamiltonian to the energy of a quantum mechanical harmonic oscillator written in terms of ladder operators  $\hat{a}_{\mathbf{k}\lambda}$  and  $\hat{a}_{\mathbf{k}\lambda}^\dagger$

$$\hat{H} = \sum_i \hbar \omega_i \left( \hat{a}_i^\dagger \hat{a}_i + \frac{1}{2} \right) = \sum_i \hbar \omega_i \frac{1}{2} \left( \hat{a}_i \hat{a}_i^\dagger + \hat{a}_i^\dagger \hat{a}_i \right). \quad (1.75)$$

In order to write the electromagnetic energy in this form, with a frequency  $\omega_i = \omega_{\mathbf{k}}$ , we identify the amplitudes  $A_{\mathbf{k}\lambda}$  with quantum operators by making the replacement

$$A_{\mathbf{k}\lambda}^{(*)} \rightarrow \sqrt{\frac{\hbar \omega_{\mathbf{k}}}{2 \varepsilon_0 V}} \hat{a}_{\mathbf{k}\lambda}^{(\dagger)}. \quad (1.76)$$

From what we know about quantum mechanics, we now also have to impose the

bosonic commutation relations on our new operators,

$$\left[ \hat{a}_{\mathbf{k}\lambda}, \hat{a}_{\mathbf{k}'\lambda'}^\dagger \right] = \delta_{\mathbf{k}\mathbf{k}'} \delta_{\lambda\lambda'}. \quad (1.77)$$

With the new operators, the quantized field operators now read

$$\hat{\mathbf{E}}(\mathbf{r}, t) = \sum_{\mathbf{k}, \lambda} \sqrt{\frac{\hbar\omega_{\mathbf{k}}}{2V\varepsilon_0}} \mathbf{e}_{\mathbf{k}\lambda} \left( \hat{a}_{\mathbf{k}\lambda} e^{i(\mathbf{k}\mathbf{r} - \omega t)} + \hat{a}_{\mathbf{k}'\lambda'}^\dagger e^{-i(\mathbf{k}\mathbf{r} - \omega t)} \right) \quad (1.78)$$

and

$$\hat{\mathbf{B}}(\mathbf{r}, t) = \sum_{\mathbf{k}, \lambda} -\sqrt{\frac{\hbar}{2V\varepsilon_0\omega_{\mathbf{k}}}} (\mathbf{k} \times \mathbf{e}_{\mathbf{k}\lambda}) \left( \hat{a}_{\mathbf{k}\lambda} e^{i(\mathbf{k}\mathbf{r} - \omega t)} + \hat{a}_{\mathbf{k}'\lambda'}^\dagger e^{-i(\mathbf{k}\mathbf{r} - \omega t)} \right). \quad (1.79)$$

The same method can be used in environments different from free space, as long as there is no absorption. The spatial mode functions and the allowed wave vectors need to be modified according to the environment. It can be easily verified that in a homogeneous isotropic medium these modifications are equivalent to simply making the replacements  $\varepsilon_0 \rightarrow \varepsilon$ ,  $\mu_0 \rightarrow \mu$  and  $c \rightarrow c/n$ .

For waves in open space, i.e. without boundary conditions, we can push the boundaries of the box to the limit  $L \rightarrow \infty$ . This leads to a continuity of modes with a density  $\frac{dk}{dn} = \frac{2\pi}{L}$ . We thus have to replace the sum over discrete  $\mathbf{k}$  into an integral,  $\sum_{\mathbf{k}} \rightarrow \frac{L}{2\pi} \int d\mathbf{k}$  or, as we have a three-dimensional distribution of wavevectors,

$$\sum_{\mathbf{k}} \rightarrow \left( \frac{L}{2\pi} \right)^3 \int d^3\mathbf{k}. \quad (1.80)$$

This changes the Hamiltonian to

$$H = (2\pi)^3 \int d^3\mathbf{k} \sum_{\lambda} \varepsilon_0 (A_{\mathbf{k}\lambda} A_{\mathbf{k}\lambda}^* + A_{\mathbf{k}\lambda}^* A_{\mathbf{k}\lambda}), \quad (1.81)$$

leading to replacements

$$A_{\mathbf{k}\lambda}^{(*)} \rightarrow \sqrt{\frac{\hbar\omega_{\mathbf{k}}}{2(2\pi)^3\varepsilon_0}} \hat{a}_{\mathbf{k}\lambda}^{(\dagger)}. \quad (1.82)$$

with commutators

$$\left[ \hat{a}_{\mathbf{k}\lambda}, \hat{a}_{\mathbf{k}'\lambda'}^\dagger \right] = \delta(\mathbf{k} - \mathbf{k}') \delta_{\lambda\lambda'} \quad (1.83)$$

now following a continuous delta-distribution for the wave-vector. The final quantized field operators take the form

$$\hat{\mathbf{E}}(\mathbf{r}, t) = \int d^3\mathbf{k} \sum_{\lambda} \sqrt{\frac{\hbar\omega_{\mathbf{k}}}{2(2\pi)^3\epsilon_0}} \mathbf{e}_{\mathbf{k}\lambda} \left( \hat{a}_{\mathbf{k}\lambda} e^{i(\mathbf{k}\mathbf{r} - \omega t)} + \hat{a}_{\mathbf{k}'\lambda'}^\dagger e^{-i(\mathbf{k}\mathbf{r} - \omega t)} \right) \quad (1.84)$$

and

$$\hat{\mathbf{B}}(\mathbf{r}, t) = \int d^3\mathbf{k} \sum_{\lambda} -\sqrt{\frac{\hbar}{2(2\pi)^3\epsilon_0\omega_{\mathbf{k}}}} (\mathbf{k} \times \mathbf{e}_{\mathbf{k}\lambda}) \left( \hat{a}_{\mathbf{k}\lambda} e^{i(\mathbf{k}\mathbf{r} - \omega t)} + \hat{a}_{\mathbf{k}'\lambda'}^\dagger e^{-i(\mathbf{k}\mathbf{r} - \omega t)} \right). \quad (1.85)$$

## 1.5 Atom-photon interactions: Dipole radiation

The main concern of this thesis is with the interaction of the electromagnetic field with single (oscillating) dipoles, in particular with the impact of medium permeability and permittivity on the rate of spontaneous emission. This is, if we treat the dipole as a quantum mechanical object with two distinct energy states, the rate at which it decays from the excited state to the ground state. Spontaneous emission is purely mediated by the vacuum fluctuations of the electromagnetic field, in contrast to stimulated emission which is due to interaction with excited field modes.

The spontaneous emission rate can be derived from the quantized electromagnetic field to a very good accuracy using perturbation theory, i.e. treating the interaction of the dipole with the field modes as a small perturbation (see for example [5, 6]) which leads to the well-known Fermi golden rule [7]. The total Hamiltonian, without the vacuum energy of the system reads

$$\hat{H} = \sum_{\mathbf{k}, \lambda} \hbar\omega_{\mathbf{k}} \hat{a}_{\mathbf{k}\lambda}^\dagger \hat{a}_{\mathbf{k}\lambda} + \hbar\omega_A |e\rangle \langle e| + \hat{\mathbf{d}} \cdot \hat{\mathbf{E}} \quad (1.86)$$

where the first term is the electromagnetic field energy, the second the energy of the dipole, described as a two-level system with energy difference  $\hbar\omega_A$ , and the last

term describes the interaction, which we will treat as a small perturbation. We have chosen the energy levels so that zero energy coincides with the ground state of the dipole and the field.  $\hat{\mathbf{d}} = \mathbf{d}\hat{\sigma}_x = \mathbf{d}(|e\rangle\langle g| + |g\rangle\langle e|)$  is the dipole operator with  $\mathbf{d}$  being the classical transition dipole moment of the system of interest (for example an atom). The dipole operator can also be described by raising/lowering operators  $\hat{\pi}^{+/-}$  for the atomic levels  $|e\rangle$  and  $|g\rangle$  as  $\hat{\mathbf{d}} = \mathbf{d}(\hat{\pi}^+ + \hat{\pi}^-)$ , so the coupling between dipole and field modes can be understood as an exchange of a single excitation. In the rotating frame of the atomic and bosonic frequencies we can then write the Hamiltonian as

$$\hat{H}_I = i\hbar \sum_{\mathbf{k}\lambda} g_{\mathbf{k}\lambda} \left( \hat{a}_{\mathbf{k}\lambda} e^{i(\mathbf{k}\mathbf{r} - \omega t)} - \hat{a}_{\mathbf{k}\lambda}^\dagger e^{-i(\mathbf{k}\mathbf{r} - \omega t)} \right) (\hat{\pi}^+ e^{i\omega_A t} + \hat{\pi}^- e^{-i\omega_A t}) \quad (1.87)$$

with

$$g_{\mathbf{k}\lambda} = \mathbf{d} \cdot \mathbf{e}_{\mathbf{k}\lambda} \sqrt{\frac{\omega_{\mathbf{k}}}{2\varepsilon_0 \hbar V}} \quad (1.88)$$

being the coupling strength in vacuum. We will assume the system to be initially in the state  $|e\rangle|0\rangle = |e, 0\rangle$ , the atom is excited and the field is in the vacuum state. After a time  $t$ , we describe the state of the evolved system by the eigenstates of the unperturbed Hamiltonian, i.e. the joint eigenstates of the uncoupled electric field and the atom:

$$|\psi(t)\rangle = \sum_n c_n(t) |n\rangle \quad (1.89)$$

The coefficients  $c_n(t)$  can be found in first order time-dependent perturbation theory by

$$c_n^{(1)}(t) = -\frac{i}{\hbar} \int_0^t d\tau \langle n | \hat{H}_I(\tau) | e, 0 \rangle. \quad (1.90)$$

We are interested in the decay of the atomic excitation into a single field excitation with mode indices  $\mathbf{k}$  and  $\lambda$ . Therefore we write

$$\begin{aligned} c_{\mathbf{k}\lambda}^{(1)}(t) &= - \int_0^t d\tau \langle g, 1_{\mathbf{k}\lambda} | g_{\mathbf{k}\lambda} \hat{a}_{\mathbf{k}\lambda}^\dagger e^{-i(\mathbf{k}\mathbf{r} - \omega\tau)} \hat{\pi}^- e^{-i\omega_A\tau} | e, 0 \rangle \\ &= i g_{\mathbf{k}\lambda} e^{i\mathbf{k}\mathbf{r}} \frac{e^{i(\omega_{\mathbf{k}} - \omega_A)t} - 1}{(\omega_{\mathbf{k}} - \omega_A)}. \end{aligned} \quad (1.91)$$

The spontaneous emission rate is determined by the transition probability of the dipole excitation to any field mode after a time  $t$ ,

$$\gamma = \frac{\partial}{\partial t} \sum_{\mathbf{k}\lambda} |c_{\mathbf{k}\lambda}^{(1)}(t)|^2. \quad (1.92)$$

We start by calculating the transition probability to an arbitrary field mode:

$$|c_{\mathbf{k}\lambda}^{(1)}(t)|^2 = |g_{\mathbf{k}\lambda}|^2 t^2 \text{sinc}^2 \left( \frac{\omega_{\mathbf{k}} - \omega_A}{2} t \right) \quad (1.93)$$

To get the contribution of all allowed modes in an infinite space we have to approach the limit  $V \rightarrow \infty$  first, so instead of summing over discrete modes we again integrate, using the mode density

$$D(k_i) = \left( \frac{dk_i}{dn_i} \right)^{-1} = \frac{L}{2\pi}. \quad (1.94)$$

Thus, the overall transition probability can be written as

$$|c^{(1)}(t)|^2 = \int d^3\mathbf{k} \frac{V}{(2\pi)^3} \sum_{\lambda} |c_{\mathbf{k}\lambda}^{(1)}(t)|^2 \quad (1.95)$$

which, together with equations 1.88 and 1.93 can be broken down to a frequency integral

$$|c^{(1)}(t)|^2 = \frac{|\mathbf{d}|^2 t^2}{6\pi^2 \epsilon_0 \hbar c^3} \int \omega^3 \text{sinc}^2 \left( \frac{\omega - \omega_A}{2} t \right) d\omega. \quad (1.96)$$

For sufficiently large timescales we can approximate the square sinc-function by a delta-distribution which picks only the value  $\omega = \omega_A$  and we thus replace  $\omega^3$  in the integral by  $\omega_A^3$  to get

$$|c^{(1)}(t)|^2 = \frac{|\mathbf{d}|^2 \omega_A^3 t}{3\pi \epsilon_0 \hbar c^3} \quad (1.97)$$

and therefore

$$\gamma = \frac{|\mathbf{d}|^2 \omega_A^3}{3\pi \epsilon_0 \hbar c^3}. \quad (1.98)$$

This is the spontaneous emission rate of a dipole in vacuum.

### 1.5.1 Generalized considerations

As has been suggested already in 1946 by Purcell [8], the existence of a medium can change the local density of electromagnetic field modes and therefore have an effect on the spontaneous emission rate of atoms embedded in such a medium. Therefore it makes sense to derive a general formula for the spontaneous emission rate valid for arbitrary environmental configurations. We start with equation 1.90 but now leave the electric field operator unspecified,

$$\begin{aligned}
c_{\mathbf{k}\lambda}^{(1)}(t) &= -\frac{i}{\hbar} \int_0^t d\tau \langle g, \mathbf{k}\lambda | \hat{\mathbf{d}} \cdot \hat{\mathbf{E}} e^{i(\omega_k - \omega_A)\tau} | e, 0 \rangle \\
&= -\frac{i}{\hbar} \mathbf{d} \langle \mathbf{k}\lambda | \hat{\mathbf{E}} | 0 \rangle \int_0^t d\tau e^{i(\omega_k - \omega_A)\tau} \\
&= -\frac{i}{\hbar} \mathbf{d} \langle \mathbf{k}\lambda | \hat{\mathbf{E}} | 0 \rangle \frac{e^{i(\omega_k - \omega_A)t} - 1}{i(\omega_k - \omega_A)}
\end{aligned} \tag{1.99}$$

where we use the time-independent representations of the field and dipole operators. Note that the electric field still has a spatial dependence (on the position of the dipole). With that, the spontaneous emission rate can be written as

$$\begin{aligned}
\gamma &= \frac{d}{dt} \sum_{\mathbf{k}\lambda} |c_{\mathbf{k}\lambda}^{(1)}(t)|^2 \\
&= \frac{d}{dt} \sum_{\mathbf{k}\lambda} \frac{d^2}{\hbar^2} |\langle \mathbf{k}\lambda | \hat{E}_{\parallel} | 0 \rangle|^2 t^2 \text{sinc}^2 \left( \frac{\omega_k - \omega_A}{2} t \right) \\
&\approx \frac{d}{dt} \sum_{\mathbf{k}\lambda} \frac{2\pi d^2}{\hbar^2} |\langle \mathbf{k}\lambda | \hat{E}_{\parallel} | 0 \rangle|^2 t \delta(\omega_k - \omega_A) \\
&= \sum_{\mathbf{k}\lambda} \frac{2\pi d^2}{\hbar^2} |\langle \mathbf{k}\lambda | \hat{E}_{\parallel} | 0 \rangle|^2 \delta(\omega_k - \omega_A)
\end{aligned} \tag{1.100}$$

where  $\hat{E}_{\parallel} = \frac{1}{d} \hat{\mathbf{E}} \cdot \mathbf{d}$  is the component of the electric field parallel to the dipole axis. This is the most commonly used form of Fermi's golden rule for spontaneous emission [7].

We note that the states  $|\mathbf{k}\lambda\rangle$  build an orthogonal basis of the single-photon space,

$$\sum_{\mathbf{k}\lambda} |\mathbf{k}\lambda\rangle \langle \mathbf{k}\lambda| = \mathbb{1}. \quad (1.101)$$

To make use of this, we write the delta-distribution of equation 1.100 in its integral representation

$$\begin{aligned} \gamma &= \int_{-\infty}^{\infty} dt \sum_{\mathbf{k}\lambda} \frac{d^2}{\hbar^2} |\langle \mathbf{k}\lambda | \hat{E}_{\parallel} | 0 \rangle|^2 e^{i(\omega_k - \omega_A)t} \\ &= \int_{-\infty}^{\infty} dt \sum_{\mathbf{k}\lambda} \frac{d^2}{\hbar^2} \langle 0 | \hat{E}_{\parallel} e^{i\omega_k t} | \mathbf{k}\lambda \rangle \langle \mathbf{k}\lambda | \hat{E}_{\parallel} | 0 \rangle e^{-i\omega_A t} \\ &= \int_{-\infty}^{\infty} dt \sum_{\mathbf{k}\lambda} \frac{d^2}{\hbar^2} \langle 0 | \hat{E}_{\parallel} e^{i\hat{H}t/\hbar} | \mathbf{k}\lambda \rangle \langle \mathbf{k}\lambda | \hat{E}_{\parallel} | 0 \rangle e^{-i\omega_A t} \end{aligned}$$

where in the last step we used the fact that  $\hbar\omega_k$  is the eigenvalue of the field Hamiltonian  $\hat{H}$  for the state vector  $|\mathbf{k}\lambda\rangle$ , in order to replace the dependence on the wavevector  $k$ . Now we can use the completeness relation from equation 1.101, to obtain

$$\gamma = \int_{-\infty}^{\infty} dt \frac{d^2}{\hbar^2} \langle 0 | \hat{E}_{\parallel} e^{i\hat{H}t/\hbar} \hat{E}_{\parallel} | 0 \rangle e^{-i\omega_A t}. \quad (1.102)$$

Rewriting this to

$$\gamma = \int_{-\infty}^{\infty} dt \frac{d^2}{\hbar^2} \langle 0 | \hat{E}_{\parallel} e^{i\hat{H}t/\hbar} \hat{E}_{\parallel} e^{-i\hat{H}t/\hbar} e^{i\hat{H}t/\hbar} | 0 \rangle e^{-i\omega_A t} \quad (1.103)$$

and applying the Hamiltonian operators to the field operator and state vectors,  $e^{i\hat{H}t/\hbar} \hat{E}_{\parallel} e^{-i\hat{H}t/\hbar} = \hat{E}_{\parallel}(t)$  and  $\hat{H} | 0 \rangle = 0$  in the Heisenberg picture, leads to

$$\gamma = \int_{-\infty}^{\infty} dt \frac{d^2}{\hbar^2} \langle 0 | \hat{E}_{\parallel}(0) \hat{E}_{\parallel}(t) | 0 \rangle e^{-i\omega_A t}. \quad (1.104)$$

Hence, the spontaneous emission rate in a medium is entirely determined by vacuum fluctuations of the electric field operator. These can be obtained from quantizing the electromagnetic field as shown above, however, this is not always easy. Another method for obtaining these field fluctuations is using Green's functions, as will be described in section 1.6. We will finish with a quick example of a case when it is

indeed easy to quantize the electromagnetic field and use equation 1.100 to calculate the medium modifications to the spontaneous emission rate.

### 1.5.2 Example: Magnetodielectrics

Let us consider a medium with a homogeneous, real permittivity  $\varepsilon$  and permeability  $\mu$ . Following the same quantization procedure as introduced in section 1.4 for the macroscopic medium, we find that the quantized electric field operator reads

$$\hat{\mathbf{E}}(\mathbf{r}, t) = \int d^3\mathbf{k} \sum_{\lambda} \sqrt{\frac{\hbar\omega_k}{2(2\pi)^3\varepsilon}} \mathbf{e}_{\mathbf{k}\lambda} \left( \hat{a}_{\mathbf{k}\lambda} e^{i(\mathbf{k}\mathbf{r}-\omega t)} + \hat{a}_{\mathbf{k}'\lambda}^{\dagger} e^{-i(\mathbf{k}\mathbf{r}-\omega t)} \right) \quad (1.105)$$

with a dispersion relation of

$$\omega = kv = \frac{k}{\sqrt{\varepsilon\mu}}. \quad (1.106)$$

We start with Fermi's golden rule in integral form

$$\gamma = \frac{2\pi d^2}{\hbar^2} \sum_{\lambda} \int d^3k |\langle \mathbf{k}\lambda | \hat{E}_{\parallel} | 0 \rangle|^2 \delta(\omega_k - \omega_A). \quad (1.107)$$

Now the meaning of the delta-distribution becomes obvious, we thus change the integration variables to spherical coordinates and substitute  $k$  by  $\omega = \frac{k}{\sqrt{\varepsilon\mu}}$ ,

$$\begin{aligned} \gamma &= \frac{2\pi d^2}{\hbar^2} \sum_{\lambda} \int \sqrt{\varepsilon\mu} d\omega \int d\varphi \int \varepsilon\mu\omega^2 \sin\theta d\theta |\langle \mathbf{k}\lambda | \hat{E}_{\parallel} | 0 \rangle|^2 \delta(\omega_k - \omega_A) \\ &= \frac{2\pi d^2}{\hbar^2} \sqrt{\varepsilon\mu}^3 \omega_A^2 \sum_{\lambda} \int d\varphi \int \sin\theta d\theta |\langle \mathbf{k}\lambda | \hat{E}_{\parallel} | 0 \rangle|^2 \end{aligned} \quad (1.108)$$

The transition element of the electric field  $|\langle \mathbf{k}\lambda | \hat{E}_{\parallel} | 0 \rangle|^2$  narrows down to the only non-vanishing component

$$|\langle \mathbf{k}\lambda | i \sqrt{\frac{\hbar\omega_k}{2(2\pi)^3\varepsilon}} \frac{1}{d} \mathbf{d} \cdot \mathbf{e}_{\mathbf{k}\lambda} \hat{a}_{\mathbf{k}\lambda}^{\dagger} e^{-i(\mathbf{k}\mathbf{r}-\omega_k t)} | 0 \rangle|^2 = \frac{\hbar\omega_k}{2(2\pi)^3\varepsilon} \left| \frac{1}{d} \mathbf{d} \cdot \mathbf{e}_{\mathbf{k}\lambda} \right|^2. \quad (1.109)$$

We can always choose angular coordinates such that  $|\frac{1}{d} \mathbf{d} \cdot \mathbf{e}_{\mathbf{k}\lambda}|^2 = \cos^2\theta$ , and we can do this for each polarization separately as they both appear in two separate integrals

which are merely being summed up. With this, the emission rate becomes

$$\begin{aligned}\gamma &= \frac{d^2\omega_A^3}{2(2\pi)^2\hbar\varepsilon}\sqrt{\varepsilon\mu^3}\sum_{\lambda}\int d\varphi\int\sin\theta\cos^2\theta d\theta \\ &= \frac{d^2\omega_A^3}{3\pi\hbar}\mu^{\frac{3}{2}}\varepsilon^{\frac{1}{2}}.\end{aligned}\tag{1.110}$$

We see that the modification of  $\mu^{\frac{3}{2}}\varepsilon^{\frac{1}{2}}$  or, equivalently,  $n\mu$  comes from the changed density of modes  $\frac{dk}{d\omega}$  together with the different form of the quantized field operator. In the case of a purely dielectric material the rate is simply

$$\frac{d^2\omega_A^3}{3\pi\hbar}\mu_0^{\frac{2}{3}}\varepsilon^{\frac{1}{2}} = \gamma_0\varepsilon_r^{\frac{1}{2}}\tag{1.111}$$

which is often interpreted as a modification to the vacuum rate of  $n = \sqrt{\varepsilon_r}$ . Here we see the dangers of such terminology as one might be tempted to infer from this a modification for magnetodielectrics of  $n = \sqrt{\mu_r\varepsilon_r}$ , but the magnetic permeability does not come into the formula with the same power as the permittivity.

## 1.6 Method of Green's functions

Green's functions are powerful tools in a wide range of mathematical and physical applications. They were developed as a means for dealing with inhomogeneous differential equations but can be used in a broad spectrum of situations. In physics, they are extensively used to describe the linear response of a system to an external perturbation like for example the scattering of a light beam in a complex medium. Together with the fluctuation dissipation theorem [9], one can also obtain field fluctuations of a quantum operator as in our case, the electric field fluctuations. We will start by giving a general definition of the mathematical framework of Green's functions and then show the applications for quantum electromagnetism.

### 1.6.1 Mathematical definition

A Green's function in its most general form is the solution of a differential equation

$$\mathcal{D}G(t - t') = \delta(t - t') \quad (1.112)$$

together with corresponding boundary conditions, where  $\mathcal{D}$  can be any differential operator. With this function  $G(t)$ , one can reconstruct the solution to any inhomogeneous differential equation of the form

$$\mathcal{D}f(t) = g(t) \quad (1.113)$$

by integrating

$$f(t) = \int dt' G(t - t')g(t'). \quad (1.114)$$

We can interpret this intuitively as solving the dynamics of a system  $f(t)$  for a single point-source, and then using this to derive the solutions for arbitrary systems by just summing up or, in fact, integrating over all sources that are actually present, giving each of them the solution of the initial point source.

If we want to describe the problem with oscillating functions we can use a Fourier decomposition

$$f(t) = \frac{1}{2\pi} \int d\omega e^{-i\omega t} f(\omega) \quad (1.115)$$

and

$$g(t) = \frac{1}{2\pi} \int d\omega e^{-i\omega t} g(\omega). \quad (1.116)$$

Now equation 1.114 can be written in frequency space in the simple form

$$f(\omega) = G(\omega)g(\omega) \quad (1.117)$$

where  $G(\omega) = \int dt e^{i\omega t} G(t)$  is the Fourier transform of the Green's function. In other words, the Green's function in frequency space relates one frequency-component of the solution  $f(\omega)$  to the same frequency-component of the source  $g(\omega)$ .

This formalism can be generalized to more than one dimension. The most general form then reads

$$\mathcal{D}_{ik} G_{kj}(t - t') = \delta_{ij}(t - t') \quad (1.118)$$

with  $\delta_{ij}(t - t') = \delta_{ij}\delta(t - t')$ , so that

$$f_i(t) = \int dt' G_{ij}(t - t') g_j(t') \quad (1.119)$$

$$\Rightarrow \mathcal{D}_{ij} f_j(t) = g_i(t), \quad (1.120)$$

or in Fourier space

$$f_i(\omega) = G_{ij}(\omega) g_j(\omega) \quad (1.121)$$

where the summation convention is implied whenever an index repeats.

## 1.6.2 Green's Functions in quantum physics: Kubo Formula

In physics we can find a relation between Green's functions and the linear response of a system of interest. Consider a perturbation to a system given by a Hamiltonian in the interaction picture of the form

$$\hat{H}_{\text{source}}(t) = -\phi_j(t) \hat{O}_j(t). \quad (1.122)$$

We can approximate the time evolution of the expectation value  $\langle \hat{O}_i(t) \rangle$  using first order perturbation theory as

$$\langle \hat{O}_i(t) \rangle = \langle \hat{O}_i(t) \rangle \Big|_{\phi=0} + \frac{i}{\hbar} \int_{-\infty}^t dt' \langle [\hat{H}_{\text{source}}(t'), \hat{O}_i(t)] \rangle, \quad (1.123)$$

or if we are interested in the change of the operator due to the perturbation,

$$\delta \langle \hat{O}_i(t) \rangle = \frac{i}{\hbar} \int_{-\infty}^t dt' \langle [\hat{H}_{\text{source}}(t'), \hat{O}_i(t)] \rangle \quad (1.124)$$

$$= -\frac{i}{\hbar} \int_{-\infty}^{\infty} dt' \theta(t - t') \phi_j(t') \langle [\hat{O}_j(t'), \hat{O}_i(t)] \rangle. \quad (1.125)$$

Comparing this to equation 1.114, we can identify a Green's function as

$$G_{ij}(t - t') = \frac{i}{\hbar} \theta(t - t') \langle [\hat{O}_i(t), \hat{O}_j(t')] \rangle \quad (1.126)$$

so that

$$\delta \langle \hat{O}_i(t) \rangle = \int_{-\infty}^{\infty} dt' G_{ij}(t-t') \phi_j(t'). \quad (1.127)$$

This expectation value can in principle be with respect to any quantum state of the system, typically one is interested in the vacuum state or the more general thermal state

$$\hat{\rho} = \frac{e^{-\beta \hat{H}}}{\text{Tr}(e^{-\beta \hat{H}})} \quad (1.128)$$

with  $\beta = 1/k_B T$ . With this, we can describe the response of the physical quantity  $\langle \hat{O}(t) \rangle$ , i.e. the expectation value, or the classical average of the operator  $\hat{O}$ , to any linear perturbation  $\phi(t)$ .

### 1.6.3 Example: Green's function of the vector potential

We are now interested in the response of the vector potential to an external current (see for example [10] for more detail). The corresponding interaction Hamiltonian has the form

$$\hat{H}_{source}(t) = - \int d^3 \mathbf{r} j_i(t, \mathbf{r}) \hat{A}_i(t, \mathbf{r}). \quad (1.129)$$

As we are in the interaction picture, the time dependency of the field operators  $\hat{A}_i(t, \mathbf{r})$  is still given by the free Hamiltonian of equation 1.81 and thus the operators have the same form as derived above. In addition to the sum over indices we also have a continuous integration over space here. This however does not change the general structure. In analogy to section 1.6.2 we write

$$\delta \langle \hat{A}_i(t, \mathbf{r}) \rangle = -\frac{i}{\hbar} \int_{-\infty}^{\infty} dt' \int d^3 \mathbf{r}' \theta(t-t') j_k(t', \mathbf{r}') \langle [\hat{A}_k(t', \mathbf{r}'), \hat{A}_i(t, \mathbf{r})] \rangle \quad (1.130)$$

and identify the Green's function as

$$G_{ij}(t, \mathbf{r}, \mathbf{r}') = \frac{i}{\hbar} \theta(t) \langle [\hat{A}_i(t, \mathbf{r}), \hat{A}_j(0, \mathbf{r}')] \rangle \quad (1.131)$$

and its Fourier transform with respect to the time coordinate

$$G_{ij}(\omega, \mathbf{r}, \mathbf{r}') = \int dt e^{i\omega t} G_{ij}(t, \mathbf{r}, \mathbf{r}'). \quad (1.132)$$

Now, the response of a single frequency component can be described by

$$\delta \langle \hat{A}_i(\omega, \mathbf{r}) \rangle = \int d^3 \mathbf{r}' G_{ik}(\omega, \mathbf{r}, \mathbf{r}') j_k(\omega, \mathbf{r}') \quad (1.133)$$

with summation convention implied. At the same time, we know that Maxwell's equations can be used to describe the dynamics of the classical vector potential. Since the change in expectation value indeed represents the classical value (the averaged field absence of sources is always zero, and both the operators and the classical fields follow the same equations of motion), we should be able to obtain this Green's function directly from solving the corresponding classical wave equations where the electrical current takes the role of the source term and is replaced by a Dirac delta-function. This can also be verified by showing that the Greens function as defined in expression 1.131 still satisfies the same equation as the corresponding classical Greens function.

#### 1.6.4 Application to spontaneous emission rates

We can use the framework developed above to calculate the field fluctuations from equation 1.104 in terms of the Green's function. We start by rewriting the decay rate in terms of the vector potential, considering only the transverse part for now, so that  $E_\omega = i\omega A_\omega$ ,

$$\gamma = \frac{\omega_A^2 d_i d_j}{\hbar^2} S_{ji}(\omega_A, \mathbf{r}, \mathbf{r})$$

where  $S_{ji}(\omega, \mathbf{r}, \mathbf{r}') = \int dt e^{i\omega t} S_{ij}(t, \mathbf{r}, \mathbf{r}')$  is the frequency representation of the correlation function

$$S_{ij}(t, \mathbf{r}, \mathbf{r}') = \langle \hat{A}_i(t, \mathbf{r}) \hat{A}_j(0, \mathbf{r}') \rangle. \quad (1.134)$$

Now we can use the fluctuation dissipation theorem [9]

$$\text{Im } G_{ij}(\omega, \mathbf{r}, \mathbf{r}') = \frac{1}{2\hbar} (1 - e^{-\beta\omega}) S_{ij}(\omega, \mathbf{r}, \mathbf{r}') \quad (1.135)$$

at zero temperature, i.e.  $e^{-\beta\omega} = 0$ , which corresponds to expectation values with respect to the vacuum state, to relate the decay rate to the imaginary part of the

Green's function,

$$\gamma = \frac{2\omega_A^2 d_i d_j}{\hbar} \text{Im} G_{ij}(\omega_A, \mathbf{r}, \mathbf{r}). \quad (1.136)$$

The main idea behind the fluctuation dissipation theorem is that due to the causality of the Green's function, the imaginary part of its spectrum can be written as (for simplicity, we omit the spacial dependency in the following derivation)

$$\begin{aligned} \text{Im} G_{ij}(\omega) &= \frac{1}{2i} (G_{ij}(\omega) - G_{ji}(-\omega)) \\ &= -\frac{1}{2\hbar} \int_{-\infty}^{\infty} dt e^{i\omega t} \left\langle [\hat{A}_j(0), \hat{A}_i(t)] \right\rangle, \end{aligned}$$

and the remaining commutator can be reduced to a simple expectation value: If we look at the first part of the commutator for a thermal state we see that we can rewrite it to

$$\begin{aligned} \left\langle \hat{A}_j(0) \hat{A}_i(t) \right\rangle &= \text{Tr} \left( e^{-\beta \hat{H}} \hat{A}_j(0) \hat{A}_i(t) \right) \\ &= \text{Tr} \left( \hat{A}_i(t) e^{-\beta \hat{H}} \hat{A}_j(0) \right) \\ &= \text{Tr} \left( e^{-\beta \hat{H}} e^{\beta \hat{H}} \hat{A}_i(t) e^{-\beta \hat{H}} \hat{A}_j(0) \right) \\ &= \text{Tr} \left( e^{-\beta \hat{H}} \hat{A}_i(t - i\beta) \hat{A}_j(0) \right) \\ &= \left\langle \hat{A}_i(t - i\beta) \hat{A}_j(0) \right\rangle \end{aligned}$$

and incorporate the additional imaginary time into a change of variable in the integral,

$$\begin{aligned} \text{Im} G_{ij}(\omega_A) &= -\frac{1}{2\hbar} \int_{-\infty}^{\infty} dt e^{i\omega t} \left( \left\langle \hat{A}_i(t - i\beta) \hat{A}_j(0) \right\rangle - \left\langle \hat{A}_i(t) \hat{A}_j(0) \right\rangle \right) \\ &= -\frac{1}{2\hbar} \left( \int_{-\infty}^{\infty} dt e^{i\omega(t+i\beta)} \left\langle \hat{A}_i(t) \hat{A}_j(0) \right\rangle - \int_{-\infty}^{\infty} dt e^{i\omega t} \left\langle \hat{A}_i(t) \hat{A}_j(0) \right\rangle \right), \end{aligned}$$

finally leading to the result of equation 1.135.

We have thus replaced the quantum vacuum fluctuations by an expression containing the Green's function which, even though still quantum, can be easily obtained from classical Maxwell's equations.

## 1.7 Local fields

Let us come back to macroscopic media again which shall be the main concern of this work. We must make ourselves aware of some of the peculiarities one can run into when working with this rather phenomenological theory. In fact, no medium is truly macroscopic, there are no continuous homogeneous polarization or magnetization densities. Usually approximating the distributions to be homogeneous over larger scales is fine, but when dealing with the emission properties of single dipoles or other microscopic bodies we need to be a bit more careful.

Whenever we are treating such objects in macroscopic electromagnetic fields, we need to take into account the fact that the microscopic elements do not see the averaged macroscopic field but rather the actual microscopic field at the particular position. This microscopic field will still be the sum of the external field and the contributions from the dipoles that make the medium, but we can no longer just do a volume average of all those dipoles. Or at least, the volume over which we could average without introducing inaccuracies is much smaller than the typical dimensions of the material structure. Practically, of course, treating every medium dipole individually is computationally impossible. Luckily however, there are still some assumptions and simplifications which can be made to get an insight on the actual locally acting field. The most intuitive and straightforward model is the Clausius-Mossotti model, sometimes also named after Lorentz and Lorenz who both derived an equivalent formula [11, 12].

In this model, the vicinity of the body of interest is treated microscopically, while the rest of the medium is described as a macroscopic homogeneous medium. This can be understood equivalently as defining a virtual cavity around our body, the inside of which we treat as vacuum ( $\varepsilon = \varepsilon_0$ ) filled with a discrete array of dipoles. This cavity has no effect on the macroscopic fields outside as it is purely a theoretical construct (and on average it has the same dipole density as the rest of the medium), which is why this model is also referred to as the virtual cavity model.

In the following we shall see two different but mathematically equivalent derivations of this virtual cavity model.

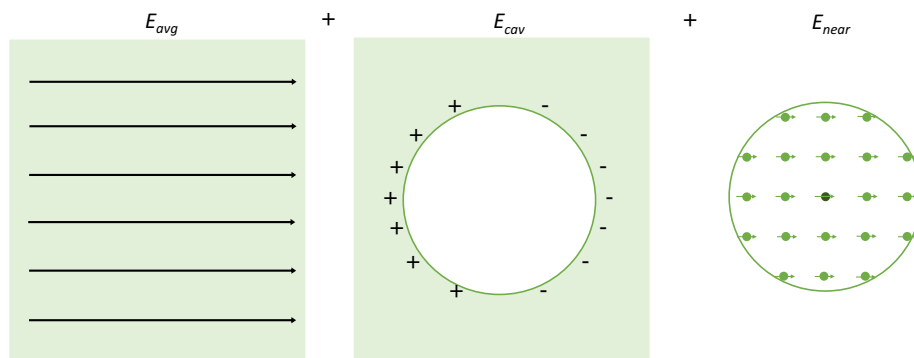


Figure 1.2: “Macroscopic” local field model: The field at the dipole position is the sum of the average macroscopic field  $\mathbf{E}_{\text{avg}}$ , the field due to the surface charges induced by the macroscopic medium at the boundary to the cavity  $\mathbf{E}_S$ , and the contributions from the dipoles inside the cavity taken into account microscopically.

**Macroscopic derivation** Let us first come to the textbook derivation of the Clausius-Mossotti local field (see for example [13–15]). We start by separating the medium into two regions. A spherical region around the dipole which forms the virtual cavity in which we treat the medium microscopically, and the region around that sphere which we shall treat macroscopically. This means we describe the region in the cavity not as a homogeneous medium but as a region of vacuum, filled with dipoles at discrete positions.

The electric field at the centre of the sphere can be described by the sum of three different fields, as shown in figure 1.2: The average field in the medium  $\mathbf{E}_{\text{avg}}$ , the field due to surface charges building up at the cavity boundary  $\mathbf{E}_S$  and the field from the dipoles inside the sphere  $\mathbf{E}_{\text{near}}$ . Note that there are no real unbound surface charges accumulating anywhere. However, as we are treating the dipoles inside the sphere separately, we cannot “use” them to neutralize the charges at the boundary (if we would, then some of the discrete dipoles would remain as unpaired charges and we’d have the same surface contribution again, just somewhere else).

The average field  $\mathbf{E}_{\text{avg}}$  is by definition the macroscopic field  $\mathbf{E}$  in the medium. The field  $\mathbf{E}_S$  due to surface contributions can be calculated using the charge distribution  $\rho_S = -\nabla \cdot \mathbf{P}$  caused by the inhomogeneity of the polarization field at the virtual

boundary,

$$\begin{aligned}
\mathbf{E}_S(\mathbf{r}) &= -\nabla\phi = -\nabla \int dV' \frac{\rho_S}{4\pi\epsilon_0|\mathbf{r}-\mathbf{r}'|} \\
&= \nabla \int dV' \frac{(\nabla' \cdot \mathbf{P}(\mathbf{r}'))}{4\pi\epsilon_0|\mathbf{r}-\mathbf{r}'|} \\
&= - \int dV' \frac{(\nabla' \cdot \mathbf{P}(\mathbf{r}'))}{4\pi\epsilon_0} \frac{(\mathbf{r}-\mathbf{r}')}{|\mathbf{r}-\mathbf{r}'|^3}
\end{aligned} \tag{1.137}$$

with  $\mathbf{P}(r) = \mathbf{P}\Theta(r-R)$  being the macroscopic polarization of the medium around the virtual cavity of radius  $R$ . Using either the derivative of the Heaviside-theta or equivalently Gauss's theorem we can write this as an integral over the sphere surface

$$\mathbf{E}_S(\mathbf{r}) = - \int R^2 \sin\theta' d\theta' d\varphi' \frac{\hat{\mathbf{r}} \cdot \mathbf{P}(\mathbf{r}-\mathbf{r}')}{4\pi\epsilon_0 |\mathbf{r}-\mathbf{r}'|^3} \tag{1.138}$$

with  $\hat{\mathbf{r}}$  being the outward normal unit vector. We are interested in the field at the centre of the sphere,

$$\begin{aligned}
\mathbf{E}_S(0) &= \int \sin\theta' d\theta' d\varphi' \frac{\hat{\mathbf{r}} \cdot \mathbf{P}}{4\pi\epsilon_0} \hat{\mathbf{r}} \\
&= \frac{1}{3} \frac{\mathbf{P}}{\epsilon_0}.
\end{aligned} \tag{1.139}$$

Now the last part missing is the electric field of the dipoles  $\mathbf{d}_i$  inside the sphere,

$$\mathbf{E}_{\text{near}} = \sum_i \mathbf{E}(\mathbf{d}_i, \mathbf{r}_i) = - \sum_i \nabla \left( \frac{\mathbf{d}_i \cdot \hat{\mathbf{r}}_i}{r_i^2} \right) \tag{1.140}$$

where the dipole positions  $\mathbf{r}_i$  are given relative to the centre of the sphere. For sufficiently symmetric dipole orderings it can be shown by explicitly summing up all dipoles in a shell that this contribution is exactly zero at the position of the dipole in the centre of the sphere:

$$\mathbf{E}_{\text{near}}(0) = 0 \tag{1.141}$$

With this, the total acting field at the centre of the sphere is simply

$$\mathbf{E}_{\text{loc}} = \mathbf{E}_{\text{avg}} + \mathbf{E}_S(0) + \mathbf{E}_{\text{near}}(0) = \mathbf{E} + \frac{1}{3} \frac{\mathbf{P}}{\epsilon_0} \tag{1.142}$$

or in terms of macroscopic fields,

$$\mathbf{E}_{\text{loc}} = \frac{1}{3\epsilon_0}\mathbf{D} + \frac{2}{3}\mathbf{E}. \quad (1.143)$$

**Microscopic derivation** The previous derivation can seem a bit unintuitive, so I will briefly present a more simple, rather fundamental approach to the problem (see [14] for more details about the two different approaches) as depicted in figure 1.3. First we note, that if we were to apply an external field, then every dipole within a symmetric configuration of dipoles would feel only this external field, since as we have shown before, the fields of the other dipoles in the vicinity cancel out. So the local field is indeed exactly equal to the externally applied field. All we need to do is simply relate the externally applied field to the average macroscopic field in the medium. This can be done by averaging over a sufficiently large volume, for example the sphere we have already introduced above:

$$\begin{aligned} \mathbf{E} = \mathbf{E}_{\text{avg}} &= \mathbf{E}_{\text{ext}} + \mathbf{E}_{\text{dip}} \\ &= \mathbf{E}_{\text{ext}} + \frac{1}{V} \int dV \sum_i \mathbf{E}(\mathbf{d}_i, \mathbf{r}_i) \\ &= \mathbf{E}_{\text{ext}} - \frac{1}{V} \sum_i \frac{1}{3} \mathbf{d}_i \\ &= \mathbf{E}_{\text{ext}} - \frac{1}{3} \mathbf{P} \end{aligned} \quad (1.144)$$

And therefore

$$\mathbf{E}_{\text{loc}} = \mathbf{E}_{\text{ext}} = \mathbf{E} + \frac{1}{3} \mathbf{P}. \quad (1.145)$$

We can in fact interpret the averaging of the dipole fields as analogously to calculating the field due to surface charges/currents as it has been done in the previous derivation, only now we calculated the surface contributions due to the polarization inside the sphere and not outside of it.

**Some additional remarks** In principal this way of deriving the local field is valid in a broad range of materials. However, one must be careful in some cases. First of all, we have assumed here that the dipole of interest is part of the medium, and thus has the same polarizability as the surrounding dipoles. If the dipole itself is

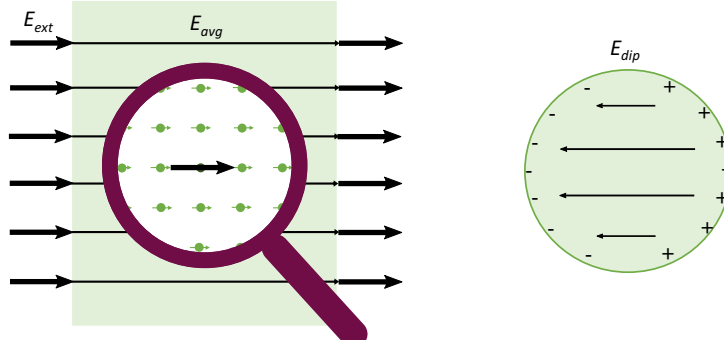


Figure 1.3: “Microscopic” local field model: The field at the dipole position is equal to the externally applied electric field  $E_{\text{ext}}$ . The macroscopic field  $E_{\text{avg}}$  inside the medium is the sum of the external field and the average of the fields from the induced dipoles  $E_{\text{dip}}$ . This average can be calculated from the surface charges of a spherical cavity, i.e. the charges due to dipoles *inside* the cavity. The local field can hence be calculated from the average field  $E_{\text{avg}}$  by *subtracting* the dipole contribution  $E_{\text{dip}}$ .

an impurity in the medium, its different polarizability can have an effect on the surrounding fields and one must use different methods, like for example the Onsager model [16, 17] which considers a tiny empty cavity, or even more general models [18]. Furthermore, the assumption that the fields of the surrounding dipoles cancel out can only be made in sufficiently symmetric configurations. In anisotropic media, to which we will come shortly, this must be taken into account as well and the model must be adjusted [18–22]. In absorbing media the model in principle remains valid, however, only in the classical realm. If we are dealing with a quantized description of the field one must make sure to include the noise fluctuations of the polarization appropriately [23, 24]. A generalization of this in the magnetic media will be addressed in chapter 4.3.

## 1.8 (Meta)materials

The main focus of this thesis is to generalize some aspects of the theory of light-matter interactions to more general kinds of media. The recently emerging field of metamaterials [25–32] gives rise to numerous new medium properties and thereby physical effects that have been ignored for the most part of history. This section shall give a general introduction to metamaterials and the novel properties they can exhibit, with a special focus on magnetodielectric and anisotropic media.

In contrast to normal materials, the fundamental building unit of metamaterials are not atoms but larger, specifically engineered objects which give the material their desired properties. In principal, this can be done as long as the desired wavelength is large compared to the dimensions of the fundamental building blocks. In that case, we can infer the macroscopic properties of the medium from the individual building blocks just like they are inferred from the atoms or molecules in a conventional material. This makes it possible to engineer novel electromagnetic properties which are otherwise hard or impossible to obtain, ranging from strong magnetic permeabilities to the famous example of negative refractive indices.

The basic idea in engineering specific metamaterials is often to arrange components of different electromagnetic properties in periodic structures to get the desired combination when taken in the macroscopic average. These objects can simply be alternating slices of bulk media, or more elaborate structures like tiny electric circuit elements. In the following we will give an overview of the specific materials which will be treated in this thesis: magnetodielectric media and anisotropic media.

### 1.8.1 Magnetodielectric media

Strong magnetodielectric media are something that is found only very rarely in nature. Conventional materials usually do not possess high permeabilities as atoms have extremely weak magnetic dipole moments, their magnetic polarizability is two orders of magnitude smaller than the electric polarizability. This is understandable in the context of the complications of making a magnetic dipole out of purely electric material. The magnetic permeability is often simply approximated by the vacuum permeability  $\mu_0$ . This makes it very hard to determine how magnetic media actually impact on physical effects. Part of this thesis is to rigorously derive formulas for the spontaneous emission rate for magnetodielectric media without making any approximations about the permeability. In particular, we allow the permeability to have large, but also complex or negative values.

With metamaterials, one is not limited to the polarizability of atoms or molecules anymore, and using more complex structures, arbitrary permeabilities can be engineered. Custom magnetic materials can be extremely useful for optical data processing and quantum information technologies, most notably is the potential in mag-

netic resonance imaging [29, 33, 34]. The most famous example of customization of the magnetic permeability is the split ring resonator [35], which is composed of two concentric rings in a plane, each with a gap. Every ring can be understood as the minimal example of an LC resonator which still exhibits a notable inductive element, namely one loop of a coil. With these resonators, one can reach an effective negative permeability, which is an essential ingredient for negative refractive index materials.

**Negative refractive index materials** In the 1960s, Veselago first considered the possibility of the refractive index of a medium being negative [36, 37]. A negative refractive index would be obtained when both the permeability  $\mu$  and the permittivity  $\varepsilon$  are negative. In such a case, the negative root of  $n = \sqrt{\mu_r \varepsilon_r}$  has to be chosen to describe the effect of the medium properly.<sup>9</sup>In conventional materials, even though materials with negative  $\mu$ , and materials with negative  $\varepsilon$  are known, these do not occur at the same time. Silver and gold for example have negative  $\varepsilon$  even at the visible spectrum, but positive  $\mu$ . Combining materials of negative  $\varepsilon$  with negative  $\mu$  materials can lead to effective materials of simultaneous negative  $\varepsilon$  and  $\mu$ . The split ring resonators introduced above are among the earliest artificial realizations to exhibit negative  $\mu$ . Combined with a lattice of conducting wires for the negative permittivity, one can obtain a composite material with a frequency band in which both  $\varepsilon$  and  $\mu$  and thus the refractive index  $n$  are indeed negative [25].

The applications are wide: Negative index materials have been proposed to be used for sub-wavelength imaging or cloaking devices. In both cases, the advantage lies in the way that light beams are deflected in the material. From Snell's law

$$\sin \theta_{\text{in}} = n \sin \theta_{\text{out}} \quad (1.146)$$

it follows that in a material with  $n < 0$ , the light beam is deflected to the opposite side of the surface normal. Figure 1.4 shows how a slab of negative index material effectively acts like negative space in the optical sense, which opens completely new paths to focusing. In theory, this could be used as a perfectly focussing lens [38]

---

<sup>9</sup>In principle the sign of  $n$  is arbitrary. It has by convention been set to be the positive root in usual materials so that the imaginary part is positive when describing a lossy medium. For consistency with this convention, in the case that both  $\varepsilon$  and  $\mu$  are negative,  $n$  must be chosen as the negative root as well.

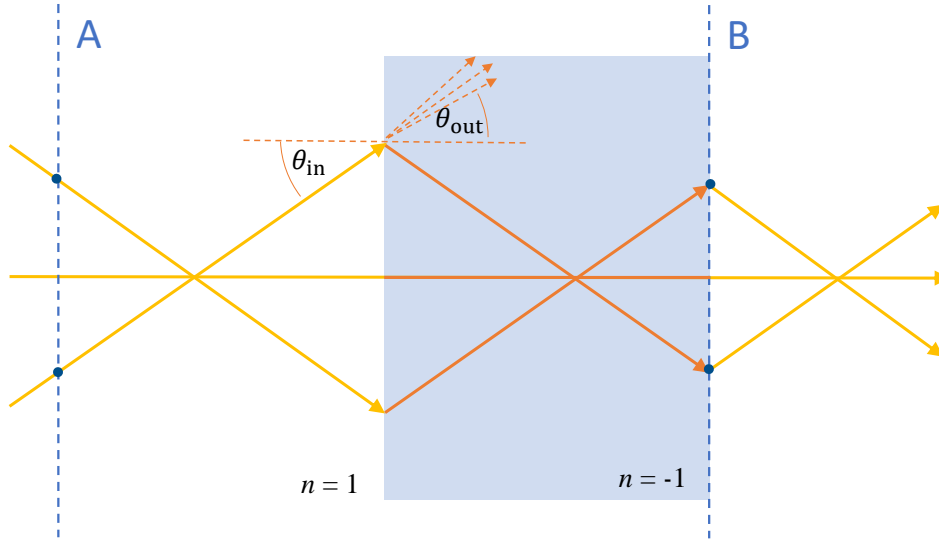


Figure 1.4: Light beams entering a negative refractive index material. The red dashed arrows show typical deflection in positive index materials. A material of refractive index  $-1$  of length  $l$  effectively removes a free-space distance of equal length: At position B behind the metamaterial, the light beams have exactly the same position and momentum as at a point A, which is at a distance  $l$  from the material. One could also understand this as negative optical path length inside the material.

which removes the restrictions to the resolution known from usual lenses as it deflects all parts of a beam at the interface.

The simultaneous negativity of  $\varepsilon$  and  $\mu$  has more consequences. Electromagnetic waves in negative refractive index materials are said to be left-handed, as the fields  $\mathbf{E}$ ,  $\mathbf{H}$  and the wavevector  $\mathbf{k}$  form a left-handed system instead of the usual right-handed relation. Hence, the Poynting vector points in the opposite direction from the wavevector, and the directions of energy propagation (phase velocity) and information propagation (group velocity) are opposed<sup>10</sup>. This opens questions in the framework of quantum information and communication, one example is the spontaneous emission rate of a dipole embedded in a negative-index medium. The form often used in literature of  $\gamma = n\gamma_{free}$  [39] would suggest a negative value for the emission rate. This can only be resolved by re-deriving the spontaneous emission rate for magnetodielectrics, with which the formula correctly reads  $\gamma = n\mu_r\gamma_{free}$  [40,41]. The negative permeability now makes up for the negative value of the refractive index,

<sup>10</sup>Note that negative refractive index alone does not necessarily lead to opposite signs of phase and group velocity. There have been rare cases reported [28] where both the group and the phase velocity had negative signs (this is the case when both  $n < 0$  and  $n + \omega \frac{dn}{d\omega} < 0$ ).

therefore leading to a positive rate again.

The possibility for losses in the medium, which will inevitably be present in any realistic materials, calls for an even more rigorous treatment, which will be the basis of chapter 4.

## 1.8.2 Anisotropic media

Anisotropic media have different properties in different directions. In particular, in the case of optical anisotropy, or birefringence, electromagnetic fields feel a different refractive index depending on which direction they are pointed. This can be the result of a certain kind of metamaterial construction, but also occurs naturally in many crystals with non-cubic lattice structure or in certain materials under stress. Common naturally occurring birefringent crystals are for example quartz or calcite, but also anthracene which has current applications in quantum optics [42,43]. Metamaterials can often have anisotropies as unintended side-effects, especially when stacking together lower-dimensional structures like metal strips, cylinders, or the split ring resonator described earlier [25].

The most famous effect of anisotropy is double-refraction: When a light beam enters the medium, it is split into two polarization components, each being deflected to a different angle due to the different refractive index they feel. Double-refraction has already been observed in 1669 [44] in calcite crystal, even though it took until the 19th century for it to be theoretically explained with different polarizations.

Mathematically, anisotropic media can be described by a matrix-valued permittivity  $\varepsilon$  or permeability  $\mu$ . For dielectrics for example, this means the permittivity  $\varepsilon$  takes the form of a tensor  $\varepsilon_{ij}$  such that  $D_i = \varepsilon_{ij}E_j$ , or in matrix form

$$\mathbf{D} = \underline{\underline{\varepsilon}}\mathbf{E}. \quad (1.147)$$

It can be shown that one can always find an orthogonal basis in which the permittivity matrix is diagonal, these basis vectors are called the principal axes of the crystal. In the following we will refer to the permittivity matrix  $\underline{\underline{\varepsilon}}$  as this diagonal matrix in the basis of the principal axes.

As we can see from equation 1.147, the electric field and the displacement field are no longer parallel in general, and the electric field is not necessarily divergence-free

anymore, even in the absence of free charges.

For a propagating wave, the electric field is in general not orthogonal to the wavevector, nor are two different polarization vectors orthogonal to each other, as will be shown later. Instead, the corresponding orthogonality constraints can now be understood to be under a different metric obtained by multiplying  $\underline{\underline{\epsilon}}$  in between the two vectors. The wavevector is thus orthogonal to the displacement field  $\mathbf{k} \cdot \mathbf{D} = \mathbf{k}^T \underline{\underline{\epsilon}} \mathbf{E} = 0$  and for two quantum-mechanically orthogonal polarization states, the displacement field of one is orthogonal to the electric field of the other,  $\mathbf{E}_1 \cdot \mathbf{D}_2 = \mathbf{E}_1^T \underline{\underline{\epsilon}} \mathbf{E}_2 = 0$  and vice versa. Hence, no orthogonal basis can be formed with any three of the vectors  $\mathbf{E}_i$ ,  $\mathbf{D}_i$ , and  $\mathbf{k}$ . Figure 1.5 illustrates the alignment of the different vectors compared to the plane orthogonal to the wave propagation.<sup>11</sup>

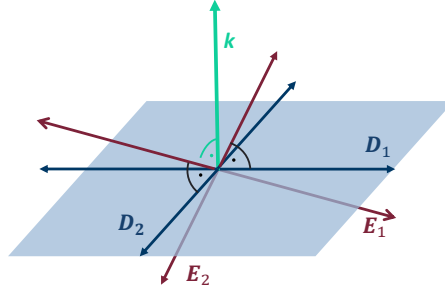


Figure 1.5: Electric and displacement field polarization vectors of a wave with wave vector  $\mathbf{k}$  in an anisotropic medium. Both  $\mathbf{D}_1$  and  $\mathbf{D}_2$  are orthogonal to  $\mathbf{k}$ , but not orthogonal to each other. Instead,  $\mathbf{D}_1 \perp \mathbf{E}_2$  and  $\mathbf{D}_2 \perp \mathbf{E}_1$ . The blue plane depicts the plane orthogonal to  $\mathbf{k}$ , or equivalently the plane formed by  $\mathbf{D}_1$  and  $\mathbf{D}_2$ .

**Uniaxial media** A special but very common case of anisotropy is the uniaxial medium, in which two of the three entries of the diagonal permittivity matrix are equal<sup>12</sup>. The third entry marks the optic axis of the medium, rotation around this axis keeps the optical properties invariant. Electromagnetic waves with wavevector parallel to the optic axis propagate just like in an isotropic medium: The displace-

<sup>11</sup>One must be careful when talking about propagation as in fact, the Poynting vector and the wave vector are not aligned either, hence the direction of energy transport and signal transport are different as well. The Poynting vector is not even unique as it is different for the two polarizations (double-refraction!).

<sup>12</sup>Anisotropic magnetodielectrics are rather rare but can exist, in that case by uniaxial we mean a medium in which permittivity and permeability tensors have the same symmetry.

ment field will always be in the plane orthogonal to the special axis, so the refractive index is the same for any polarization. In this case, also the electric field will be in the same plane and parallel to the corresponding displacement field.

For arbitrary wavevectors, one can always find one polarization which is in the plane orthogonal to the optic axis. For this polarization, again, the electric and the displacement field are parallel and the wave behaves like in an isotropic medium. Therefore, this polarization mode is also called the ordinary wave. The polarization orthogonal to the ordinary wave is called the extraordinary wave, for such waves the medium effect is completely anisotropically, i.e. these waves experience all the anisotropic effects described above.

**Biaxial media** The term biaxial itself might be a bit misleading at first, as biaxial media actually describe the most general case with three different values in the permittivity tensor. One can however always find two unique axes which have a special role, similar to the single optic axis of the uniaxial medium. There is now exactly two directions of  $\mathbf{k}$  for which all polarizations feel the same refractive index. These are called the wave-normal optic axes [45], they always lie in the plane of the two principal axes with the largest and the smallest permittivity. Apart from those two special cases, wave propagation in a biaxial medium is rather complicated, and always depends both on the polarization and the direction of propagation. In general, there are no ordinary waves in biaxial media.

Anisotropic media, both biaxial and uniaxial, have a lot of applications in optics and quantum information technologies. Polarizers for example have stronger absorption for certain directions of the fields and thereby only let light of a certain polarization pass unaffected. They can be made in a metamaterial fashion as for example a simple grid of parallel wires, but also exist on the atomic scale in some anisotropic crystals. By aligning polymer chains in one direction one can enforce that valence electrons only move freely in this direction but not orthogonal to it. Polarizers are present in all branches of technology. They are used in a lot of medical applications for diagnostics, in quantum information and communication for polarization measurements, but also in every day objects such as LCD displays, sunglasses or photographic filters. The other big application in quantum optics is the polarizing beam splitter, which makes use of the double-refraction property of birefringent crys-

tals and thereby separates the two polarizations of a beam or even a single photon. This can be used for example to entangle path and polarization degrees of freedom of photonic qubits.

Apart from the intended applications, birefringence also appears in a lot of situations as a side effect, as certain materials wanted for other applications happen to be anisotropic. Most importantly, nonlinear crystals used for the generation of second harmonics are almost always anisotropic [46, 47]. Furthermore, some materials used as host crystals for single impurities in quantum computing or communication applications are strongly anisotropic. It is especially these unintended anisotropies that have often been ignored so far, which calls for a deeper investigation of the effects, especially quantum mechanical effects which are affected by the anisotropy. Chapter 3 aims to solve some of the open questions related to anisotropic materials, especially the form of the quantized field operators and the case of emitting atoms embedded in such media.

# Chapter 2

## The $\mathbf{B}$ vs. $\mathbf{H}$ debate

“The unhappy term ‘magnetic field’ for  $\mathbf{H}$  should be avoided as far as possible. It seems that this term has led into error none less than Maxwell himself”

A. Sommerfeld

For the most part in literature, the magnetic fields<sup>1</sup>  $\mathbf{B}$  and  $\mathbf{H}$  are used almost interchangeably. This is due to the fact that almost all materials we find in nature are purely dielectric or at least only very weakly magnetic. In non-magnetic media the two fields are related only by a constant factor and it does not make any difference which field is used to describe physical effects. However, when magnetic responses become stronger, we need to clearly distinguish between the two fields, just like we do for the electric fields, in order to specify whether and how the macroscopic magnetization of the medium contributes to certain effects and interactions. There is great dispute in the field already about which field to actually call the magnetic field (e.g. [1] vs. [48]), but more importantly, about which field a magnetic dipole couples to [49, 50].

Maxwell’s equations are only of limited help here as they do not explicitly state the form of the interaction of fields and matter. A Lagrangian or Hamiltonian formalism can give more information, however, any derivation of the Hamiltonian is based on initial assumptions which are only verified by comparing the resulting equations

---

<sup>1</sup>I will make no choice of which field to call *the* magnetic field, but instead just call them  $\mathbf{B}$ - or  $\mathbf{H}$ - field and refer to them both as magnetic fields.

of motion to Maxwell's equations. Hence, in principle, different versions of the interaction energy can be derived, using different macroscopic fields.

Nevertheless, there are a few clues on which we can base some basic statements. In the following I aim to answer two questions. First, the question of which is the fundamental field, as compared to the non-fundamental field which is to be understood as the field "loaded" by the magnetizations/polarizations of the medium. Second, which fields do electric and magnetic dipoles couple to? For electric dipoles, after similar discussions [51], there is now a wide consensus that both these fields are the  $E$ -field [2, 3], for the magnetic fields there are some arguments for both  $\mathbf{B}$  and  $\mathbf{H}$ . In the following we shall see how different arguments for either field arise depending on which fundamental physical principal we base the discussion on. We will also present a potential solution to the coupling of magnetic dipoles which does not violate any of the arguments that favour a particular field.

## 2.1 What is the "fundamental" field?

Before we come to this question, we should make ourselves aware that the term fundamental is no physically rigorous definition, but merely an intuition, and interpretation for our understanding of the world. Deciding which field is more fundamental would have no actual physical implication on anything we could measure or observe. This is maybe already the first part of the answer: All fields,  $\mathbf{E}$ ,  $\mathbf{D}$ ,  $\mathbf{H}$ ,  $\mathbf{B}$  are in some sense fundamental and we can in principle describe the world in any combination of magnetic and electric fields. Especially, in free space, there is no difference between those quantities. Once we introduce charges and currents, and thereby electric and magnetic dipoles we simply define a relationship between  $\mathbf{E}$  and  $\mathbf{D}$ , and between  $\mathbf{B}$  and  $\mathbf{H}$  so that we can write Maxwell's equations in a macroscopic manner without explicitly having to include all the dipoles in the equations. But of course these fields have a slightly different character, which can be readily observed for example at their behaviour across interfaces. In the following, I will present different arguments showing how both the fields  $\mathbf{B}$  and  $\mathbf{H}$  can be seen as fundamental in some sense and why, in my personal opinion, the  $\mathbf{B}$ -field is the truly fundamental one.

### 2.1.1 Duality arguments

It was shown by Heaviside and Larmor that in the absence of free charges or currents, Maxwell's equations are completely symmetric between the electric and magnetic fields [52, 53]. More specifically, if we introduce new fields according to the transformation

$$\tilde{\mathbf{E}}(\theta) = \mathbf{E} \cos \theta + \sqrt{\frac{\mu_0}{\varepsilon_0}} \mathbf{H} \sin \theta \quad (2.1)$$

$$\tilde{\mathbf{H}}(\theta) = \mathbf{H} \cos \theta - \sqrt{\frac{\varepsilon_0}{\mu_0}} \mathbf{E} \sin \theta \quad (2.2)$$

and

$$\tilde{\mathbf{D}}(\theta) = \mathbf{D} \cos \theta + \sqrt{\frac{\varepsilon_0}{\mu_0}} \mathbf{B} \sin \theta \quad (2.3)$$

$$\tilde{\mathbf{B}}(\theta) = \mathbf{B} \cos \theta - \sqrt{\frac{\mu_0}{\varepsilon_0}} \mathbf{D} \sin \theta \quad (2.4)$$

these fields follow the same set of equations as the original fields. Not only Maxwell's equations, but in fact any physical property, like for example the energy density  $\frac{1}{2}(\mathbf{E} \cdot \mathbf{D} + \mathbf{B} \cdot \mathbf{H})$  or the Poynting vector  $\mathbf{E} \times \mathbf{H}$  are invariant under this transformation. Just like the macroscopic fields transform, we must transform the dipole moments, polarization / magnetization and permeability/permittivity accordingly. One particularly interesting transformation is the case of  $\theta = \pi/2$  which transforms the fields into their dual counterparts

$$\mathbf{E} \leftrightarrow \mathbf{H} \quad (2.5)$$

$$\mathbf{D} \leftrightarrow \mathbf{B} \quad (2.6)$$

(apart from a constant factor which is really just a question of definition).

This symmetry can be seen directly in Maxwell's equations, for example the fields  $\mathbf{D}$  and  $\mathbf{B}$  are divergence-free while  $\mathbf{E}$  and  $\mathbf{H}$  are not. In a similar manner, in electro-/magnetostatics,  $\mathbf{E}$  and  $\mathbf{H}$  are curl-free while  $\mathbf{D}$  and  $\mathbf{B}$  are not. Consequently, at an interface to a macroscopic medium, the perpendicular components  $\mathbf{D}^\perp$  and  $\mathbf{B}^\perp$  are continuous while the field strengths of  $\mathbf{E}^\perp$  and  $\mathbf{H}^\perp$  are lower inside the medium

as the dipoles act to screen part of the field.

Arguing by the duality of the electromagnetic fields, it becomes apparent that if we understand  $\mathbf{E}$  as the fundamental electric field, the fundamental magnetic field should be its dual,  $\mathbf{H}$ .

### 2.1.2 Experimental accessibility

In the laboratory, people usually talk about  $\mathbf{H}$  and  $\mathbf{E}$ , i.e. experiments are usually designed in terms of those fields, and measurements reveal exactly these, independent of the materials in play. This seems to fit well with the duality argument. However, the reason for this is more of a practical nature and has not much to do with duality [48]. Magnetic fields are created by building up a current in a loop or coil. The quantity readily accessible to the experimentalist is the current, which directly determines  $\mathbf{H}$ . The field  $\mathbf{B}$  in turn, would depend on the permeability of the medium in which we want to create the field.

When creating electric fields, for example at a capacitor, the easiest way to quantify the field strength is to read the voltage of the electricity source, which is related to the field  $\mathbf{E}$  between the two plates. If one were to measure the more fundamental quantity of the charge on the plates, then the medium-independent quantity one could determine from this information would be indeed the displacement field  $\mathbf{D}$ .

So if we study this situation carefully we see that indeed  $\mathbf{D}$  and  $\mathbf{H}$  are the fields which purely depend on free charges and currents but not on the macroscopic quantities of magnetization or polarization of a medium. In the next argument we will look a little deeper into this connection between  $\mathbf{D}$  and  $\mathbf{H}$  or, equivalently, between  $\mathbf{E}$  and  $\mathbf{B}$ .

### 2.1.3 No magnetic monopoles

There is a reason why we all learnt about  $\mathbf{E}$  and  $\mathbf{B}$  long before even knowing that there are more fields than these two. Before making the transition to macroscopic electrodynamics, Maxwell's equations are usually written in terms of  $\mathbf{E}$  and  $\mathbf{B}$  only, even though any other choice would work just as well. This is because it is the only combination of fields with which we can introduce magnetic and electric dipoles and with them, polarization and magnetization in terms of electric charges and currents

<b>E</b>  dual to each other 	<b>B</b> 	<b>I.</b> $\nabla \cdot E = \rho - \nabla \cdot P$ $\nabla \cdot B = 0$ $\nabla \times E = -\dot{B}$ $\nabla \times B = \dot{E} + J + \dot{P} + \nabla \times M$ <div style="display: flex; justify-content: space-around; font-size: small;"> <span><math>J_P</math></span> <span><math>J_M</math></span> </div>
<b>H</b>	<b>D</b>	<b>II.</b> $\nabla \cdot D = \rho$ $\nabla \cdot H = -\nabla \cdot M$ $\nabla \times D = -\dot{H} - \dot{M} - \nabla \times P$ $\nabla \times H = \dot{D} + J$
<b>III.</b> $\nabla \cdot E = \rho - \nabla \cdot P$ $\nabla \cdot H = -\nabla \cdot M$ $\nabla \times E = -\dot{H} - \dot{M}$ $\nabla \times H = \dot{E} + J + \dot{P}$	<b>VI.</b> $\nabla \cdot D = \rho$ $\nabla \cdot B = 0$ $\nabla \times D = -\dot{B} - \nabla \times P$ $\nabla \times B = \dot{D} + J + \nabla \times M$	

Figure 2.1: Maxwell's equations, written in terms of either possible pair of electric and magnetic fields, with  $\rho$  and  $\mathbf{J}$  being the free charges and currents. In representation I., all matter terms can be accounted for as electric charges and currents, while in II., we would need magnetic charges and currents to describe the matter terms in a similar manner. For better visibility, natural units of  $c = \epsilon_0 = 1$  are used in this diagram.

and thereby reduce all macroscopic considerations to the bare fundamental quantities. Let us have a look at figure 2.1, which shows Maxwell's equations written in all of the four possible pairs of electric and magnetic fields. We see that in any other combination of fields, the polarization or magnetization appears in places which usually do not contain any contributions from matter.

It turns out that if we were to include magnetic monopoles/charges into the equations, those occurrences could be easily described as dipole moments formed by magnetic charges in the same manner as we usually describe all dipoles to be formed by electric charges: So in analogy of the correspondence between dipole moments to electric charge and current

$$\nabla \cdot \mathbf{P} = -\rho_P, \quad \dot{\mathbf{P}} = \mathbf{J}_P, \quad \nabla \times \mathbf{M} = \mathbf{J}_M \quad (2.7)$$

we could as well describe them as formed by magnetic charges  $\tilde{\rho}$  and currents  $\tilde{\mathbf{J}}$ :

$$\nabla \cdot \mathbf{M} = -\tilde{\rho}_M, \quad \dot{\mathbf{M}} = \tilde{\mathbf{J}}_M, \quad \nabla \times \mathbf{P} = \tilde{\mathbf{J}}_P \quad (2.8)$$

Just like the set of equations **I.** is written in terms of electric charges and currents, the dual version of them, **II.** now look as if all polarization and magnetization came from magnetic charges and currents.

Of course none of these equations actually require the existence of magnetic (monopole) charges, as they all occur in the form of dipoles. But it tells us that there is something very fundamental about the fields  $\mathbf{E}$  and  $\mathbf{B}$ , at least if we deny the existence of magnetic monopoles. Then these are exactly the two fields we need to write Maxwell's equations without even needing to introduce the concept of polarization or magnetization, as we can express everything in terms of electric charges and currents.

In principle we can use any combination of fields to write any of the four equations. The combination used usually in macroscopic electrodynamics, a mix of all four fields, does not even require to include any (bound) currents or charges:

$$\nabla \cdot \mathbf{D} = 0 \quad (2.9)$$

$$\nabla \cdot \mathbf{B} = 0 \quad (2.10)$$

$$\nabla \times \mathbf{E} = -\frac{\partial \mathbf{B}}{\partial t} \quad (2.11)$$

$$\nabla \times \mathbf{H} = \frac{\partial \mathbf{D}}{\partial t} \quad (2.12)$$

However, we again see that the fields  $\mathbf{D}$  and  $\mathbf{H}$  carry a special role: They appear exactly in those equations in which we would include the matter contributions due to electric monopoles, so we can indeed understand them as those fields which contain the polarizations and magnetizations caused by electric charges and currents<sup>2</sup>. So with this in mind, we make the final conclusion:

---

<sup>2</sup>At the same time we could say that  $\mathbf{E}$  and  $\mathbf{B}$  can in principle contain polarizations and magnetizations caused by magnetic monopoles.

In the absence of magnetic monopoles, the magnetic field  $\mathbf{B}$  is fundamental in the sense that only in a formulation of Maxwell's equations in  $\mathbf{E}$  and  $\mathbf{B}$ , we can account for all matter contributions in terms of electric currents and charges.

Coming back to the dual symmetry of the fields, this conclusion is not necessarily in contradiction with duality: While the dual symmetry connects the fields  $\mathbf{E}$  and  $\mathbf{H}$ , and  $\mathbf{D}$  and  $\mathbf{B}$ , this same symmetry thereby also naturally pairs up the fields  $\mathbf{E}$  and  $\mathbf{B}$ , as compared to their dual counterparts  $\mathbf{H}$  and  $\mathbf{D}$ . In a world with only electric monopoles,  $\mathbf{E}$  and  $\mathbf{B}$  are fundamental just like in a world with only magnetic monopoles (which would be its dual),  $\mathbf{D}$  and  $\mathbf{H}$  would be fundamental. It is in fact exactly this circumstance of no magnetic monopoles that breaks the symmetry between the fields and makes one pair more workable than the other. Just imagine how beautifully symmetric Maxwell's equations would be in a world with both magnetic and electric monopoles.

### 2.1.4 Lorentz transformation

Another argument supporting our choice of  $\mathbf{E}$  and  $\mathbf{B}$  as the natural, fundamental couple comes from a completely different point of view:

The Lorentz transformation of the electromagnetic field tensor  $F^{\mu\nu}$  couples exactly the two fields  $\mathbf{E}$  and  $\mathbf{B}$ , which we just declared fundamental, with each other, while  $\mathbf{D}$  couples to  $\mathbf{H}$  [54]. A Lorentz-boost of velocity  $\mathbf{v}$  transforms the components of the field parallel ( $B_{\parallel}$  and  $E_{\parallel}$ ) and orthogonal ( $B_{\perp}$  and  $E_{\perp}$ ) to the translation axis according to

$$B'_{\parallel} = B_{\parallel}, \quad (2.13)$$

$$E'_{\parallel} = E_{\parallel}, \quad (2.14)$$

$$B'_{\perp} = \frac{1}{\sqrt{1 - \frac{v^2}{c^2}}} (\mathbf{B} - \mathbf{v} \times \mathbf{E})_{\perp}, \quad (2.15)$$

$$E'_{\perp} = \frac{1}{\sqrt{1 - \frac{v^2}{c^2}}} (\mathbf{E} + \mathbf{v} \times \mathbf{B})_{\perp} \quad (2.16)$$

and the fields  $\mathbf{D}$  and  $\mathbf{H}$  similarly as

$$H'_{\parallel} = H_{\parallel}, \quad (2.17)$$

$$D'_{\parallel} = D_{\parallel}, \quad (2.18)$$

$$H'_{\perp} = \frac{1}{\sqrt{1 - \frac{v^2}{c^2}}} (\mathbf{H} - \mathbf{v} \times \mathbf{D})_{\perp}, \quad (2.19)$$

$$D'_{\perp} = \frac{1}{\sqrt{1 - \frac{v^2}{c^2}}} (\mathbf{D} + \mathbf{v} \times \mathbf{H})_{\perp}. \quad (2.20)$$

This is a nice reassurance as it comes from a rather different theoretical background and yet still results in the same natural pairing of field variables.

## 2.2 Which field does a dipole interact with?

The more important question is that of the coupling between magnetic matter to the electromagnetic field, most fundamentally, the magnetic dipole coupling. A quick comparison of units shows that  $\mathbf{m} \cdot \mathbf{H}$  can't be correct as it does not describe an energy, the options with the correct units would be either  $\mathbf{m} \cdot \mu_0 \mathbf{H}$  or  $\mathbf{m} \cdot \mathbf{B}$ . At first glance one might be tempted to think that the correct coupling term thus must be  $\mathbf{m} \cdot \mathbf{B}$ . First, there is no additional constants in the electric coupling, and second, if we follow the usual procedure of replacing every occurrence of  $\mu_0$  by  $\mu$  of the medium, we get  $\mathbf{m} \cdot \mu \mathbf{H} = \mathbf{m} \cdot \mathbf{B}$  again.

On the other hand, duality tells us that, if we assume the coupling of electric dipoles  $\mathbf{d} \cdot \mathbf{E}$  to be correct, the magnetic dipole must couple to the field  $\mathbf{H}$ , and in order to keep the units correct, to  $\mathbf{m} \cdot \mu_0 \mathbf{H}$ . In fact, this additional factor  $\mu_0$  is purely historically originated, due to a different definition of the magnetic dipole moment as compared to the electric dipole. So in a duality transform, the corresponding dipole moment to  $\mathbf{d}$  would be  $\mu_0 \mathbf{m}$ . In refs. [55, 56] a coupling Hamiltonian of the form  $\mathbf{d} \cdot \mathbf{E} + \mu_0 \mathbf{m} \cdot \mathbf{H}$  is indicated which supports the duality argument, while in other sources [49] a coupling to the field  $\mathbf{B}$  is implied.

As it seems impossible to make fully justified arguments about the coupling of a dipole to either one of the macroscopic fields, we present in the following a different

solution or even circumvention of the problem:

It appears that a point dipole should never be treated within a purely macroscopic formalism in the first place, as the dimensions of the dipole if treated as a point-source (even with a position-uncertainty) are clearly not significantly larger than, if at all compatible with, the atomic lattice spacing of the medium. Therefore we must treat the dipole as being in the vacuum it really is in, and describe its environment microscopically. If we do that, the question of the coupling to the electromagnetic field in fact becomes redundant as both fields  $\mathbf{B}$  and  $\mu_0\mathbf{H}$  are equal in vacuum.

For obvious reasons we can't calculate the coupling of our dipole to every single other dipole in the medium. However, it turns out that the local field as introduced in section 1.7 is a perfect candidate for a description in terms of macroscopic fields while keeping the dipole itself in vacuum.

The only fully justifiable answer to the question which field a dipole couples to will thus be “the local field”.

In the electric case, equation 1.143, it can be directly seen that the fields  $E_{\text{loc}}$  and  $D_{\text{loc}}$  at the dipole position indeed only differ by  $\epsilon_0$  (they must, as we imposed a vacuum at the dipole position) and thus are both equally valid candidates. According to the Clausius-Mossotti local field approximation, the dipole actually couples to a mix of the macroscopic fields  $E$  and  $D$ :

$$\mathbf{d} \cdot \mathbf{E}_{\text{loc}} = \frac{1}{\epsilon_0} \mathbf{d} \cdot \mathbf{D}_{\text{loc}} = \mathbf{d} \cdot \left( \frac{1}{3\epsilon_0} \mathbf{D} + \frac{2}{3} \mathbf{E} \right) \quad (2.21)$$

In the following we will derive an analogous relationship for the magnetic fields which similarly lets us answer the question of the coupling of magnetic dipoles by “the local magnetic field”.

### 2.2.1 Derivation of the local magnetic field

The derivation of the local magnetic field follows a similar approach as in section 1.7: We describe the medium microscopically in a spherical cavity around the dipole of interest and divide the locally acting field into macroscopic contributions  $\mathbf{B}_{\text{avg}}$ , boundary contributions  $\mathbf{B}_{\text{S}}$  and contributions from the magnetic dipoles inside the cavity  $\mathbf{B}_{\text{near}}$ . Instead of surface charges we now have to include surface currents  $\mathbf{J}_M = \nabla \times (\mathbf{M}\Theta(r))$  going around the sphere to compensate for the discontinuity of

macroscopic permeability at the virtual cavity boundary. Their contribution to the magnetic field in the centre can be calculated as

$$\begin{aligned} \mathbf{B}_S(\mathbf{r}) &= \nabla \times \mathbf{A} = \nabla \times \int dV' \frac{\mu_0 \mathbf{J}_M}{4\pi |\mathbf{r} - \mathbf{r}'|} \\ &= \int dV' \frac{\mu_0 (\hat{\mathbf{r}} \times \mathbf{M}) \delta(\mathbf{r}')}{4\pi} \left( \nabla \times \frac{1}{|\mathbf{r} - \mathbf{r}'|} \right) \end{aligned} \quad (2.22)$$

which evaluated at  $r = 0$  is

$$\begin{aligned} \mathbf{B}_S(0) &= \int \sin \theta' d\theta' d\varphi' \frac{\mu_0 (\hat{\mathbf{r}} \times \hat{\mathbf{r}} \times \mathbf{M})}{4\pi} \\ &= \int \sin \theta' d\theta' d\varphi' \frac{\mu_0 ((\hat{\mathbf{r}} \cdot \mathbf{M}) \hat{\mathbf{r}} - \mathbf{M})}{4\pi} \\ &= \frac{\mu_0}{4\pi} \left( \frac{4\pi}{3} \mathbf{M} - 4\pi \mathbf{M} \right) \\ &= -\frac{2}{3} \mu_0 \mathbf{M}. \end{aligned} \quad (2.23)$$

The contributions from local dipoles inside the sphere cancel out just like the electric dipoles. With this, we have

$$\mathbf{B}_{\text{loc}} = \mathbf{B}_{\text{avg}} + \mathbf{B}_S(0) + \mathbf{B}_{\text{near}}(0) = \mathbf{B} - \frac{2}{3} \mu_0 \mathbf{M} \quad (2.24)$$

or equivalently

$$\mathbf{B}_{\text{loc}} = \frac{1}{3} \mathbf{B} + \frac{2}{3} \mu_0 \mathbf{H} \quad (2.25)$$

which, since we treated the dipole as in vacuum, can also be written in a dual symmetric form of equation 1.143

$$\mathbf{H}_{\text{loc}} = \frac{1}{\mu_0} \mathbf{B}_{\text{loc}} = \frac{1}{3\mu_0} \mathbf{B} + \frac{2}{3} \mathbf{H}. \quad (2.26)$$

We arrive at the same conclusion as for the electric field, the magnetic dipole couples neither purely to one of the macroscopic fields  $\mathbf{B}$  or  $\mathbf{H}$ , but to the local field, which

is a mixture of both<sup>3</sup>:

$$\mathbf{m} \cdot \mathbf{B}_{\text{loc}} = \mu_0 \mathbf{m} \cdot \mathbf{H}_{\text{loc}} = \mathbf{m} \cdot \left( \frac{1}{3} \mathbf{B} + \frac{2}{3} \mu_0 \mathbf{H} \right) \quad (2.27)$$

When comparing this to the electric coupling we note that this is exactly the dual version of the electric dipole coupling. We should stress here the universality of this approach: Even though in the derivation we used the magnetic field  $\mathbf{B}$ , which appears fundamental but not dual to  $\mathbf{E}$ , we finally arrived at an expression which is exactly the dual version of the electric local field. This is reassuring in that the local field is indeed a solution which does not rely on any assumptions to the different nature of the two magnetic fields or their coupling.

## 2.2.2 Weak-permeability approximation

Just like in the case of an electric dipole, which is often taken to couple to the (macroscopic) electric field  $\mathbf{E}$ , we can make a similar approximation for the magnetic dipole. If we take  $\mu$  to be similar to but not exactly  $\mu_0$ , the magnetic dipole coupling can be approximated by

$$\mathbf{m} \cdot \mathbf{B}_{\text{loc}} = \mu_0 \mathbf{m} \cdot \mathbf{H}_{\text{loc}} \approx \mathbf{m} \cdot \mu_0 \mathbf{H} \quad (2.28)$$

rather than  $\mathbf{m} \cdot \mathbf{B}$ . Of course, this is a very rough and bold approximation as for the same justification we could as well set  $\mathbf{B} \approx \mu_0 \mathbf{H}$  which then would remove any distinction of which field the dipole couples to. The only reason for favouring  $\mathbf{m} \cdot \mu_0 \mathbf{H}$  to  $\mathbf{m} \cdot \mathbf{B}$  is that this term appears with a larger factor of  $2/3$ , so  $\mathbf{m} \cdot \mu_0 \mathbf{H}$  is a slightly less bad approximation than  $\mathbf{m} \cdot \mathbf{B}$ . The main point of this approximation is merely to show the connection to the electric dipole coupling for which local field effects are often not taken into account but instead, the dipole is taken to couple to the field  $\mathbf{E}$ . So in the same framework, one then would have to say that the magnetic dipole couples to the field  $\mathbf{H}$ . This again agrees perfectly with the dual symmetry of electromagnetic fields in which  $\mathbf{H}$  is indeed the dual correspondence of  $\mathbf{E}$ .

---

<sup>3</sup>Note that the derivation could equivalently be carried out in terms of the magnetic field  $\mathbf{H}$ . We have simply chosen to use  $\mathbf{B}$  so that the magnetization of the medium can be straightforwardly described by electric currents in the most familiar way.

# Chapter 3

## Dipole emission in anisotropic media

Optical anisotropy is a very common phenomenon not only in metamaterials but also in nature, and makes the generalization of macroscopic media descriptions [57,58] to take into account a direction-dependency of the medium responses to external fields. The optical properties of anisotropic media have been widely studied for dielectric materials [45,58–68], given that many quantum technologies and optics experiments rely on the use of uniaxial or biaxial crystals [42,43,46,47]. However, spontaneous emission of atoms embedded in an anisotropic host medium has not been the focus of research as in most cases, the anisotropy is rather a side product of the experimental setup than an intended property<sup>1</sup>. In the following we will present a derivation of the spontaneous emission properties of an electric dipole in a uniaxial host crystal and propose a numerical model to approximate the emission rate in general biaxial media. This work has been published in [70]<sup>2</sup>. Furthermore we generalize the formula for uniaxial media to magnetodielectrics and show that the emission rate of magnetic dipoles in such a medium takes the dual form of the electric dipole expression.

---

<sup>1</sup>In the appendix of [69], an expression for the spontaneous emission rate in a uniaxial medium has been derived from a classical approach, however, a quick check of the derivation shows an error along the calculation which leads to an incorrect final result.

<sup>2</sup>Material reprinted with permission from A. Messinger, N. Westerberg, and S. M. Barnett, *Phys. Rev. A*, vol. 102, p. 013721, 2020. Copyright 2020 by the American Physical Society.

### 3.1 Quantization of the electromagnetic field

We can calculate the spontaneous emission rate using Fermi's golden rule, equation 1.100, so we first need the form of the quantized electric field operators. We thus start with the wave equation from equations 1.57-1.60 for the electric field,

$$\nabla \times \nabla \times \mathbf{E} = -\mu_0 \ddot{\mathbf{D}} = -\mu_0 \underline{\underline{\varepsilon}} \ddot{\mathbf{E}}. \quad (3.1)$$

In an anisotropic dielectric, the electric field is no longer divergence-free, so we cannot replace the double curl by a Laplacian as we did in section 1.4 to find the usual wave equation. However, we can still introduce a decomposition of the (complex<sup>3</sup>) electric field into plane waves,

$$\mathbf{E}(r, t) = \int d^3\mathbf{k} \mathbf{E}_{\mathbf{k}} e^{i(\mathbf{k}r - \omega_{\mathbf{k}}t)} \quad (3.2)$$

and try to find solutions for  $\mathbf{E}_{\mathbf{k}}$ . Equation 3.1 in the reciprocal space now reads

$$\mathbf{k} \times \mathbf{k} \times \mathbf{E}_{\mathbf{k}} = -\omega_{\mathbf{k}}^2 \mu_0 \underline{\underline{\varepsilon}} \mathbf{E}_{\mathbf{k}} \quad (3.3)$$

which we can also write as

$$\frac{1}{\mu_0 \underline{\underline{\varepsilon}}} (k^2 \mathbf{E}_{\mathbf{k}} - \mathbf{k}(\mathbf{k} \cdot \mathbf{E}_{\mathbf{k}})) = \omega_{\mathbf{k}}^2 \mathbf{E}_{\mathbf{k}}. \quad (3.4)$$

This is nothing but an eigenvalue problem with  $\mathbf{E}_{\mathbf{k}}$  and  $\omega_{\mathbf{k}}^2$  being the eigenvectors and eigenvalues of a matrix  $\underline{\underline{M}}$  with entries

$$M_{ij} = \frac{1}{\mu_0} \sum_l \varepsilon_{il}^{-1} (k^2 \delta_{lj} - k_l k_j). \quad (3.5)$$

If we choose our coordinate system so that the permittivity tensor is diagonal, its inverse is also diagonal,  $\varepsilon_{ij}^{-1} = \delta_{ij} \frac{1}{\varepsilon_{ij}} \equiv \delta_{ij} \frac{1}{\varepsilon_i}$ , and we can simplify

$$M_{ij} = \frac{1}{\mu_0 \varepsilon_i} (k^2 \delta_{ij} - k_i k_j). \quad (3.6)$$

---

<sup>3</sup>Again, the complex conjugate of each frequency component is omitted for simplicity here.

Note that in this notation the doubly occurring index  $i$  is not summed over. From the structure of  $\underline{\underline{M}}$  we can infer some properties of the solutions already, which will prove helpful later:

**Theorem 1**

1. There are no more than two non-trivial solutions (with eigenvalues  $\neq 0$ ).
2. All solutions  $\lambda$  satisfy  $\omega_{\mathbf{k},\lambda} = \omega_{-\mathbf{k},\lambda}$  and  $\mathbf{E}_{\mathbf{k},\lambda} \parallel \mathbf{E}_{-\mathbf{k},\lambda}$  and
3.  $\mathbf{k} \cdot (\underline{\underline{\varepsilon}}\mathbf{E}_{\mathbf{k},\lambda}) = 0$ .
4.  $\mathbf{E}_{\mathbf{k},\lambda} \cdot (\underline{\underline{\varepsilon}}\mathbf{E}_{\mathbf{k},\lambda'}) = 0$  for different solutions  $\omega_{\mathbf{k},\lambda} \neq \omega_{\mathbf{k},\lambda'}$ .
5.  $\frac{1}{\mu_0}(\mathbf{k} \times \mathbf{E}_{\mathbf{k},\lambda}) \cdot (\mathbf{k} \times \mathbf{E}_{\mathbf{k},\lambda'}) = -\omega_{\mathbf{k},\lambda}\omega_{\mathbf{k},\lambda'}\mathbf{E}_{\mathbf{k},\lambda} \cdot (\underline{\underline{\varepsilon}}\mathbf{E}_{\mathbf{k},\lambda'})$ .

**Proof:**

1. This can be seen by explicitly checking that  $\text{Rank}(\underline{\underline{M}}) \leq 2$ .
2. Equality of forward and backward frequencies follows from the symmetry of equation 3.3. The Eigenvectors are identical apart from an arbitrary pre-factor.
3. This can be seen in equation 3.3, where the left side is clearly orthogonal to  $\mathbf{k}$ , and the right side parallel to  $\underline{\underline{\varepsilon}}\mathbf{E}_{\mathbf{k},\lambda}$ :

$$\mathbf{k} \cdot (\underline{\underline{\varepsilon}}\mathbf{E}_{\mathbf{k},\lambda}) = \frac{1}{-\omega_{\mathbf{k}}^2\mu_0}\mathbf{k} \cdot (\mathbf{k} \times \mathbf{k} \times \mathbf{E}_{\mathbf{k}}) = 0 \quad (3.7)$$

4. This proof is best understood as a variation of the well-known proof of eigenvector orthogonality of real symmetric matrices: The matrix  $\underline{\underline{M}}$  is a product of the diagonal matrix  $\underline{\underline{\varepsilon}}^{-1}$  and the symmetric matrix  $\underline{\underline{N}} := \frac{1}{\mu_0}(k^2\mathbb{1} - \mathbf{k}\mathbf{k}^\top)$ . For a fixed  $\mathbf{k}$  (we ignore the index in the following as it is not relevant) and two

different polarizations  $\mathbf{E}_1$  and  $\mathbf{E}_2$ , we can write

$$\underline{\underline{\varepsilon}}^{-1} \underline{\underline{N}} \mathbf{E}_1 = \omega_1^2 \mathbf{E}_1 \quad (3.8)$$

$$\Leftrightarrow \underline{\underline{N}} \mathbf{E}_1 = \omega_1^2 \underline{\underline{\varepsilon}} \mathbf{E}_1 \quad (3.9)$$

$$\Leftrightarrow (\underline{\underline{N}} \mathbf{E}_1) \cdot \mathbf{E}_2 = \omega_1^2 (\underline{\underline{\varepsilon}} \mathbf{E}_1) \cdot \mathbf{E}_2 \quad (3.10)$$

$$\Leftrightarrow \mathbf{E}_1 \cdot (\underline{\underline{N}} \mathbf{E}_2) = \omega_1^2 \mathbf{E}_1 \cdot (\underline{\underline{\varepsilon}} \mathbf{E}_2) \quad (3.11)$$

where in the last step we made use of the fact that both  $\underline{\underline{N}}$  and  $\underline{\underline{\varepsilon}}$  are symmetric. For the second solution  $\mathbf{E}_2$ , we also know that  $\underline{\underline{N}} \mathbf{E}_2 = \omega_2^2 \underline{\underline{\varepsilon}} \mathbf{E}_2$ . Plugging this in the left side of equation 3.11 gives

$$\omega_2^2 \mathbf{E}_1 \cdot (\underline{\underline{\varepsilon}} \mathbf{E}_2) = \omega_1^2 \mathbf{E}_1 \cdot (\underline{\underline{\varepsilon}} \mathbf{E}_2) \quad (3.12)$$

$$\Leftrightarrow (\omega_1^2 - \omega_2^2) \mathbf{E}_1 \cdot (\underline{\underline{\varepsilon}} \mathbf{E}_2) = 0 \quad (3.13)$$

So for two different frequencies  $\omega_1 \neq \omega_2$  we must have  $\mathbf{E}_1 \cdot (\underline{\underline{\varepsilon}} \mathbf{E}_2) = 0$ .

5. We know that  $-\omega_{\mathbf{k},\lambda}^2 \mu_0 \underline{\underline{\varepsilon}} \mathbf{E}_{\mathbf{k},\lambda} = \mathbf{k} \times \mathbf{k} \times \mathbf{E}_{\mathbf{k},\lambda}$  for solutions  $\mathbf{E}_{\mathbf{k},\lambda}$  and  $\omega_{\mathbf{k},\lambda}$ . Multiplying a second solution  $\mathbf{E}_{\mathbf{k},\lambda'}$  from the left, we get

$$-\omega_{\mathbf{k},\lambda}^2 \mu_0 \mathbf{E}_{\mathbf{k},\lambda'} \cdot (\underline{\underline{\varepsilon}} \mathbf{E}_{\mathbf{k},\lambda}) = \mathbf{E}_{\mathbf{k},\lambda'} \cdot (\mathbf{k} \times \mathbf{k} \times \mathbf{E}_{\mathbf{k},\lambda}) \quad (3.14)$$

$$= (\mathbf{k} \times \mathbf{E}_{\mathbf{k},\lambda}) \cdot (\mathbf{k} \times \mathbf{E}_{\mathbf{k},\lambda'}). \quad (3.15)$$

This is nearly what we wanted to show apart from the pre-factor  $\omega_{\mathbf{k},\lambda}^2$ . For  $\lambda = \lambda'$ , we have  $\omega_{\mathbf{k},\lambda'} = \omega_{\mathbf{k},\lambda}$  and we are done. In the case that  $\omega_{\mathbf{k},\lambda'} \neq \omega_{\mathbf{k},\lambda}$ , we have shown that  $\mathbf{E}_{\mathbf{k},\lambda} \cdot (\underline{\underline{\varepsilon}} \mathbf{E}_{\mathbf{k},\lambda'}) = 0$ , so the whole left side is zero and the pre-factor does not matter.

We can interpret these observations the following way: The first statement simply states the fact that the waves can have two different polarizations as the third degree of freedom is taken away by  $\nabla \cdot \mathbf{D} = 0$ . We can also go a bit deeper and say that we indeed only have exactly two choices now, as linear combinations of those two solutions are not eigenvectors. Physically, this means that even though electromagnetic waves in linear combinations of the two polarization modes can exist, such a

state could not be described by one unique frequency or dispersion because the two polarization modes are affected differently by the medium. This is exactly what the effect of double-refraction describes.

Observation (2.) is simply describing the reciprocity of the medium. (3.) tells us that in the medium, it is  $\mathbf{D} = \underline{\underline{\epsilon}}\mathbf{E}$  and not  $\mathbf{E}$  that is orthogonal to the wave vector. This naturally fulfils the first Maxwell equation. Similarly, (4.) means that for different polarizations,  $\mathbf{E}_{\mathbf{k},\lambda} \perp \mathbf{D}_{\mathbf{k},\lambda'}$ , i.e. the electric field polarization of one mode is orthogonal to the displacement field polarization of the other. This comes in handy when calculating the energy stored in the electric field which requires knowledge of the term  $\mathbf{E} \cdot \mathbf{D}$ . Finally, (5.) draws the connection to the magnetic field, i.e.  $\mathbf{H}_{\mathbf{k},\lambda} \cdot \mathbf{B}_{\mathbf{k},\lambda'} = \mathbf{E}_{\mathbf{k},\lambda} \cdot \mathbf{D}_{\mathbf{k},\lambda'}$ . In particular, for different polarizations we have  $\mathbf{H}_{\mathbf{k},\lambda} \perp \mathbf{B}_{\mathbf{k},\lambda'}$ , although in this case we could as well write  $\mathbf{B}_{\mathbf{k},\lambda} \perp \mathbf{B}_{\mathbf{k},\lambda'}$  or  $\mathbf{H}_{\mathbf{k},\lambda} \perp \mathbf{H}_{\mathbf{k},\lambda'}$  because we still treat the permeability  $\mu$  as a scalar and  $\mathbf{H}$  and  $\mathbf{B}$  are parallel.

With these solutions, let us write the electric and magnetic field as

$$\mathbf{E}(r, t) = \int d^3\mathbf{k} \sum_{\lambda} \mathbf{e}_{\mathbf{k}\lambda} (A_{\mathbf{k}\lambda} e^{i(\mathbf{k}\mathbf{r} - \omega_{\mathbf{k},\lambda}t)} + A_{\mathbf{k}\lambda}^* e^{-i(\mathbf{k}\mathbf{r} - \omega_{\mathbf{k},\lambda}t)}) \quad (3.16)$$

$$\mathbf{D}(r, t) = \int d^3\mathbf{k} \sum_{\lambda} \underline{\underline{\epsilon}} \mathbf{e}_{\mathbf{k}\lambda} (A_{\mathbf{k}\lambda} e^{i(\mathbf{k}\mathbf{r} - \omega_{\mathbf{k},\lambda}t)} + A_{\mathbf{k}\lambda}^* e^{-i(\mathbf{k}\mathbf{r} - \omega_{\mathbf{k},\lambda}t)}) \quad (3.17)$$

$$\mathbf{B}(r, t) = \int d^3\mathbf{k} \sum_{\lambda} -\frac{1}{\omega_{\mathbf{k},\lambda}} \mathbf{k} \times \mathbf{e}_{\mathbf{k}\lambda} (A_{\mathbf{k}\lambda} e^{i(\mathbf{k}\mathbf{r} - \omega_{\mathbf{k},\lambda}t)} + A_{\mathbf{k}\lambda}^* e^{-i(\mathbf{k}\mathbf{r} - \omega_{\mathbf{k},\lambda}t)}) \quad (3.18)$$

$$\mathbf{H}(r, t) = \int d^3\mathbf{k} \sum_{\lambda} -\frac{1}{\mu_0 \omega_{\mathbf{k},\lambda}} \mathbf{k} \times \mathbf{e}_{\mathbf{k}\lambda} (A_{\mathbf{k}\lambda} e^{i(\mathbf{k}\mathbf{r} - \omega_{\mathbf{k},\lambda}t)} + A_{\mathbf{k}\lambda}^* e^{-i(\mathbf{k}\mathbf{r} - \omega_{\mathbf{k},\lambda}t)}) \quad (3.19)$$

with  $\mathbf{e}_{\mathbf{k}\lambda} = \mathbf{E}_{\mathbf{k},\lambda}/|\mathbf{E}_{\mathbf{k},\lambda}|$  the normalized eigenvectors and  $A_{\mathbf{k}\lambda}$  the field amplitudes, and calculate the energy stored in the field

$$\begin{aligned} H &= \frac{1}{2} \int \mathbf{E}(r, t) \cdot \mathbf{D}(r, t) + \mathbf{H}(r, t) \cdot \mathbf{B}(r, t) dV \\ &\stackrel{(2.)}{=} 4\pi^3 \int d^3\mathbf{k} \sum_{\lambda\lambda'} \left( \mathbf{e}_{\mathbf{k}\lambda} \cdot \underline{\underline{\epsilon}} \mathbf{e}_{\mathbf{k}\lambda'} + \frac{1}{\mu_0 \omega \omega'} (\mathbf{k} \times \mathbf{e}_{\mathbf{k}\lambda}) \cdot (\mathbf{k} \times \mathbf{e}_{\mathbf{k}\lambda'}) \right) (A_{\mathbf{k}\lambda} A_{\mathbf{k}\lambda'} e^{-i(\omega + \omega')t} + c.c.) \\ &\quad + 4\pi^3 \int d^3\mathbf{k} \sum_{\lambda\lambda'} \left( \mathbf{e}_{\mathbf{k}\lambda} \cdot \underline{\underline{\epsilon}} \mathbf{e}_{\mathbf{k}\lambda'} - \frac{1}{\mu_0 \omega \omega'} (\mathbf{k} \times \mathbf{e}_{\mathbf{k}\lambda}) \cdot (\mathbf{k} \times \mathbf{e}_{\mathbf{k}\lambda'}) \right) (A_{\mathbf{k}\lambda} A_{-\mathbf{k}\lambda'}^* e^{-i(\omega - \omega')t} + c.c.) \end{aligned}$$

where we have used the integral representation of the Dirac delta function to elimi-

nate integration over  $\mathbf{k}'$  and written  $\omega^{(l)}$  short for  $\omega_{\mathbf{k},\lambda^{(l)}}$ . Using (5.) we see that the pre-factors in the first line cancel out,

$$\mathbf{e}_{\mathbf{k}\lambda} \cdot \underline{\underline{\varepsilon}} \mathbf{e}_{\mathbf{k}\lambda'} \pm \frac{1}{\mu_0 \omega \omega'} (\mathbf{k} \times \mathbf{e}_{\mathbf{k}\lambda}) \cdot (\mathbf{k} \times \mathbf{e}_{\mathbf{k}\lambda'}) = \mathbf{e}_{\mathbf{k}\lambda} \cdot \underline{\underline{\varepsilon}} \mathbf{e}_{\mathbf{k}\lambda'} \mp \mathbf{e}_{\mathbf{k}\lambda} \cdot \underline{\underline{\varepsilon}} \mathbf{e}_{\mathbf{k}\lambda'} \quad (3.20)$$

and we additionally use (4.) on the second line to obtain

$$H = (2\pi)^3 \int d^3\mathbf{k} \sum_{\lambda} \mathbf{e}_{\mathbf{k}\lambda} \cdot \underline{\underline{\varepsilon}} \mathbf{e}_{\mathbf{k}\lambda} (A_{\mathbf{k}\lambda} A_{\mathbf{k}\lambda}^* + A_{\mathbf{k}\lambda}^* A_{\mathbf{k}\lambda}). \quad (3.21)$$

Comparing this to the Hamiltonian of a quantum harmonic oscillator, we see that we must introduce ladder operators  $\hat{a}_{\mathbf{k}\lambda}$  and  $\hat{a}_{\mathbf{k}\lambda}^\dagger$  with commutation relations

$$[\hat{a}_{\mathbf{k}\lambda}, \hat{a}_{\mathbf{k}'\lambda'}^\dagger] = \delta(\mathbf{k} - \mathbf{k}') \delta_{\lambda\lambda'} \quad (3.22)$$

and make the replacements

$$A_{\mathbf{k}\lambda}^{(*)} \rightarrow \sqrt{\frac{\hbar \omega_{\mathbf{k},\lambda}}{2(2\pi)^3 \mathbf{e}_{\mathbf{k}\lambda} \cdot \underline{\underline{\varepsilon}} \mathbf{e}_{\mathbf{k}\lambda}}} \hat{a}_{\mathbf{k}\lambda}^{(\dagger)}. \quad (3.23)$$

With this we can write the field operators as

$$\hat{\mathbf{E}}(\mathbf{r}, t) = \int d^3\mathbf{k} \sum_{\lambda} \mathbf{e}_{\mathbf{k}\lambda} \hat{u}_{\mathbf{k},\lambda}(\mathbf{r}, t) \quad (3.24)$$

$$\hat{\mathbf{D}}(\mathbf{r}, t) = \int d^3\mathbf{k} \sum_{\lambda} \underline{\underline{\varepsilon}} \mathbf{e}_{\mathbf{k}\lambda} \hat{u}_{\mathbf{k},\lambda}(\mathbf{r}, t) \quad (3.25)$$

$$\hat{\mathbf{B}}(\mathbf{r}, t) = \int d^3\mathbf{k} \sum_{\lambda} \frac{-1}{\omega_{\mathbf{k},\lambda}} \mathbf{k} \times \mathbf{e}_{\mathbf{k}\lambda} \hat{u}_{\mathbf{k},\lambda}(\mathbf{r}, t) \quad (3.26)$$

$$\hat{\mathbf{H}}(\mathbf{r}, t) = \int d^3\mathbf{k} \sum_{\lambda} \frac{-1}{\omega_{\mathbf{k},\lambda}} \frac{1}{\mu_0} (\mathbf{k} \times \mathbf{e}_{\mathbf{k}\lambda}) \hat{u}_{\mathbf{k},\lambda}(\mathbf{r}, t) \quad (3.27)$$

with

$$\hat{u}_{\mathbf{k},\lambda}(\mathbf{r}, t) = \sqrt{\frac{\hbar\omega_{\mathbf{k},\lambda}}{2(2\pi)^3 \mathbf{e}_{\mathbf{k}\lambda} \cdot \underline{\underline{\epsilon}}_{\mathbf{k}\lambda}}} \times \quad (3.28)$$

$$\left( \hat{a}_{\mathbf{k}\lambda} e^{i(\mathbf{k}\cdot\mathbf{r} - \omega_{\mathbf{k},\lambda}t)} + \hat{a}_{\mathbf{k}\lambda}^\dagger e^{-i(\mathbf{k}\cdot\mathbf{r} - \omega_{\mathbf{k},\lambda}t)} \right). \quad (3.29)$$

Note that the biggest difference from the quantized field in an isotropic medium is the potential dependency of the frequency on the polarization and on the full vector  $\mathbf{k}$  instead of its length only. Furthermore, the pre-factor of  $\hat{u}_{\mathbf{k},\lambda}(\mathbf{r}, t)$  introduced for the quantization, and with this inevitably also the vacuum fluctuations of the fields, have an additional dependency on the alignment of the polarization vectors with respect to the crystal axes,  $\mathbf{e}_{\mathbf{k}\lambda} \cdot \underline{\underline{\epsilon}}_{\mathbf{k}\lambda}$ .

## 3.2 Spontaneous emission of electric dipoles

We now have everything we need to calculate the spontaneous emission rate in such a medium. We simply plug the field operator into Fermi's golden rule, and then have to solve the emerging integral

$$\begin{aligned} \gamma &= \frac{2\pi}{\hbar^2} \sum_f |\langle f | \hat{\mathbf{d}} \cdot \hat{\mathbf{E}} | 0 \rangle|^2 \delta(\omega_{\mathbf{k}\lambda} - \omega_A) \\ &= \frac{1}{8\hbar\pi^2} \int d^3\mathbf{k} \sum_\lambda \frac{\omega_{\mathbf{k}\lambda} |\mathbf{d} \cdot \mathbf{e}_{\mathbf{k}\lambda}|^2}{\mathbf{e}_{\mathbf{k}\lambda} \cdot \underline{\underline{\epsilon}}_{\mathbf{k}\lambda}} \delta(\omega_{\mathbf{k}\lambda} - \omega_A). \end{aligned} \quad (3.30)$$

The problem is, in general anisotropic media, even though solutions can be found, the form of the polarization vectors and frequencies is a complicated function of the wave vector orientation. Nevertheless, we can make a few general steps towards the solution already without explicitly knowing the eigenvectors and eigenvalues of  $\underline{\underline{M}}$ . Just like in the isotropic case, we need to convert the  $k$ -integral into a frequency integral to apply the delta-distribution. We thus make the substitution  $k \rightarrow \omega_{\mathbf{k}\lambda}$  with  $dk = n_{\mathbf{k},\lambda} d\omega_{\mathbf{k}\lambda}/c$  to rewrite equation 3.30 into

$$\gamma = \frac{1}{8\hbar\pi^2} \sum_\lambda \int \sin\theta d\varphi d\theta \left( \frac{n_{\mathbf{k},\lambda}}{c} \right)^3 \omega_{\mathbf{k}\lambda}^2 d\omega_{\mathbf{k}\lambda} \frac{\omega_{\mathbf{k}\lambda} |\mathbf{d} \cdot \mathbf{e}_{\mathbf{k}\lambda}|^2}{\mathbf{e}_{\mathbf{k}\lambda} \cdot \underline{\underline{\epsilon}}_{\mathbf{k}\lambda}} \delta(\omega_{\mathbf{k}\lambda} - \omega_A) \quad (3.31)$$

and evaluate the delta-distribution,

$$\gamma = \frac{\omega_A^3}{8\hbar\pi^2} \sum_{\lambda} \int \sin\theta d\varphi d\theta \left(\frac{n_{\mathbf{k},\lambda}}{c}\right)^3 \frac{|\mathbf{d} \cdot \mathbf{e}_{\mathbf{k}\lambda}|^2}{\mathbf{e}_{\mathbf{k}\lambda} \cdot \underline{\underline{\epsilon}} \mathbf{e}_{\mathbf{k}\lambda}} \quad (3.32)$$

where the  $\mathbf{k}$  index now is to be understood as the wavevector corresponding to the atomic frequency  $\omega_A$  with the orientation given by the angles  $\theta$  and  $\varphi$ . All we are left with now is an integral over the angular degrees of freedom of the wavevector. These integrals are not straightforward to solve for general anisotropic media<sup>4</sup>. This is why we will start with the more symmetric case of uniaxial media, in which the solutions have a more simple form and we can solve the integral analytically.

### 3.2.1 Uniaxial dielectrics

We define our medium to have a permittivity tensor  $\underline{\underline{\epsilon}} = \text{diag}(\epsilon_1, \epsilon_2, \epsilon_2)$ . The wave equation 3.3 for such a medium has the (un-normalized) solutions

$$\mathbf{e}_{\mathbf{k}_o} = \begin{pmatrix} 0 \\ -k_3 \\ k_2 \end{pmatrix}, \quad \mathbf{e}_{\mathbf{k}_e} = \begin{pmatrix} -\epsilon_2(k_2^2 + k_3^2) \\ \epsilon_1 k_1 k_2 \\ \epsilon_1 k_1 k_3 \end{pmatrix} \quad (3.33)$$

with corresponding angular frequencies

$$\omega_{\mathbf{k}_o} = \frac{ck}{n_o} = \frac{1}{\sqrt{\mu_0 \epsilon_2}} k \quad (3.34)$$

$$\omega_{\mathbf{k}_e} = \frac{ck}{n_e} = \sqrt{\frac{\boldsymbol{\kappa} \cdot \underline{\underline{\epsilon}} \boldsymbol{\kappa}}{\mu_0 \epsilon_1 \epsilon_2}} k, \quad (3.35)$$

where  $\boldsymbol{\kappa} = \mathbf{k}/k$  is the normalized wave vector. We call  $n_o$  and  $n_e$  the ordinary and extraordinary refractive indices, they describe the effective dispersion that a wave of a certain electromagnetic field mode feels. The first solution corresponds to the ordinary wave. Its polarisation vector  $\mathbf{e}_{\mathbf{k}_o}$  is orthogonal to the wavevector, and the frequency  $\omega_o$  does not depend on the orientation of  $\mathbf{k}$ , just like it is the case in an isotropic medium. The extraordinary wave,  $\mathbf{e}_{\mathbf{k}_e}$ , exhibits more complicated

<sup>4</sup>To the best of our knowledge, there is no analytical solution.

behaviour as it feels the full anisotropy of the medium. In particular, as can be seen from equation 3.35, the extraordinary refractive index depends on the orientation of the wave vector with respect to the crystal axes.

Using these solutions, we can now write down an explicit expression for the spontaneous emission rate of an atomic dipole. We define the dipole moment as  $\mathbf{d} = (d_1, d_2 \cos \phi, d_2 \sin \phi)$  according to the symmetry of the medium. As there is nothing distinguishing the  $y$ -axis and  $z$ -axis, we choose  $\phi = 0$  for the dipole orientation without loss of generality, but note that for any other angle the result will be the same. We furthermore choose spherical coordinates to match the same symmetry,

$$\mathbf{k} = k(\cos \theta, \sin \theta \cos \varphi, \sin \theta \sin \varphi)^T. \quad (3.36)$$

The expression in equation 3.32 is now most easily solved by considering the two polarization modes separately, and summing them up at the end.

**Contributions from ordinary waves:** The first integral to solve is

$$\gamma_o = \frac{\omega_A^3}{8\hbar\pi^2} \int \sin \theta d\varphi d\theta \left( \frac{n_{\mathbf{k},o}}{c} \right)^3 \frac{|\mathbf{d} \cdot \mathbf{e}_{\mathbf{k}o}|^2}{\mathbf{e}_{\mathbf{k}o} \cdot \underline{\underline{\varepsilon}} \mathbf{e}_{\mathbf{k}o}} \quad (3.37)$$

which describes the rate of transition into an ordinary wave excitation. The component  $d_1$  of the dipole does not contribute to this rate, as ordinary waves have polarisations in the plane with permittivity  $\varepsilon_2$  only. The emission rate due to ordinary waves thus simplifies to

$$\gamma_o = \frac{d_2^2 \omega_A^3}{8\hbar\pi^2} \int_0^{2\pi} d\varphi \int_0^\pi d\theta (\mu_0 \varepsilon_2)^{3/2} \frac{\sin^3 \theta}{\varepsilon_2}, \quad (3.38)$$

which can be easily solved,

$$\gamma_o = \frac{d_2^2 \omega_A^3 \mu_0^{3/2}}{4\pi\hbar} \varepsilon_2^{1/2} = \frac{d_2^2 \omega_A^3}{4\pi\hbar \varepsilon_0 c^3} n_o. \quad (3.39)$$

The result has a dependency on the ordinary refractive index  $n_o = \sqrt{\varepsilon_2/\varepsilon_0}$  only. This is in agreement with our expectations of the ordinary waves behaving like in an isotropic medium of permittivity  $\varepsilon_2$ . Note however the factor of  $\frac{3}{4}$  as compared

to the total emission rate of such an isotropic medium. We can understand this in the isotropic limit as the ordinary waves contributing to three quarters of the total emission rate for a dipole in the y-z plane.

**Contributions from extraordinary waves:** Extraordinary waves can have field components in any direction, so we cannot omit any parts of  $\mathbf{d}$  for this calculation and have to include the whole term  $|\mathbf{d} \cdot \mathbf{e}_{\mathbf{k}\lambda}|^2$ . However, products of two different spatial components of the polarization vector,  $e_{\mathbf{k}\epsilon}^{(i)} e_{\mathbf{k}\epsilon}^{(j)}$  can be omitted due to its structure: The products are always anti-symmetric in  $k_i$  and  $k_j$  and therefore will cancel in symmetric integration domains. For example,

$$e_{\mathbf{k}\epsilon}^{(1)} e_{\mathbf{k}\epsilon}^{(2)} \propto (k_2^2 + k_3^2) k_1 k_2 \quad (3.40)$$

$$e_{\mathbf{k}\epsilon}^{(2)} e_{\mathbf{k}\epsilon}^{(3)} \propto k_1 k_2 k_1 k_3 = k_1^2 k_2 k_3. \quad (3.41)$$

We therefore replace  $|\mathbf{d} \cdot \mathbf{e}_{\mathbf{k}\epsilon}|^2$  by the only non-vanishing terms  $(d_1 e_{\mathbf{k}\epsilon}^{(1)})^2 + (d_2 e_{\mathbf{k}\epsilon}^{(2)})^2$ . This yields

$$\begin{aligned} \gamma_e &= \frac{\omega_A^3}{2\hbar(2\pi)^2} \int_0^{2\pi} d\varphi \int_0^\pi d\theta \frac{(\mu_0 \epsilon_1 \epsilon_2)^{3/2} \sin \theta}{\epsilon_1 \epsilon_2 (\epsilon_2 \sin^2 \theta + \epsilon_1 \cos^2 \theta)^{5/2}} \\ &\quad \times [d_2^2 \epsilon_1^2 \cos^2 \theta \cos^2 \varphi + d_1^2 \epsilon_2^2 \sin^2 \theta] \end{aligned} \quad (3.42)$$

$$= \frac{\omega_A^3}{3\pi\hbar} \mu_0^{3/2} \left( \frac{d_2^2 \epsilon_1 + 4d_1^2 \epsilon_2}{4\sqrt{\epsilon_2}} \right). \quad (3.43)$$

This cannot be expressed as a simple function of the extraordinary refractive index

$$n_e = \epsilon_0^{-1/2} (\cos^2 \theta / \epsilon_2 + \sin^2 \theta / \epsilon_1)^{-1/2} \quad (3.44)$$

anymore, which is in stark contrast with both the contribution from the ordinary wave, and the emission rate in isotropic media. The difference is in the fact that there are now two dipole orientations which both contribute with different factors to the rate as well as that the extraordinary refractive index itself is a function of the emission direction.

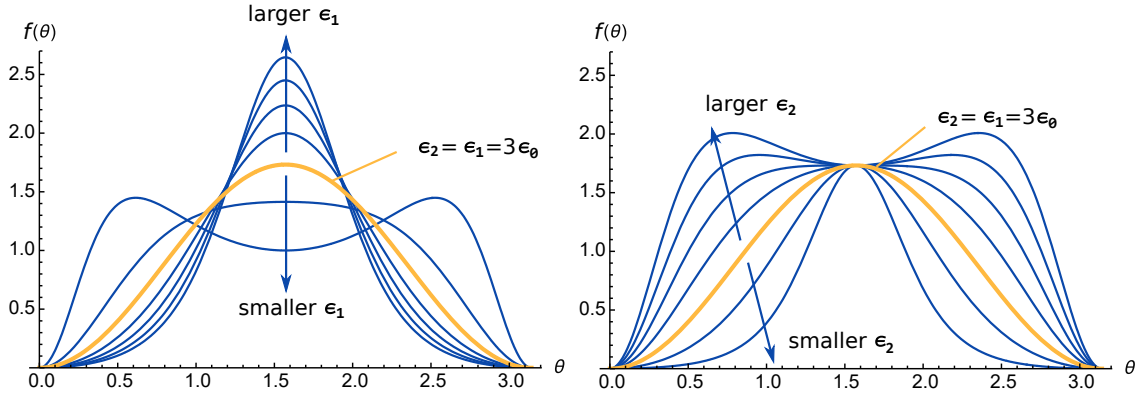


Figure 3.1: Angular distribution  $f(\theta)$  of the spontaneous emission rate (in units of the vacuum emission rate) to a fixed polar angle  $\varphi$ , for various configurations  $\epsilon_{o,e} \in \{1, 7\}$  of a uniaxial medium with fixed  $\epsilon_o$  (left) and fixed  $\epsilon_e$  (right). A change in  $\epsilon_o$  only changes the sides of the distribution, leaving the emission to an angle  $\theta = \pi/2$  constant, while a change in  $\epsilon_e$  impacts on the relative distribution, leaving the total rate (integrated over all angles) constant.

**Total emission rate:** The total emission rate can now be calculated from the sum of extraordinary and ordinary rates,

$$\begin{aligned} \gamma &= \gamma_o + \gamma_e \\ &= \frac{\omega_A^3 \mu_0^{3/2}}{3\pi\hbar} \left( \frac{\epsilon_1 + 3\epsilon_2}{4\sqrt{\epsilon_2}} d_2^2 + \sqrt{\epsilon_2} d_1^2 \right). \end{aligned} \quad (3.45)$$

We note that for a dipole oriented parallel to the  $\epsilon_1$ -axis, the emission rate is that of an isotropic medium with permittivity  $\epsilon_2$ . This is surprising as one intuitively might expect that the dipole will couple most strongly to the electric field components which are parallel to the dipole axis, i.e. in this case to the  $x$ -component  $\mathbf{E}^{(1)}$ . This field component feels only the permittivity  $\epsilon_1$ , so we would expect a very strong dependency of the emission rate to  $\epsilon_1$  and not  $\epsilon_2$ .

To resolve this paradox, we must take into account variations of the angular emission distribution. The typical donut-shaped emission pattern only occurs in an isotropic medium, where the angular dependency in the integrand is simply the  $\cos^2 \theta$  term describing the overlap between the dipole and the emission direction. In our case we have additional dependencies from the anisotropy. Consider the emission per unit angle by a dipole  $\mathbf{d} = (d_1, 0, 0)$ . Extraordinary waves are the only modes that contribute to the emission for such a dipole. The emission rate for this case is

the  $d_1$  component of equation 3.42:

$$\gamma_{\parallel} = \frac{\omega_A^3 d_1^2}{8\pi^2 \hbar} \int_0^{2\pi} d\varphi \int_0^{\pi} d\theta \frac{\sqrt{\mu_0^3 \varepsilon_1 \varepsilon_2} \sin^2 \theta \varepsilon_2^2}{(\varepsilon_2 \sin^2 \theta + \varepsilon_1 \cos^2 \theta)^{5/2}} \sin \theta \quad (3.46)$$

From this we extract the emission rate per solid angle  $d\Omega = d\varphi d\theta \sin \theta$  as

$$\begin{aligned} \frac{d\gamma_{\parallel}}{d\Omega} &= \frac{\omega_A^3 d_1^2 \sqrt{\mu_0^3 \varepsilon_0}}{8\pi^2 \hbar c^3} \left[ \frac{1}{\varepsilon_1^2} n_e^5(\theta) \sin^2 \theta \right] \\ &\equiv \frac{\omega_A^3 d_1^2 \sqrt{\mu_0^3 \varepsilon_0}}{8\pi^2 \hbar c^3} [f(\theta)/\varepsilon_0^2] \end{aligned} \quad (3.47)$$

so that the total emission rate is given by

$$\gamma_{\parallel} = \frac{3}{4} \gamma_{\text{vac}} \int_0^{\pi} d\theta f(\theta) \sin \theta. \quad (3.48)$$

If we look at the case  $\theta = \pi/2$  we see that the emission towards directions orthogonal to the dipole indeed solely depends on  $\varepsilon_1$ , just like we expected. The dependency of the total rate on  $\varepsilon_2$  must therefore come from the other possible emission directions, which we deemed less dominant. Figure 3.1 shows the angular dependency of the dimensionless per-angle emission rate  $f(\theta) = \frac{\varepsilon_2^2}{\varepsilon_1^2} n_e^5(\theta) \sin^2 \theta$ .

The shape of the angular distribution arises from an interplay between the preferred emission angle orthogonal to the dipole axis (that is the  $|\mathbf{d}_{\parallel} \cdot \mathbf{e}_{\mathbf{k}_e}|^2 \propto \cos^2 \theta$  term), and the preferred direction of wave propagation, which is determined by the effective refractive index  $n_e$ . Hence, for a large enough ratio  $\varepsilon_2/\varepsilon_1$ , the emission will peak towards two azimuthal angles  $\theta_{\text{max}} = \pi/2 \pm \Delta\theta$ . The shift of the emission peak can be calculated from maximizing the function  $f(\theta)$  which leads to the condition

$$\frac{df}{d\theta} = 0 \quad (3.49)$$

$$\Leftrightarrow \sin \theta \cos \theta (2(\varepsilon_2 \sin^2 \theta + \varepsilon_1 \cos^2 \theta) - 5(\varepsilon_2 - \varepsilon_1) \sin^2 \theta) = 0. \quad (3.50)$$

We see that according to the  $\cos \theta$  term, in the centre of the distribution, orthogonal to the dipole axis there is always an extremum, but we do not know yet if it is a minimum or a maximum. As we know the emission towards the dipole axis is always zero, the nature of the extremum is determined by the existence of further extrema

in the interval  $[0, \pi]$ . We thus set

$$(2(\varepsilon_2 \sin^2 \theta + \varepsilon_1 \cos^2 \theta) - 5(\varepsilon_2 - \varepsilon_1) \sin^2 \theta) = 0 \quad (3.51)$$

to find additional minima, which simplifies to

$$2\varepsilon_1 + 3 \sin^2 \theta (\varepsilon_1 - \varepsilon_2) = 0. \quad (3.52)$$

This has solutions

$$\theta = \arcsin \sqrt{\frac{2}{3(\frac{\varepsilon_2}{\varepsilon_1} - 1)}} \quad (3.53)$$

whenever  $\frac{\varepsilon_2}{\varepsilon_1} > \frac{5}{3}$ <sup>5</sup>. Hence, whenever these additional solutions exist, the extremum at the centre of the distribution is a minimum while these additional two angles are the new maxima. The shift of these emission peaks

$$\Delta\theta = \arccos \sqrt{\frac{2}{3(\frac{\varepsilon_2}{\varepsilon_1} - 1)}} \quad (3.54)$$

further increases with the larger ratios  $\varepsilon_2/\varepsilon_1$ , while the emission towards an angle  $\theta = \pi/2$  is fixed only by  $\varepsilon_1$ . In fact, the relative angular distribution with respect to the total emission  $f(\theta)/[\int f(\theta) \sin \theta d\theta]$  indeed only depends on the ratio  $r = \varepsilon_2/\varepsilon_1$ . It is this interplay of angular distributions which in the end leads to a cancelling of the dependencies on  $\varepsilon_1$  in the total rate.

**Random dipole orientation** The lack of an appearance of  $\varepsilon_1$  in the emission of a dipole  $\mathbf{d} = (d_1, 0, 0)$  also has consequences for another scenario. If we average equation 3.45 for random dipole alignments, one might expect  $\varepsilon_1$  to appear at least with a factor of  $\frac{1}{3}$ . However, the averaged spontaneous emission rate of unordered emitters is

$$\gamma_{\text{avg}} = \frac{\omega_A^3 \mu_0^{3/2} d^2}{3\pi\hbar} \left( \frac{1}{6} \frac{\varepsilon_1}{\sqrt{\varepsilon_2}} + \frac{5}{6} \sqrt{\varepsilon_2} \right). \quad (3.55)$$

---

<sup>5</sup>One might argue that the spherical nature of the coordinates play a role as well and we should indeed consider the function  $\tilde{f}(\theta) = f(\theta) \sin \theta$  (i.e. the total emission towards a certain azimuthal angle instead of fixing a polar angle  $\phi$  as well). This does not lead to any qualitative differences, and merely changes the condition for two maxima to  $\frac{\varepsilon_2}{\varepsilon_1} > \frac{5}{2}$ .

We see that indeed  $\varepsilon_1$  only appears in one of six parts and the total rate is by no means an average of the permittivities in the three directions. This should be kept in mind as it can lead to unexpectedly strong impacts of  $\varepsilon_2$  in uniaxial media.

### 3.2.2 Biaxial dielectrics

The wave equation of a medium with three different permittivity values,  $\underline{\underline{\varepsilon}} = \text{diag}(\varepsilon_x, \varepsilon_y, \varepsilon_z)$  is far more complicated than a uniaxial medium as there are no more symmetries present. The eigenvectors and eigenvalues can still be found, from solving an eigenvalue equation quadratic in  $\omega^2$  [60] we can write them as

$$\mathbf{e}_{\mathbf{k}\pm} = \begin{pmatrix} k_1/(\varepsilon_x - \varepsilon_{\mathbf{k}}) \\ k_2/(\varepsilon_y - \varepsilon_{\mathbf{k}}) \\ k_3/(\varepsilon_z - \varepsilon_{\mathbf{k}}) \end{pmatrix} \quad (3.56)$$

$$\omega_{\mathbf{k}\pm} = \frac{ck}{n_{\pm}} = \frac{1}{\sqrt{\mu_0 \varepsilon_{\mathbf{k}\pm}}} k \quad (3.57)$$

with an effective permittivity

$$\varepsilon_{\mathbf{k}\pm} = \frac{2\varepsilon_x \varepsilon_y \varepsilon_z}{t_{\mathbf{k}} \pm s_{\mathbf{k}}} \quad (3.58)$$

for  $t_{\mathbf{k}} = \boldsymbol{\kappa} \cdot \underline{\underline{\varepsilon}} (\text{Tr}(\underline{\underline{\varepsilon}}) \mathbf{I} - \underline{\underline{\varepsilon}}) \boldsymbol{\kappa}$ ,  $s_{\mathbf{k}} = \sqrt{t_{\mathbf{k}}^2 - 4\varepsilon_x \varepsilon_y \varepsilon_z \boldsymbol{\kappa} \cdot \underline{\underline{\varepsilon}} \boldsymbol{\kappa}}$  and  $\boldsymbol{\kappa} = \mathbf{k}/k$ . This specific form of writing the eigenvectors can lead to singularities for certain configurations of  $\varepsilon_i$ . This should not concern us as it is only a feature of the unnormalized eigenvectors as we express them here and we should simply note that one can always find an alternative expression with finite entries (for example by multiplying the whole vector by  $(\varepsilon_i - \varepsilon_{\mathbf{k}})$ ).

The integral arising from Fermi's golden rule with these solutions appears to be beyond analytic solvability. However, as the dispersion is still linear in  $k$  and the polarization vectors (apart from normalization) also do not depend on the length of  $\mathbf{k}$  but only its directionality, we can perform the integration over  $k$  in a similar manner to equation 3.32 to arrive at

$$\gamma = \frac{\omega_A^3}{2\hbar(2\pi)^2} \int \sum_{\lambda=\pm} \frac{|\mathbf{d} \cdot \mathbf{e}_{\mathbf{k}_0\lambda}|^2}{\mathbf{e}_{\mathbf{k}_0\lambda} \cdot \underline{\underline{\varepsilon}} \mathbf{e}_{\mathbf{k}_0\lambda}} (\mu_0 \varepsilon_{\mathbf{k}})^{3/2} \sin \theta d\theta d\varphi \quad (3.59)$$

where we have used the dispersion  $\frac{dk}{d\omega} = \sqrt{\mu_0 \varepsilon_{\mathbf{k}}}$  and applied the delta-distribution over the frequency. The remaining integral can only be solved numerically. In the following we propose a model to approximate the solution of this integral with an analytic expression based on the results from uniaxial media:

We choose a dipole orientated along the z-axis to start with, and explore the limits where  $\varepsilon_y$  takes the same value as either of the other two permittivities. For instance, we know that if  $\varepsilon_y = \varepsilon_x$ , the dipole points along the extraordinary axis, so we can identify  $\varepsilon_x = \varepsilon_y$  with  $\varepsilon_2$  and  $\varepsilon_z$  with  $\varepsilon_3$  of a uniaxial medium, and from equation 3.45, the emission rate follows as

$$\gamma^{(a)} = \frac{d^2 \omega_A^3 \mu_0^{3/2}}{3\pi \hbar} \sqrt{\varepsilon_x}. \quad (3.60)$$

Likewise, if  $\varepsilon_y = \varepsilon_z$  the dipole points along the ordinary axis and we identify  $\varepsilon_y = \varepsilon_z$  with  $\varepsilon_2$  and  $\varepsilon_x$  with  $\varepsilon_1$  so that in that case the rate must be

$$\gamma^{(b)} = \frac{d^2 \omega_A^3 \mu_0^{3/2} (\varepsilon_x + 3\varepsilon_z)}{3\pi \hbar 4\sqrt{\varepsilon_z}}. \quad (3.61)$$

Now we are interested in the behaviour of the emission rate with  $\varepsilon_y$  in between and beyond these two known points. We do this by studying the numerical solutions of equation 3.59 which are calculated using Wolfram Mathematica.

If we fix  $\varepsilon_x$  and  $\varepsilon_z$ , we find nearly linear behaviour with  $\varepsilon_y$  (see Fig. 3.2, crosses). This suggests that we try a linear interpolation in  $\varepsilon_y$  between the two known values from the uniaxial cases,

$$\gamma(\varepsilon_y) = \gamma^{(a)} + (\varepsilon_y - \varepsilon_x) \frac{\gamma^{(b)} - \gamma^{(a)}}{\varepsilon_z - \varepsilon_x} \quad (3.62)$$

$$= \frac{d^2 \omega_A^3 \mu_0^{3/2}}{3\pi \hbar} \left( \sqrt{\varepsilon_x} - \frac{\varepsilon_y - \varepsilon_x}{4\sqrt{\varepsilon_z}} + \frac{\varepsilon_y - \varepsilon_x}{\sqrt{\varepsilon_x} + \sqrt{\varepsilon_z}} \right), \quad (3.63)$$

which is drawn in Fig. 3.2, blue line. The result is already close to the numerical solution but not perfect, especially as the expression 3.63 puts  $\varepsilon_y$  in a special role even though our choice of fixing  $\varepsilon_x$  and  $\varepsilon_z$  was arbitrary.

As there is nothing distinguishing  $\varepsilon_x$  and  $\varepsilon_y$  from each other ( $\varepsilon_z$  is special because of the dipole alignment we chose), we can derive an equivalent formula to be linear

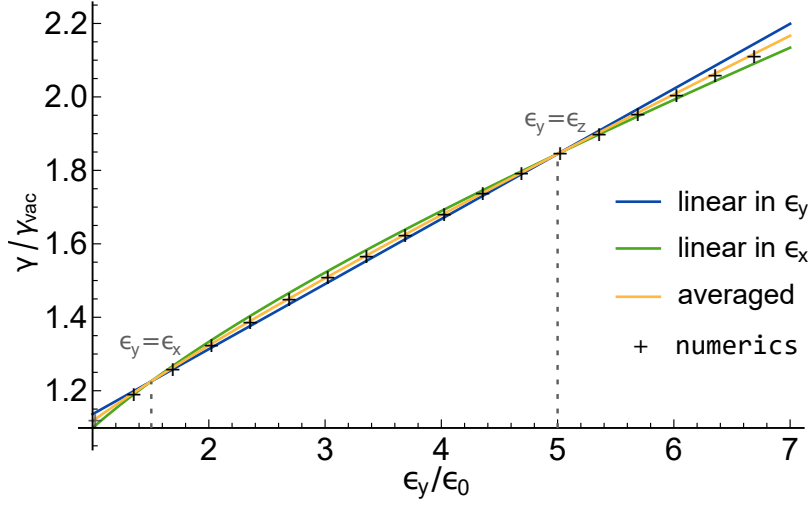


Figure 3.2: Dependency of the spontaneous emission rate in units of the vacuum emission rate on the relative permittivity  $\epsilon_y/\epsilon_0$  with fixed values of  $\epsilon_x = 1.5\epsilon_0$  and  $\epsilon_z = 5\epsilon_0$  for a dipole aligned with the  $\epsilon_z$ -axis. Analytical models obtained from linear interpolation with  $\epsilon_x$ , linear interpolation with  $\epsilon_y$  and an average of both (solid lines) are compared to numerical results (crosses).

in  $\epsilon_x$  (green line in Fig. 3.2)

$$\gamma(\epsilon_x) = \frac{d^2\omega_A^3\mu_0^{3/2}}{3\pi\hbar} \left( \sqrt{\epsilon_y} + \frac{\epsilon_y - \epsilon_x}{4\sqrt{\epsilon_z}} - \frac{\epsilon_y - \epsilon_x}{\sqrt{\epsilon_y} + \sqrt{\epsilon_z}} \right) \quad (3.64)$$

and take the mean of both to make the model fully symmetric,

$$\gamma = \frac{\gamma(\epsilon_x) + \gamma(\epsilon_y)}{2} \quad (3.65)$$

$$= \frac{d^2\omega_A^3\mu_0^{3/2}}{6\pi\hbar} \left[ \sqrt{\epsilon_x} + \sqrt{\epsilon_y} + \frac{\epsilon_y - \epsilon_x}{\sqrt{\epsilon_x} + \sqrt{\epsilon_z}} + \frac{\epsilon_x - \epsilon_y}{\sqrt{\epsilon_y} + \sqrt{\epsilon_z}} \right]. \quad (3.66)$$

As can be seen in Fig. 3.2 (orange curve), this now perfectly fits the numerical data. To check the range in which this model is valid, various configurations for  $\epsilon_x$  and  $\epsilon_z$  are shown in Figure 3.3. We note that the permittivity parallel to the dipole orientation has the weakest impact on the emission rate, as variations in  $\epsilon_z$  barely change the graph unless there is a large difference between  $\epsilon_x$  and  $\epsilon_y$ , for example the blue curve on the left which has large  $\epsilon_x$  but small  $\epsilon_y$  and similarly the right end of the green curve.

To simplify the expression a bit we can also introduce new variables,  $n_+ =$

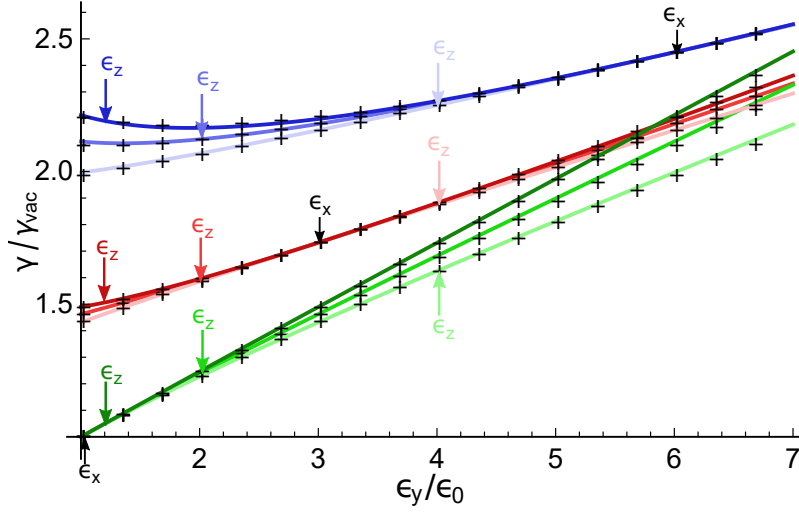


Figure 3.3: Comparison of the averaged model (solid lines) with numerical results (crosses) for various different configurations of  $\epsilon_x/\epsilon_0 = 6, 3, 1$  (blue, red, green group of graphs) and  $\epsilon_z/\epsilon_0 = 4, 2, 1.2$  (light, medium, dark graph from each group) for a dipole aligned with  $\epsilon_z$ . The corresponding values for  $\epsilon_x$  and  $\epsilon_z$  are also indicated by arrows where they match the value of  $\epsilon_y$  for each curve.

$\frac{1}{2\sqrt{\epsilon_0}}(\sqrt{\epsilon_y} + \sqrt{\epsilon_x})$ ,  $n_- = \frac{1}{2\sqrt{\epsilon_0}}(\sqrt{\epsilon_y} - \sqrt{\epsilon_x})$  and  $n_{\parallel} = \sqrt{\frac{\epsilon_z}{\epsilon_0}}$  to write Eq. (3.65) as

$$\gamma = n_+ \frac{(n_+ + n_{\parallel})^2 + 3n_-^2}{(n_+ + n_{\parallel})^2 - n_-^2} \gamma_{\text{vac}}. \quad (3.67)$$

This again shows that approximations such as  $\gamma = n_{\text{avg}} \gamma_{\text{vac}}$  with  $n_{\text{avg}} = \frac{1}{3\sqrt{\epsilon_0}}(\sqrt{\epsilon_x} + \sqrt{\epsilon_y} + \sqrt{\epsilon_z})$  as they are often done are not always advisable as the parallel permittivity  $\epsilon_z$  indeed has a very different role compared to the other two. In the limit of small  $n_-$  for example the easiest approximation would be  $\gamma = n_+ \gamma_{\text{vac}}$ , i.e. an average without  $\epsilon_z$ .

**Arbitrary dipole alignment** So far we have only considered a dipole which points exactly along one of the principal axes of the medium. In order to get a general expression we first need to deal with the term  $|\mathbf{d} \cdot \mathbf{e}_{\mathbf{k}\lambda}|^2$ , which may include cross-terms. If we take a closer look at the polarization vectors in Eq. (3.56), we see that, again, the product of two different components  $i$  and  $j$  of an eigenvector is antisymmetric in both  $k_i$  and  $k_j$ :  $\mathbf{e}_{\mathbf{k}1}$  does not have any asymmetric parts,  $\mathbf{e}_{\mathbf{k}2} \propto k_1 k_2$  and  $\mathbf{e}_{\mathbf{k}3} \propto k_1 k_3$  for both modes. Therefore, all cross-terms cancel out over symmetric integration domains and we can simply write the emission rate for arbitrary dipole

alignment as the sum of the three dipole component contributions,

$$\gamma = \frac{1}{d^2} (d_x^2 \gamma_{\parallel \varepsilon_x} + d_y^2 \gamma_{\parallel \varepsilon_y} + d_z^2 \gamma_{\parallel \varepsilon_z}), \quad (3.68)$$

with  $\gamma_{\parallel \varepsilon_i}$  being the emission rate for the same dipole if it was aligned to the principal axis of  $\varepsilon_i$ .

### 3.2.3 Local Field effects

So far we derived a purely macroscopic theory. However, as we have seen in section 1.7, microscopic elements like dipoles indeed feel the locally acting microscopic field rather than the averaged macroscopic field. In isotropic media for example, the local field correction to the spontaneous emission rate is given by

$$\gamma_{\text{loc}} = L^2 \gamma \quad (3.69)$$

where  $L$  is the local field factor defined by  $\mathbf{E}_{\text{loc}} = L\mathbf{E}$ , the form of which depends on the model used.

In anisotropic media, we must assume that the correction will also depend on the direction of the electric field. Independently of the local field model, a general ansatz would be a correction tensor of the form

$$\mathbf{E}_{\text{loc}} = \underline{\underline{L}}\mathbf{E}. \quad (3.70)$$

We will not focus on the model to use and on the exact form of the correction here, as other works have covered this topic already, see for example [16, 20–22, 71] to name a few.

We will instead show how any local field correction can be incorporated into the expressions for the spontaneous emission rate, as long as the effects are linear in the electric field:

For a tensor-valued correction, the  $|\mathbf{d} \cdot \mathbf{E}|^2$  term in the integral needs to be replaced by  $|\mathbf{d} \cdot \underline{\underline{L}}\mathbf{E}|^2 = |\sum d_i L_{ij} E_j|^2$ . Instead of solving the integral again for this new corrected field, we let  $\underline{\underline{L}}$  act on the dipole vector to its left,  $|(\mathbf{d}^T \underline{\underline{L}})\mathbf{E}|^2 \equiv |\tilde{\mathbf{d}} \cdot \mathbf{E}|^2$  and plug the adjusted dipole vector  $\tilde{\mathbf{d}} = \underline{\underline{L}}^T \mathbf{d}$  into the previously obtained solutions.

For a local field correction represented by a diagonal matrix  $L_{ij} = \delta_{ij}L_i$  which does not depend on the wave vector, we obtain the new expressions for the corrected spontaneous emission rate

$$\gamma_{\text{loc}} = \frac{\omega_A^3 \mu_0^{3/2}}{3\pi\hbar} \left( \frac{\varepsilon_1 + 3\varepsilon_2}{4\sqrt{\varepsilon_2}} L_2^2 d_2^2 + \sqrt{\varepsilon_2} L_1^2 d_1^2 \right) \quad (3.71)$$

in uniaxial, and

$$\gamma_{\text{loc}} = \frac{1}{d^2} (d_x^2 L_1^2 \gamma_{\parallel \varepsilon_x} + d_y^2 L_2^2 \gamma_{\parallel \varepsilon_y} + d_z^2 L_3^2 \gamma_{\parallel \varepsilon_z}) \quad (3.72)$$

in biaxial media. As in this case the correction is a scalar factor for every dipole component, we don't expect any qualitative difference in the efficiency or accuracy of our model.

To conclude, we have developed a model to approximate the emission rate of an electric dipole in a biaxial dielectric medium with a closed analytic expression which holds for a wide range of medium configurations and is easily adjustable according to local field models. The advantage of our analytic form is that it is not only a better approximation than the average refractive index, but also holds the potential for qualitative studies of the dependency of the emission rate on each of the permittivities and the interplay between them. We expect that this will prove useful in designing novel media or choosing tailored materials for specific applications.

### 3.3 Magnetic generalization

We now want to include magnetic effects into our treatment of anisotropic media. First we extend the general theory to anisotropic magnetodielectrics, that is, materials for which both the permeability and the permittivity are described by a matrix quantity which is not the identity. Later we will calculate an expression for the emission rate of magnetic dipoles in a special uniaxial magnetodielectric medium and compare it to the electric dipole.

#### 3.3.1 Waves in general anisotropic magnetodielectrics

The wave equation to solve for the electric field now reads

$$\mathbf{k} \times \underline{\underline{\mu}}^{-1}(\mathbf{k} \times \mathbf{E}_{\mathbf{k}}) = -\omega_{\mathbf{k}}^2 \underline{\underline{\varepsilon}} \mathbf{E}_{\mathbf{k}}, \quad (3.73)$$

where we have used again the expansion of the electric field into plane waves,

$$\mathbf{E}(r, t) = \int d^3\mathbf{k} \mathbf{E}_{\mathbf{k}} e^{i(\mathbf{k}\mathbf{r} - \omega_{\mathbf{k}}t)}. \quad (3.74)$$

Despite it being more complicated we can still formulate the wave equation as an eigenvalue problem of a new matrix  $\underline{\underline{M}}$  which represents the operation

$$\underline{\underline{M}} \cdot = \underline{\underline{\varepsilon}}^{-1} \left( \mathbf{k} \times \underline{\underline{\mu}}^{-1}(\mathbf{k} \times \cdot) \right). \quad (3.75)$$

For a medium in which  $\underline{\underline{\varepsilon}}$  and  $\underline{\underline{\mu}}$  are diagonal in the same basis (this is not necessarily always the case, but a reasonable assumption), we can write  $\underline{\underline{M}}$  in that basis as

$$M_{ij} = \frac{1}{|\mu| \varepsilon_i} \left( \left( \mathbf{k} \cdot \underline{\underline{\mu}} \mathbf{k} \right) \mu_i \delta_{ij} - k_i k_j \mu_i \mu_j \right) \quad (3.76)$$

with  $|\mu| = \det \underline{\underline{\mu}} = \mu_1 \mu_2 \mu_3$  and  $\mu_i(\varepsilon_i)$  being the diagonal entries  $\mu_{ii}(\varepsilon_{ii})$ . Even if the electric and magnetic principal axes are not the same,  $\underline{\underline{M}}$  still has well-defined entries which can be found by inverting the permeability or permittivity matrix. The solutions of this problem have similar properties as for the purely dielectric medium. In section 3.1, we have already shown that (1.) there are no more than two non-trivial solutions (with eigenvalues  $\neq 0$ ), (2.) the problem is entirely symmetric between forward and backward propagation of waves,  $\omega_{\mathbf{k},\lambda} = \omega_{-\mathbf{k},\lambda}$ ,  $\mathbf{E}_{\mathbf{k},\lambda} \parallel \mathbf{E}_{-\mathbf{k},\lambda}$ , and (3.) all eigenvectors, including the trivial solution  $\mathbf{k}$ , are mutually orthogonal with respect to the metric given by an inner product with  $\underline{\underline{\varepsilon}}$ , i.e.  $\mathbf{E}_{\mathbf{k},\lambda} \cdot (\underline{\underline{\varepsilon}} \mathbf{E}_{\mathbf{k},\lambda'}) = 0$  for  $\omega_{\mathbf{k},\lambda} \neq \omega_{\mathbf{k},\lambda'}$ . These are still valid in the magnetodielectric case, the proofs follow exactly the same line. Furthermore we now add the modified statement (4.)

$$(\mathbf{k} \times \mathbf{E}_{\mathbf{k},\lambda}) \cdot \underline{\underline{\mu}}^{-1}(\mathbf{k} \times \mathbf{E}_{\mathbf{k},\lambda'}) = -\omega_{\mathbf{k},\lambda} \omega_{\mathbf{k},\lambda'} \mathbf{E}_{\mathbf{k},\lambda} \cdot (\underline{\underline{\varepsilon}} \mathbf{E}_{\mathbf{k},\lambda'}), \quad (3.77)$$

which is the correct form to represent  $\mathbf{H}_{\mathbf{k},\lambda} \cdot \mathbf{B}_{\mathbf{k},\lambda'} = \mathbf{E}_{\mathbf{k},\lambda} \cdot \mathbf{D}_{\mathbf{k},\lambda'}$  in a magnetodielectric medium. The proof of this can be deduced from the dielectric case using  $\mathbf{E}_{\mathbf{k},\lambda'} \cdot (\mathbf{k} \times$

$\underline{\underline{\mu}}^{-1}(\mathbf{k} \times \mathbf{E}_{\mathbf{k},\lambda}) = (\mathbf{k} \times \mathbf{E}_{\mathbf{k},\lambda}) \cdot \underline{\underline{\mu}}^{-1}(\mathbf{k} \times \mathbf{E}_{\mathbf{k},\lambda'})$ . With this, the electric field quantization introduced in section 3.1 for dielectric media remains valid, and the quantized version of the magnetic fields follows straightforwardly from Maxwell's equations. We thus write the field operators in the form

$$\hat{\mathbf{E}}(\mathbf{r}, t) = \int d^3\mathbf{k} \sum_{\lambda} \mathbf{e}_{\mathbf{k}\lambda} \hat{u}_{\mathbf{k},\lambda}(\mathbf{r}, t) \quad (3.78)$$

$$\hat{\mathbf{D}}(\mathbf{r}, t) = \int d^3\mathbf{k} \sum_{\lambda} \underline{\underline{\varepsilon}} \mathbf{e}_{\mathbf{k}\lambda} \hat{u}_{\mathbf{k},\lambda}(\mathbf{r}, t) \quad (3.79)$$

$$\hat{\mathbf{B}}(\mathbf{r}, t) = \int d^3\mathbf{k} \sum_{\lambda} \frac{-1}{\omega_{\mathbf{k},\lambda}} \mathbf{k} \times \mathbf{e}_{\mathbf{k}\lambda} \hat{u}_{\mathbf{k},\lambda}(\mathbf{r}, t) \quad (3.80)$$

$$\hat{\mathbf{H}}(\mathbf{r}, t) = \int d^3\mathbf{k} \sum_{\lambda} \frac{-1}{\omega_{\mathbf{k},\lambda}} \underline{\underline{\mu}}^{-1}(\mathbf{k} \times \mathbf{e}_{\mathbf{k}\lambda}) \hat{u}_{\mathbf{k},\lambda}(\mathbf{r}, t) \quad (3.81)$$

with  $\mathbf{e}_{\mathbf{k}\lambda} = \mathbf{E}_{\mathbf{k}\lambda}/|\mathbf{E}_{\mathbf{k}\lambda}|$  being the normalized eigenvectors of the adjusted matrix  $\underline{\underline{M}}$  and

$$\hat{u}_{\mathbf{k},\lambda}(\mathbf{r}, t) = \sqrt{\frac{\hbar\omega_{\mathbf{k},\lambda}}{16\pi^3 \mathbf{e}_{\mathbf{k}\lambda} \cdot \underline{\underline{\varepsilon}} \mathbf{e}_{\mathbf{k}\lambda}}} \times \quad (3.82)$$

$$\left( \hat{a}_{\mathbf{k}\lambda} e^{i(\mathbf{k}\cdot\mathbf{r} - \omega_{\mathbf{k},\lambda}t)} + \hat{a}_{\mathbf{k}\lambda}^{\dagger} e^{-i(\mathbf{k}\cdot\mathbf{r} - \omega_{\mathbf{k},\lambda}t)} \right) \quad (3.83)$$

staying the same, so that the field Hamiltonian takes the diagonal form

$$H = \frac{1}{2} \int d^3r \left[ \hat{\mathbf{E}}(\mathbf{r}, t) \cdot \hat{\mathbf{D}}(\mathbf{r}, t) + \hat{\mathbf{H}}(\mathbf{r}, t) \cdot \hat{\mathbf{B}}(\mathbf{r}, t) \right] \quad (3.84)$$

$$= \int d^3\mathbf{k} \sum_{\lambda} \hbar\omega_{\mathbf{k}\lambda} \left( \hat{a}_{\mathbf{k}\lambda}^{\dagger} \hat{a}_{\mathbf{k}\lambda} + \frac{1}{2} \right) \quad (3.85)$$

again. Note that the dependency of the pre-factor of  $\hat{u}_{\mathbf{k},\lambda}$  on the projection of  $\underline{\underline{\varepsilon}}$  onto the electric field direction is an arbitrary choice, and could equivalently be written as the projection of  $\underline{\underline{\mu}}$  to the direction of the magnetic field  $\mathbf{H}$ , keeping in mind that  $\mathbf{H}_{\mathbf{k},\lambda} \cdot \mathbf{B}_{\mathbf{k},\lambda} = \mathbf{E}_{\mathbf{k},\lambda} \cdot \mathbf{D}_{\mathbf{k},\lambda}$ .

### 3.3.2 Solutions in uniaxial magnetodielectrics

We now consider a uniaxial medium in which the magnetic and electric anisotropy axes are aligned, so that we can write  $\underline{\underline{\varepsilon}} = \text{diag}(\varepsilon_1, \varepsilon_2, \varepsilon_2)$  and  $\underline{\underline{\mu}} = \text{diag}(\mu_1, \mu_2, \mu_2)$ . Interestingly, the electric polarization vectors are the same as in the dielectric, the magnetic anisotropy only affects the orientation of the magnetic field in this case,

$$\mathbf{e}_{\mathbf{k},\text{TE}} \propto \begin{pmatrix} 0 \\ -k_3 \\ k_2 \end{pmatrix}, \quad \mathbf{e}_{\mathbf{k},\text{TM}} \propto \begin{pmatrix} -\varepsilon_2(k_2^2 + k_3^2) \\ \varepsilon_1 k_1 k_2 \\ \varepsilon_1 k_1 k_3 \end{pmatrix}. \quad (3.86)$$

To compare, the magnetic field polarization vectors  $\mathbf{h}_{\mathbf{k},\lambda} = \underline{\underline{\mu}}^{-1}(\mathbf{k} \times \mathbf{e}_{\mathbf{k},\lambda})$  (apart from constant prefactors) can be written as

$$\mathbf{h}_{\mathbf{k},\text{TE}} \propto \begin{pmatrix} -\mu_2(k_2^2 + k_3^2) \\ \mu_1 k_1 k_2 \\ \mu_1 k_1 k_3 \end{pmatrix}, \quad \mathbf{h}_{\mathbf{k},\text{TM}} \propto \begin{pmatrix} 0 \\ -k_3 \\ k_2 \end{pmatrix}. \quad (3.87)$$

The corresponding frequencies are

$$\omega_{\mathbf{k},\text{TE}} = \frac{ck}{n_{\text{TE}}} = \sqrt{\frac{\boldsymbol{\kappa} \cdot \underline{\underline{\mu}} \boldsymbol{\kappa}}{\varepsilon_2 \mu_1 \mu_2}} k, \quad (3.88)$$

$$\omega_{\mathbf{k},\text{TM}} = \frac{ck}{n_{\text{TM}}} = \sqrt{\frac{\boldsymbol{\kappa} \cdot \underline{\underline{\varepsilon}} \boldsymbol{\kappa}}{\mu_2 \varepsilon_1 \varepsilon_2}} k \quad (3.89)$$

with  $\boldsymbol{\kappa} = \mathbf{k}/k$ . We can see that, in contrast to uniaxial dielectrics, we do not have an ordinary and an extraordinary wave anymore, as the frequency now always depends on the propagation direction. Instead, we can identify a transverse electric (TE) mode, for which only the electric field is orthogonal to the wavevector, and a transverse magnetic (TM) mode, in which only the magnetic field is. Similarly, for the TE mode, the dispersion relation depends only on the alignment of  $\mathbf{k}$  with respect to  $\underline{\underline{\mu}}$ , while the TM mode has the equivalent dependency on  $\underline{\underline{\varepsilon}}$ . In the dielectric limit the TE mode reduces to an ordinary wave just like for a purely magnetic material the TM mode would behave like an ordinary wave. We note that this is fully symmetric with respect to the electromagnetic duality.

### 3.3.3 Electric dipole radiation

We can now calculate the spontaneous emission rate of an electric dipole  $\mathbf{d} = (d_1, d_2, 0)$  like in the dielectric case by inserting these solutions into

$$\gamma = \frac{\omega_A^3}{8\hbar\pi^2} \int \sin\theta d\varphi d\theta \sum_{\lambda} \left(\frac{n_{\lambda}}{c}\right)^3 \frac{|\mathbf{d} \cdot \mathbf{e}_{\mathbf{k}\lambda}|^2}{\mathbf{e}_{\mathbf{k}\lambda} \cdot \underline{\underline{\varepsilon}} \mathbf{e}_{\mathbf{k}\lambda}}. \quad (3.90)$$

Solving the remaining integrals yields a contribution from TM waves

$$\gamma_{\text{TM}} = \frac{\omega_A^3}{3\pi\hbar} \mu_2^{3/2} \frac{d_2^2 \varepsilon_1 + 4d_1^2 \varepsilon_2}{4\sqrt{\varepsilon_2}} \quad (3.91)$$

and from TE waves

$$\gamma_{\text{TE}} = \frac{d_2^2 \omega_A^3}{4\pi\hbar} \sqrt{\varepsilon_2 \mu_2} \mu_1. \quad (3.92)$$

For the TM waves the result is the same as for a scalar permeability of  $\mu_2$ , as there are only magnetic fields in the (y,z) plane involved. Hence, the emission rate of a dipole aligned with the anisotropy axis still only depends on the medium properties in the plane orthogonal to that axis,  $\gamma_{\parallel} \propto \mu_2^{3/2} \varepsilon_2^{1/2}$ . We can write the total emission rate as

$$\gamma = \frac{\omega_A^3}{3\pi\hbar} \sqrt{\frac{\mu_2}{\varepsilon_2}} \left( d_1^2 \varepsilon_2 \mu_2 + d_2^2 \left( \frac{3}{4} \mu_1 \varepsilon_2 + \frac{1}{4} \mu_2 \varepsilon_1 \right) \right) \quad (3.93)$$

from which we deduce that for random dipole alignment, the average emission rate

$$\gamma_{\text{avg}} \propto \sqrt{\frac{\mu_2}{\varepsilon_2}} \left( \frac{1}{3} \varepsilon_2 \mu_2 + \frac{1}{2} \mu_1 \varepsilon_2 + \frac{1}{6} \mu_2 \varepsilon_1 \right) \quad (3.94)$$

has terms depending on  $\mu_1$  with a relative factor of 1/2 while  $\varepsilon_1$  occurs only with a weight of 1/6.

### 3.3.4 Magnetic dipole radiation

We now calculate the spontaneous emission rate for a magnetic dipole  $\mathbf{m} = (m_1, m_2, 0)$  in the anisotropic magnetodielectric, using Fermi's golden rule, assuming an interaction energy  $\mu_0 \hat{\mathbf{m}} \cdot \hat{\mathbf{H}}$ . We note that indeed this might not be the exact form of the coupling of the dipole to the field, but in analogy to the electric coupling, this would be the basis for calculations taking local field effects into account. The spontaneous

emission rate thus can be calculated from

$$\begin{aligned}\gamma &= \frac{2\pi}{\hbar^2} \sum_f |\langle f | \mu_0 \hat{\mathbf{m}} \cdot \hat{\mathbf{H}} | 0 \rangle|^2 \delta(\omega_{\mathbf{k}\lambda} - \omega_A) \\ &= \frac{\mu_0^2}{8\hbar\pi^2} \int d^3\mathbf{k} \sum_\lambda \frac{\left| \mathbf{m} \cdot \underline{\underline{\mu}}^{-1}(\mathbf{e}_{\mathbf{k}\lambda} \times \mathbf{k}) \right|^2}{\omega_{\mathbf{k},\lambda} \mathbf{e}_{\mathbf{k}\lambda} \cdot \underline{\underline{\varepsilon}} \mathbf{e}_{\mathbf{k}\lambda}} \delta(\omega_{\mathbf{k}\lambda} - \omega_A)\end{aligned}\quad (3.95)$$

$$= \frac{\omega_A^3 \mu_0^2}{8\hbar\pi^2} \int \sum_\lambda \left(\frac{n_\lambda}{c}\right)^5 \frac{\left| \mathbf{m} \cdot \underline{\underline{\mu}}^{-1}(\mathbf{e}_{\mathbf{k}\lambda} \times \boldsymbol{\kappa}) \right|^2}{\mathbf{e}_{\mathbf{k}\lambda} \cdot \underline{\underline{\varepsilon}} \mathbf{e}_{\mathbf{k}\lambda}} \sin\theta d\varphi d\theta. \quad (3.96)$$

Note that for the sake of symmetry we can also write this entirely in terms of the magnetic polarization vectors,

$$\gamma = \frac{\omega_A^3 \mu_0^2}{8\hbar\pi^2} \int \sum_\lambda \left(\frac{n_\lambda}{c}\right)^3 \frac{|\mathbf{m} \cdot \mathbf{h}_{\mathbf{k}\lambda}|^2}{\mathbf{h}_{\mathbf{k}\lambda} \cdot \underline{\underline{\mu}} \mathbf{h}_{\mathbf{k}\lambda}} \sin\theta d\varphi d\theta \quad (3.97)$$

We see that this is in complete analogy to the electric dipole emission rate, and by inserting the solutions from section 3.3.2, we consequently obtain a total emission rate of

$$\gamma = \frac{\omega_A^3 \mu_0^2}{3\pi\hbar} \sqrt{\frac{\varepsilon_2}{\mu_2}} \left( m_1^2 \mu_2 \varepsilon_2 + m_2^2 \left( \frac{3}{4} \varepsilon_1 \mu_2 + \frac{1}{4} \varepsilon_2 \mu_1 \right) \right). \quad (3.98)$$

In the case of an isotropic medium, this reduces to the known form of the magnetic dipole emission rate

$$\gamma_{\text{iso}} = \frac{\omega_A^3 \mu_0^2 m^2}{3\pi\hbar} \sqrt{\mu \varepsilon^3} \quad (3.99)$$

which corresponds to a Purcell enhancement of  $n\varepsilon$ . For the case of a weakly magnetic material, we can also take the approximation of  $\mu_i = \mu_0$  which would lead to an emission rate

$$\gamma_{\text{diel}} = \frac{\omega_A^3 \mu_0^2}{3\pi\hbar} \sqrt{\varepsilon_2 \mu_0} \left( m_1^2 \varepsilon_2 + m_2^2 \left( \frac{3}{4} \varepsilon_1 + \frac{1}{4} \varepsilon_2 \right) \right) \quad (3.100)$$

of a magnetic dipole embedded in a dielectric host.

In comparison of the emission rates of magnetic and electric dipoles, these results confirm the duality of the fields  $\mathbf{E}$  and  $\mathbf{H}$ , with replacements of  $\varepsilon$  to  $\mu$ , and of  $\mathbf{d}$  to  $\mu_0 \mathbf{m}$  being made. Just like for the electric dipole, the results vary significantly

from the rate obtained when considering an isotropic medium of averaged refractive index. This is true even for magnetic dipoles in purely dielectric media.

# Chapter 4

## Dipole emission in absorbing magnetodielectrics

In this chapter, we explore the emission properties of electric and magnetic dipoles in absorbing media, i.e. we derive the spontaneous emission rate for materials in which both the permittivity  $\varepsilon$  and the permeability  $\mu$  may take non-vanishing complex values. As there are losses to other degrees of freedom in the system, we cannot simply use a quantized field description as in chapter 3, such operators would not be valid quantum operators anymore. This becomes very clear when considering the Hamiltonian of the electromagnetic field in such a situation. The energy stored in the field alone is not conserved, and such a Hamiltonian would not be Hermitian and would lead to a non-unitary time evolution. In order to fully quantize the field variables in a lossy medium one must also include the medium excitations to restore overall energy conservation [72]. One could in principle use these new operators for the coupled system and calculate the rate of spontaneous emission to such joint excitations. However, we instead choose the more straightforward approach of using the Green's function method introduced in section 1.6 to obtain the emission rate from the classically derived Green's function of the system. With this method, the emission properties of electric dipoles in absorbing dielectrics have been successfully derived in previous works [39, 73, 74].

## 4.1 Electric Dipoles

While the Green's function in dielectric media has received a lot of attention in research, the more general case of magnetodielectric media has been less investigated. Especially the case of absorbing materials has so far not been covered in sufficient detail. In the following we give the most general expression for the Green's function of media with arbitrary, complex values of both the permittivity  $\varepsilon$  and the permeability  $\mu$ .

We could in principle derive the emission rate of electric dipoles from the Greens function of the vector potential  $\mathbf{A}$  as sketched in section 1.6.3. However, as we later want to make a connection to the magnetic field and its Green's function, it is preferable to use the Green's function of the electric field  $\mathbf{E}$  here which, as is shown in appendix A, differs from the vector potential Green's function only by a factor of  $-\omega^2$ .

We first split the displacement field into two components,

$$\mathbf{D} = \varepsilon \mathbf{E} + \mathbf{P}_N \quad (4.1)$$

where  $\mathbf{P}_N$  is the noise polarization which includes any part of the polarization field which is not proportional to  $\mathbf{E}$ . It has been shown [72] that in a quantum theory of absorbing media the displacement field  $\mathbf{D}$  can no longer be exactly proportional to  $\mathbf{E}$  while satisfying the fluctuation-dissipation theorem, and introducing the noise polarization is a way of including these additional fluctuations.

In our case the noise polarization simply takes the role of the dipole of interest, i.e. the source of the electric field. The wave equation in frequency space then reads

$$\nabla \times \nabla \times \mathbf{E} = -\mu\varepsilon\omega^2 \mathbf{E} + \mu\omega^2 \mathbf{P}_N. \quad (4.2)$$

For the transverse part of the electric field we rewrite this to the inhomogeneous differential equation

$$(\nabla^2 + \omega^2\mu\varepsilon) \mathbf{E}^T = \mu\omega^2 \mathbf{P}_N^T. \quad (4.3)$$

The longitudinal part has been studied in detail for dielectrics for example in [73]. As it has no dependency on  $\mu$  even in magnetodielectric media, no new results will arise by a more general treatment and therefore we restrict this work to the transverse

fields.

We treat the noise polarization  $\mathbf{P}_N$  as the source of the electric field  $\mathbf{E}$ , so want the Green's function to be the solution of

$$(\nabla^2 + \omega^2 \mu \varepsilon) G_{ij}(\omega, \mathbf{r}, \mathbf{r}') = \mu \omega^2 \delta_{ij}^T(\mathbf{r} - \mathbf{r}') \quad (4.4)$$

where  $\delta_{ij}^T(\mathbf{r})$  is the transverse delta-function which ensures we pick only the transverse component of  $\mathbf{P}_N$ . With this Green's function, the averaged electric field arising from equation 1.133 will now solve our wave equation. Note that replacing  $\delta \langle \hat{E}_i(\omega, \mathbf{r}) \rangle$  by  $E_i$  is valid here since the classical Maxwell's equations in media already describe macroscopic averaged field variables, and the mean value without any sources is always zero [10].

We can solve equation 4.4 in Fourier space by using the integral representation of the transverse delta function,

$$\delta_{ij}^T(\mathbf{r}) = \frac{1}{(2\pi)^3} \int d^3 \mathbf{k} \left( \delta_{ij} - \frac{k_i k_j}{k^2} \right) e^{i\mathbf{k}\mathbf{r}}, \quad (4.5)$$

so that

$$(-k^2 + \omega^2 \mu \varepsilon) G_{ij}(\omega, \mathbf{k}) = \mu \omega^2 \left( \delta_{ij} - \frac{k_i k_j}{k^2} \right). \quad (4.6)$$

One should mention that due to the symmetry of the problem, the Green's function does not depend on the individual positions but only on the vector translating between them,  $G_{ij}(\omega, \mathbf{r}, \mathbf{r}') = G_{ij}(\omega, \mathbf{r} - \mathbf{r}')$ . We thus calculate the Green's function of the relative coordinate  $\mathbf{R} = \mathbf{r} - \mathbf{r}'$  from the Fourier transform

$$G_{ij}(\omega, \mathbf{R}) = \frac{1}{(2\pi)^3} \int d^3 \mathbf{k} G_{ij}(\omega, \mathbf{k}) e^{i\mathbf{k}\mathbf{R}} \quad (4.7)$$

with

$$G_{ij}(\omega, \mathbf{k}) = -\mu \omega^2 \frac{\delta_{ij} - \frac{k_i k_j}{k^2}}{\omega^2 \mu \varepsilon - k^2}. \quad (4.8)$$

Solving the resulting integral is a rather tricky task. We closely follow the procedure used in [73] for dielectrics for the following derivation. We express equation 4.8 in

terms of a spatial derivative of the exponential function in the Fourier transform,

$$-\left(\delta_{ij} - \frac{k_i k_j}{k^2}\right) e^{i\mathbf{k}\mathbf{R}} = \frac{1}{k^2} (\partial_i \partial_j - \delta_{ij} \nabla^2) e^{i\mathbf{k}\mathbf{R}} \quad (4.9)$$

and solve the remaining integral after pulling out the derivatives,

$$G_{ij}(\omega, \mathbf{R}) = \frac{\mu\omega^2}{(2\pi)^3} (\partial_i \partial_j - \delta_{ij} \nabla^2) \int d^3\mathbf{k} \frac{e^{i\mathbf{k}\mathbf{R}}}{k^2 (\omega^2 \mu \varepsilon - k^2)} \quad (4.10)$$

$$-\frac{1}{4\pi\varepsilon} (\partial_i \partial_j - \delta_{ij} \nabla^2) \frac{1}{R} (e^{i\sqrt{\varepsilon\mu}\omega R} - 1) \quad (4.11)$$

$$= -\frac{1}{4\pi\varepsilon} \left( \frac{2}{3} i (\sqrt{\varepsilon\mu}\omega)^3 \delta_{ij} + \frac{1}{2} \varepsilon\mu\omega^2 \left( \frac{\delta_{ij}}{R} + \frac{R_i R_j}{R^3} \right) + \mathcal{O}(R) \right) \quad (4.12)$$

where in the last step we are omitting higher-order terms in  $R$  as we are only interested in the solution at  $\mathbf{R} = 0$ .

For real values of  $\varepsilon$  and  $\mu$ , the calculation of the spontaneous emission rate of electric dipoles from equation 4.12 is straightforward as we only need to take into account the first, explicitly imaginary term,

$$\text{Im } G_{ij}(\omega, \mathbf{R} = 0) = -\frac{1}{6\pi\varepsilon\omega^2} (\sqrt{\varepsilon\mu}\omega)^3 \delta_{ij}, \quad (4.13)$$

and we get<sup>1</sup>

$$\begin{aligned} \gamma &= -\frac{2d_i d_j}{\hbar} \text{Im } G_{ij}(\omega_A, \mathbf{R} = 0) \\ &= \frac{d^2}{3\pi\hbar\varepsilon} (\sqrt{\varepsilon\mu}\omega_A)^3 \\ &= \frac{d^2 \omega_A^3}{3\pi\hbar c^3 \varepsilon_0} \frac{n^3}{\varepsilon_r} \end{aligned} \quad (4.14)$$

Comparing with equation 1.98, we see that this differs from the free-space emission rate by the constant factor  $\gamma = \frac{n^3}{\varepsilon_r} \gamma_{vac} = n\mu_r \gamma_{vac}$  which is in agreement with literature [40, 41] and the rate we derived in section 1.5.2 using Fermi's golden rule.

If we want to allow values for  $\varepsilon$  or  $\mu$  with non-vanishing imaginary parts, greater

---

<sup>1</sup>In comparison to section 1.6.4 we note the missing  $-\omega^2$  as this is the Green's function for the electric field instead of the vector potential, and  $\langle \hat{E}_i \hat{E}_j \rangle = -\omega^2 \langle \hat{A}_i \hat{A}_j \rangle$  which is compensated by the different form of the Green's function.

care needs to be taken. In particular, complex values of  $\mu$  will give rise to a divergency of the imaginary part of the Green's function at  $\mathbf{R} = 0$  due to the second term in equation 4.12. This is a result of the macroscopic model being used in combination with a microscopic point dipole, rather than an actual physical phenomenon. A similar problem appears in the calculation of longitudinal emission rates already for imaginary values of  $\varepsilon$  [39, 73]. One way of avoiding the singularities and at least obtaining a qualitative expression is to introduce a high-frequency cutoff, or equivalently, averaging the Green's function over a small area around  $\mathbf{R} = 0$ . We do this by a Gaussian smoothing of the form

$$\begin{aligned}\tilde{G}_{ij}(\omega, 0) &= \int dV \int dV' \left(\frac{2}{\rho}\right)^3 e^{-\frac{2\pi}{\rho^2}(r^2+r'^2)} G_{ij}(\omega, \mathbf{r}, \mathbf{r}') \\ &= -\frac{\mu\omega^2}{(\pi\rho)^3} \int dV \int dV' \int d^3\mathbf{k} e^{-\frac{2\pi}{\rho^2}(r^2+r'^2)} \frac{\delta_{ij} - \frac{k_i k_j}{k^2}}{\omega^2 \mu \varepsilon - k^2} e^{i\mathbf{k}(\mathbf{r}-\mathbf{r}')}\end{aligned}$$

where we have used the the  $\mathbf{k}$ -space representation of the Green's function, equation 4.8. This way, we can perform the volume integration already without even having to deal with the exact form of  $G_{ij}(\omega, \mathbf{k})$ ,

$$\int dV \int dV' e^{-\frac{2\pi}{\rho^2}(r^2+r'^2)} e^{i\mathbf{k}(\mathbf{r}-\mathbf{r}')} = \frac{\rho^3}{8} e^{-\frac{k^2 \rho^2}{4\pi}}. \quad (4.15)$$

We are now left with

$$\begin{aligned}\tilde{G}_{ij}(\omega, 0) &= -\frac{\mu\omega^2}{(2\pi)^3} \int d^3\mathbf{k} e^{-\frac{k^2 \rho^2}{4\pi}} \frac{\delta_{ij} - \frac{k_i k_j}{k^2}}{\omega^2 \mu \varepsilon - k^2} \\ &= -\frac{\mu\omega^2 \delta_{ij}}{(2\pi)^3} \int d^3\mathbf{k} e^{-\frac{k^2 \rho^2}{4\pi}} \frac{(1 - \frac{k_i^2}{k^2})}{\omega^2 \mu \varepsilon - k^2} \\ &= -\frac{\mu\omega^2 \delta_{ij}}{3\pi^2} \int dk e^{-\frac{k^2 \rho^2}{4\pi}} \frac{k^2}{\omega^2 \mu \varepsilon - k^2}\end{aligned}$$

where in the second step we have used the fact that the integral is anti-symmetric for  $k_i$  and  $k_j$  if  $i \neq j$ . We want the width of the Gaussian to be small compared to

the wavelength, so we solve the last integral in the limit  $\varepsilon\mu\omega^2\rho^2 \ll 1$  which gives<sup>2</sup>

$$\begin{aligned}\tilde{G}_{ij}(\omega, 0) &\approx -\frac{\mu\omega^2\delta_{ij}}{3\pi} \left( \frac{1}{\rho} + \frac{1}{2}\sqrt{-\varepsilon\mu\omega} \right) \\ &= -\frac{\mu\omega^2\delta_{ij}}{3\pi} \left( \frac{1}{\rho} \pm \frac{i}{2}\sqrt{\varepsilon\mu\omega} \right).\end{aligned}\quad (4.16)$$

The sign in the second line depends on the arguments of  $\varepsilon$  and  $\mu$ , for positive imaginary parts of the refractive index, the square root is positive as well. The spontaneous emission rate follows as

$$\gamma = \frac{d^2\omega_A^3\mu_0}{3\pi\hbar c} \left( \text{Re}(n\mu_r) + 2\frac{c}{\omega_A\rho}\text{Im}(\mu_r) \right).\quad (4.17)$$

The first term of this result is equal to the already known emission rate in lossless media, the second term can be understood as an additional correction due to the medium absorption. It should be noted that there is still an undetermined factor  $\rho$  in this which describes the width of the Gaussian and which, if set to zero, leads to a divergence again.

However, this can still be used as a qualitative result from which we can deduce the scaling of the correction term with  $\varepsilon_r$  and  $\mu_r$ . As a first point, we see that the correction only depends on magnetic losses and one might think that electric losses therefore have no effect on the emission rate. However, this is only true if  $\text{Im}\mu_r = 0$  for which the calculation for the lossless medium gives the correct result again. For complex  $\mu_r$ , the effect of electric losses comes into play in the first term as the imaginary parts of  $\varepsilon_r$  and  $\mu_r$  in combination can still lead to a change of the real part of the product  $n\mu_r$ ,

$$\begin{aligned}\text{Re}\left(\mu_r^{\frac{3}{2}}\varepsilon_r^{\frac{1}{2}}\right) &\equiv \text{Re}\left(|\mu_r|^{\frac{3}{2}}e^{i\frac{3}{2}\phi_\mu}|\varepsilon_r|^{\frac{1}{2}}e^{i\frac{1}{2}\phi_\varepsilon}\right) \\ &= |\mu_r|^{\frac{3}{2}}|\varepsilon_r|^{\frac{1}{2}}\cos\left(\frac{3}{2}\phi_\mu + \frac{1}{2}\phi_\varepsilon\right).\end{aligned}$$

---

<sup>2</sup>For the very interested reader:  
 $\int dk e^{-\frac{k^2\rho^2}{4\pi}} \frac{k^2}{\omega^2\mu\varepsilon - k^2} = \frac{\sqrt{\pi}}{2} \left( \frac{\sqrt{4\pi}}{\rho} + \sqrt{-\varepsilon\mu\pi\omega^2} e^{-\varepsilon\mu\omega^2\rho^2/4\pi} + 2\sqrt{\varepsilon\mu\omega^2} \text{DawsonF}\left(\sqrt{\varepsilon\mu\omega^2\rho^2/4\pi}\right) \right)$   
 with DawsonF being the Dawson integral defined by  $\text{DawsonF}(x) = \exp(-x^2) \int_0^x \exp(y^2) dy$ .

## 4.2 Magnetic Dipoles

In order to calculate the emission rate of magnetic dipoles we need to find the Green's function of the magnetic field. Like before, we assume a coupling of the magnetic dipole to the field  $\mathbf{H}$  to calculate the emission rate to have the best possible approximation and allow for later treatment of local field models equivalent to the electric case.

In a similar manner to the noise polarization discussed earlier, we separate the noise magnetization as<sup>3</sup>

$$\mathbf{B} = \mu\mathbf{H} + \mu_0\mathbf{M}_N \quad (4.18)$$

and can now write the wave equation as

$$\nabla \times \nabla \times \mathbf{H} = -\mu\varepsilon\omega^2\mathbf{H} + \omega^2\varepsilon\mu_0\mathbf{M}_N. \quad (4.19)$$

For the transverse part of the magnetic field we can rewrite this as<sup>4</sup>

$$(\nabla^2 + \omega^2\mu\varepsilon)\mathbf{H}^T = \varepsilon\omega^2\mu_0\mathbf{M}_N^T \quad (4.20)$$

in perfect analogy to the electric field. We can therefore see that the spontaneous emission rate in absorbing media is indeed invariant under dual transformations and the magnetic dipole emission rate is simply obtained from the electric case by making the appropriate replacements, or simply identifying the corresponding elements of each wave equation with each other. We thereby follow the Green's function of the magnetic field  $\mathbf{H}$ ,

$$G_{ij}^{(H)}(\omega, \mathbf{R}) = -\frac{1}{4\pi\mu} \left( \frac{2}{3}i(\sqrt{\varepsilon\mu}\omega)^3\delta_{ij} + \frac{1}{2}\varepsilon\mu\omega^2 \left( \frac{\delta_{ij}}{R} + \frac{R_i R_j}{R^3} \right) + \mathcal{O}(R) \right) \quad (4.21)$$

---

<sup>3</sup>There is some discussion about whether to include the noise magnetization in  $\mathbf{B}$  or  $\mathbf{H}$ , which determines the prefactor of  $\mathbf{M}_N$ . However, this is not expected to make any difference in the final result as a different factor should be compensated by the Green's function, so we will keep to the given form here.

<sup>4</sup>Just like for the electric field, there can be longitudinal magnetic fields as well in specific circumstances. We will not focus on that case in this work, but a quick comparison shows that the longitudinal emission rate can be deduced from the electric case with the same dual symmetry.

yielding the spontaneous emission rate of a magnetic dipole

$$\begin{aligned}\gamma &= -\frac{2\mu_0^2 m_i m_j}{\hbar} \text{Im} G_{ij}^{(H)}(\omega_A, \mathbf{R} = 0) \\ &\approx \frac{m^2 \omega_A^3 \mu_0}{3\pi \hbar c^3} \left( \text{Re}(n\varepsilon_r) + 2\frac{c}{\omega_A \rho} \text{Im}(\varepsilon_r) \right).\end{aligned}$$

Note that the pre-factor  $\mu_0$  has been kept together with the magnetization/dipole moment, i.e. the whole expression  $\mu_0 \mathbf{M}_N^T$  makes the source term, and in the final expression for the emission rate we need  $\mu_0^2 m_i m_j$  in the place of the dipole moment again. Thereby no additional changes are necessary in the Green's function itself, and we have somewhat covered up the historical different definition of the magnetic dipole moment.

Just like the electric dipole emission can be equivalently derived from the vector potential  $\mathbf{A}$ , in which case the electric current is understood as the source of the field, we can also derive the magnetic emission rate from the same vector potential or alternatively, one can even directly derive the Green's function for the magnetic field ( $\mathbf{B}$ ) from the Green's function of the vector potential. Using the Green's function of the  $\mathbf{B}$ -field for the derivation leads to the same result in lossless media, but runs into great trouble when losses come into play, as in that case extra care needs to be taken when choosing the field variables and sources so they still satisfy the fluctuation-dissipation relation. The main difference in the result is the phase of the permeability  $\mu$ <sup>5</sup>. A derivation of the magnetic Green's function from the vector potential together with further discussion of the arising problems can be found in Appendix A.

### 4.3 Local field effects

In section 2.2 we claim that the dipoles in fact couple to the microscopic, local fields instead of the macroscopic, averaged electric or magnetic fields, so we have to adjust our results to a local field theory for absorbing media as well.

It has been shown in [23] that in absorbing media it is no longer sufficient to

---

<sup>5</sup>This is work in progress.

simply include local field effects as

$$\gamma_{\text{loc}} = \left| \frac{\varepsilon_r + 2}{3} \right|^2 \gamma \quad (4.22)$$

to the spontaneous emission rate as would follow from a classical picture. The reason is that this formalism does not take into account the fluctuations of the field operators that are due to the medium absorptions. Instead, one needs to explicitly include the noise polarization or magnetization as part of the total polarization or magnetization,

$$\hat{\mathbf{P}} = \chi_e \hat{\mathbf{E}} + \hat{\mathbf{P}}_N \quad (4.23)$$

$$\hat{\mathbf{M}} = \chi_m \hat{\mathbf{H}} + \hat{\mathbf{M}}_N, \quad (4.24)$$

and start with the local field expression in its original form,

$$\hat{\mathbf{E}}_{\text{loc}} = \hat{\mathbf{E}} + \frac{1}{3} \frac{\hat{\mathbf{P}}}{\varepsilon_0}. \quad (4.25)$$

Separating the noise term then yields

$$\begin{aligned} \hat{\mathbf{E}}_{\text{loc}} &= \hat{\mathbf{E}} + \frac{1}{3}(\varepsilon_r - 1)\hat{\mathbf{E}} + \frac{1}{3} \frac{\hat{\mathbf{P}}_N}{\varepsilon_0} \\ &= \frac{\varepsilon_r + 2}{3} \hat{\mathbf{E}} + \frac{1}{3} \frac{\hat{\mathbf{P}}_N}{\varepsilon_0} \end{aligned} \quad (4.26)$$

and equivalently

$$\hat{\mathbf{H}}_{\text{loc}} = \frac{\mu_r + 2}{3} \hat{\mathbf{H}} + \frac{1}{3} \hat{\mathbf{M}}_N \quad (4.27)$$

for the magnetic field. This means, if we replace the field operators by their local field equivalent, the spontaneous emission rate for an electric dipole<sup>6</sup> now is composed of

---

<sup>6</sup>We restrict calculations to the electric field from here, noting that the local magnetic field is indeed dual to the electric field and thus all results will be.

the commutators

$$\begin{aligned}
 & \left\langle 0 \left| \hat{E}_{\text{loc},i}^\dagger(\mathbf{r}, \omega) \hat{E}_{\text{loc},j}^\dagger(\mathbf{r}', \omega') \right| 0 \right\rangle \\
 &= \frac{\varepsilon(\omega)+2}{3} \frac{\varepsilon^*(\omega')+2}{3} \left\langle 0 \left| \hat{E}_i(\mathbf{r}, \omega) \hat{E}_j^\dagger(\mathbf{r}', \omega') \right| 0 \right\rangle \\
 &+ \frac{1}{9\varepsilon_0^2} \left\langle 0 \left| \hat{P}_{N,i}(\mathbf{r}, \omega) \hat{P}_{N,j}^\dagger(\mathbf{r}', \omega') \right| 0 \right\rangle \\
 &+ \frac{\varepsilon(\omega)+2}{9\varepsilon_0} \left\langle 0 \left| \hat{E}_i(\mathbf{r}, \omega) \hat{P}_{N,j}^\dagger(\mathbf{r}', \omega') \right| 0 \right\rangle \\
 &+ \frac{\varepsilon^*(\omega')+2}{9\varepsilon_0} \left\langle 0 \left| \hat{P}_{N,i}(\mathbf{r}, \omega) \hat{E}_j^\dagger(\mathbf{r}', \omega') \right| 0 \right\rangle.
 \end{aligned} \tag{4.28}$$

The calculation of these additional commutators for magnetodielectrics is the same as in Ref. [23] which was conducted for pure dielectric materials and leads to

$$\begin{aligned}
 \gamma_{\text{loc}} &= \left| \frac{\varepsilon_r + 2}{3} \right|^2 \gamma + \frac{2d_i d_j}{9\hbar\varepsilon_0} \text{Re}(\varepsilon_r) \overline{\delta_{ij} \delta(\boldsymbol{\rho})} \\
 &- \frac{4d_i d_j}{3\hbar\varepsilon_0 c^2} \text{Re}(\varepsilon_r) \text{Re} \left[ \frac{\varepsilon_r + 2}{3} \widetilde{G}_{ij}(\mathbf{0}, \omega_A) \right]
 \end{aligned} \tag{4.29}$$

where the bars indicate the (unphysical) limit of  $\rho \rightarrow 0$ . Just like before, we run into singularities at this point and therefore a small volume average has to be taken.

Even though the form of the equation is the same as in Ref. [23], the result is not the same for magnetodielectrics. The difference to the dielectric lies in the different Green's function of this problem<sup>7</sup> which we shall study in the following. From equation 4.16 we can readily obtain the real part of the last term,

$$\begin{aligned}
 \text{Re} \left[ \frac{\varepsilon_r + 2}{3} \widetilde{G}_{ij}(\mathbf{0}, \omega_A) \right] &= \text{Re} \left[ -\frac{\varepsilon_r + 2}{3} \left( \frac{1}{\rho} + \frac{i}{2c} \sqrt{\varepsilon_r \mu_r} \omega \right) \frac{\mu_0 \mu_r \omega^2 \delta_{ij}}{3\pi} \right] \\
 &= -\frac{\omega^3 \mu_0 \delta_{ij}}{9\pi c} \left[ \frac{c}{\omega \rho} \text{Re}(\varepsilon_r \mu_r + 2\mu_r) + \frac{1}{2} \text{Im}(\sqrt{\varepsilon_r \mu_r}^3 + 2\mu_r \sqrt{\varepsilon_r \mu_r}) \right]
 \end{aligned}$$

Again, we only consider the transverse part, as the longitudinal part does not depend on the magnetic permeability and thus remains unchanged. As we see, even in the local field corrections of the electric field we find an indirect influence of the magnetic permeability, as it changes the vacuum fluctuations of all fields.

Due to the symmetry of the problem, the results for magnetic dipoles follow

---

<sup>7</sup>On comparison to Ref. [23] one should also note that the Green's function is defined as that of the vector potential, so different pre-factors occur.

exactly analogously with the appropriate replacements. The corrected spontaneous emission rate of a magnetic dipole must therefore be

$$\begin{aligned} \gamma_{\text{loc}}^{(\text{mag})} = & \left| \frac{\mu_r + 2}{3} \right|^2 \gamma + \frac{2\mu_0 m_i m_j}{9\hbar} \text{Re}(\mu_r) \overline{\delta_{ij} \delta(\boldsymbol{\rho})} \\ & - \frac{4\mu_0 m_i m_j}{3\hbar c^2} \text{Re}(\mu_r) \text{Re} \left[ \frac{\mu_r + 2}{3} \widetilde{G}_{ij}^{(H)}(\mathbf{0}, \omega_A) \right] \end{aligned} \quad (4.30)$$

with

$$\begin{aligned} \text{Re} \left[ \frac{\mu_r + 2}{3} \widetilde{G}_{ij}^{(H)}(\mathbf{0}, \omega_A) \right] &= \text{Re} \left[ -\frac{\mu_r + 2}{3} \left( \frac{1}{\rho} + \frac{i}{2c} \sqrt{\varepsilon_r \mu_r} \omega \right) \frac{\varepsilon_0 \varepsilon_r \omega^2 \delta_{ij}}{3\pi} \right] \\ &= -\frac{\omega^3 \varepsilon_0 \delta_{ij}}{9\pi c} \left[ \frac{c}{\omega \rho} \text{Re}(\varepsilon_r \mu_r + 2\varepsilon_r) + \frac{1}{2} \text{Im}(\sqrt{\varepsilon_r \mu_r}^3 + 2\varepsilon_r \sqrt{\varepsilon_r \mu_r}) \right], \end{aligned}$$

if we assume our initial model of the noise magnetization to be correct.

# Chapter 5

## Conclusion and outlook

In this part of the thesis, we have studied the interaction of electric and magnetic dipoles with the electromagnetic field in various different situations with a special focus on the magnetic fields in macroscopic media.

We have presented a canonical quantization of the macroscopic field in a general magneto-dielectric anisotropic medium, and from that derived explicit formulas for the spontaneous emission rate of both electric and magnetic dipoles in uniaxial media. In comparison of these two, our results confirm the duality of the fields  $\mathbf{E}$  and  $\mathbf{H}$ , with replacements of  $\varepsilon$  to  $\mu$ , and of  $\mathbf{d}$  to  $\mu_0\mathbf{m}$  being made. The results vary significantly from the emission rate obtained from considering the approximation of an isotropic medium of averaged refractive index. We furthermore presented a model to describe the emission rate of an electric dipole in a biaxial dielectric medium with an analytic form. The advantage is that it is not only a better approximation than the average refractive index, but also bears the potential for qualitative studies of the dependency of the emission rate on each of the permittivities and the interplay between them. This can prove particularly useful in designing novel media or choosing tailored materials for specific applications.

We have furthermore generalized the theory of spontaneous emission including local field effects for both electric and magnetic dipoles using the Green's functions of the fields  $\mathbf{E}$  and  $\mathbf{H}$ . We have used a Gaussian averaging to obtain qualitative results in the regimes where the regular Green's function diverges due to an incompatibility between macroscopic and microscopic models in absorbing media.

We have shown that all our results are fully symmetric with respect to the electro-

magnetic duality and independent of our interpretations of the nature of the different fields  $\mathbf{E}$ ,  $\mathbf{D}$ ,  $\mathbf{B}$  and  $\mathbf{H}$  if we assume a coupling of the dipoles to the respective *local* fields. However, in the magnetic case, we also observed that different results can be obtained depending on which magnetic field is used to derive the emission rate. This difference stresses the importance of the question which fields and sources must be used for a correct and justified treatment. This goes even beyond the calculation of the spontaneous emission rate, questions like the magnetization being a function of  $\mathbf{B}$  or  $\mathbf{H}$  and the relationship of the noise magnetization to the bosonic polariton operators still need a sound and rigorous investigation. This is the matter of ongoing research and will hopefully lead to a deeper insight into the nature of the different field variables in absorbing magnetic media in the future.

## Part II

# Coherence and catalysis in the Jaynes-Cummings model

# Chapter 6

## Introduction

Coherence [75, 76], the property of a system to be in a superposition of different energy eigenstates, is one of the crucial elements of quantum physics. Together with entanglement, it marks the difference from states that can be described by classical theories. Recently, especially the role of coherence in quantum thermodynamics [77, 78] has sparked increasing interest. In the resource theory approach, coherence is described as a resource [79–82] which can enable (at least approximately) non-energy conserving operations which would otherwise be forbidden [81]. The extraction of work using quantum coherence [83] is an idea that has particularly attracted attention.

Even though coherence cannot be created from strictly energy conserving operations, it can be transferred between two systems when they interact, i.e. it can be created in one system at the cost of using it up in another. It was shown in 2014 by Åberg [84] that under certain circumstances, a coherent reservoir can enable a coherence-creating operation on an external system with an accuracy that does not degrade upon use: An observation, which leads to the paradox of the catalytic use of coherence, which is only resolved by taking correlations between the systems into account [85].

While the suggested setup of [84] is in principle physically possible, it requires very artificial conditions, both in terms of the reservoir state and the nature of the interaction. In the work presented in this chapter, which was published in [86], we present an analysis of Åberg’s idea in a more realistic framework: We study the catalytic capacity of the sequential interaction of a coherent state with a series of

two-level atoms through a Jaynes-Cummings Hamiltonian. Being one of the most important models for the interaction of light with atoms, the Jaynes-Cummings interaction presents itself as a natural choice. It allows for a fully quantum mechanical treatment whilst at the same time remaining exactly solvable [87–89], and it is easy to realize experimentally using techniques from cavity quantum electrodynamics [90]. Coherent states are the natural choice for the resource state in such a cavity, given their classical limit and intrinsic robustness. Furthermore, the quantum optical properties of coherent states have been extensively studied, and in the sense of enabling operations, lasers are routinely used to induce quantum operations on the electronic states of trapped atoms and ions [91].

## 6.1 Coherence as a resource

Let us start with a short introduction of the concept of coherence and its relevance as a resource in the framework of quantum thermodynamics. The key idea is that since coherence can be described as a thermodynamic resource it must be consumed as it is used. The word “coherence” is used in a lot of different contexts, in this work by coherence we mean specifically the property of a state being in a quantum superposition of different energy eigenstates, as opposed to a single eigenstate, or a statistical mixture thereof. A good measure [79, 80] of how much coherence a state exhibits is the off-diagonal entries of its density matrix in the energy eigenbasis, which can for example be quantified by the  $l_1$  norm of coherence,

$$C_{l_1}(\hat{\rho}) = \sum_{i \neq j} |\rho_{ij}|. \quad (6.1)$$

A "classical" mixed state would only have entries on the diagonal, so with this definition in mind, we can think of coherence as non-classicality of a state. Another measure, which also remains tractable in infinitely large Hilbert spaces is given by the relative entropy of coherence,

$$C_{\text{ent}}(\hat{\rho}) = S(\hat{\rho}_{\text{diag}}) - S(\hat{\rho}) \quad (6.2)$$

where  $S(\hat{\rho}) = -\text{Tr}(\hat{\rho} \log \hat{\rho})$  is the von-Neumann entropy and  $\hat{\rho}_{\text{diag}} = \sum_i \rho_{ii} |i\rangle \langle i|$  is the density matrix which contains only the diagonal entries of  $\hat{\rho}$ . The relative entropy of coherence thus is the difference in entropy between a quantum state and the corresponding decohered classical state: Reducing the entropy of a classical state without changing its classically obtainable statistics (the diagonal elements) is thus equivalent to increasing its coherence. The “further” away a state is from a classical mixture, the more coherence it exhibits, with the maximal possible coherence always corresponding to a state of zero entropy. Both definitions, although not giving the same number for the same state, work equally well, at least for finite dimensional Hilbert spaces. To properly describe coherence as resource we need the following basic ingredients of resource theories:

**Free states** These are states without any resource value, which should be easy to create. In our case this is incoherent states (energy eigenstates or classical mixtures thereof).

**Free operations** Operations which do not increase the resource, here those are incoherent operations. It can be shown that these are exactly the strictly energy preserving operations, that is, operations that commute with the system Hamiltonian.

**Maximal states** Maximally coherent states, in our case, should be able to allow for the creation of any other quantum state of same dimension with the use of incoherent operations only. A maximal coherent state of dimension  $d$  is for example the equal superposition  $\frac{1}{\sqrt{d}} \sum_i |i\rangle$ .

Both coherence measures we have introduced allow for a treatment as a resource<sup>1</sup> in this framework: They do not increase under incoherent operations, they are zero for incoherent states, and both have their maximal value for maximally coherent states, which are equally weighted coherent superpositions of arbitrary phase.

Now let us see how coherence can enrich the landscape of thermodynamics, which traditionally only deals with statistical mixtures of energy eigenstates. Taking co-

---

<sup>1</sup>One must be careful not to confuse the resource theory of coherence with the thermodynamic resource theory in which coherence is only one type of resource. While in thermodynamics, only Gibbs (thermal) states are considered free, in coherence resource theory all incoherent states, including pure energy eigenstates, are free.

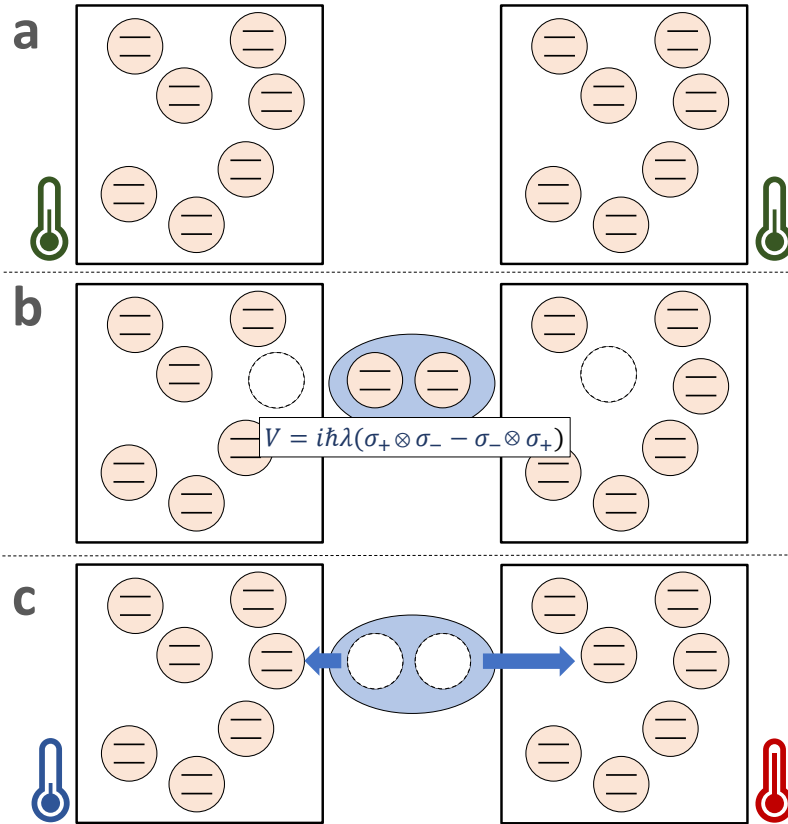


Figure 6.1: Possible energy transfer protocol between two identical reservoirs using coherence. a: The initial state, with both baths having the same energy distributions. b: One atom from each bath is chosen randomly, and allowed to interact via equation 6.3. c: If the atoms are initially in coherent superpositions, then an interaction time can be chosen such that the atom from the right reservoir ends up with more energy than the left, so that the average energy in the right reservoir increases while it decreases on the left. If the atoms are instead described by a statistical mixture, no energy transfer between the reservoirs is possible.

herence into the picture fundamentally changes some of its basic principles, indeed it may fairly be stated that the inclusion of superposition is the principal defining feature of *quantum* thermodynamics [78,92]. In particular, it can be shown that more work can be extracted from a system that exhibits coherence than from an incoherent system with exactly the same energy probability distribution. Let us illustrate this with a simple example. Suppose we have two identical baths of two-level atoms at equal temperature, as shown in Figure 6.1a. One atom from each bath is chosen randomly and interacts with the other via the unitary interaction

$$\hat{V} = i\hbar\lambda(\hat{\sigma}_+ \otimes \hat{\sigma}_- - \hat{\sigma}_- \otimes \hat{\sigma}_+), \quad (6.3)$$

as illustrated in Figure 6.1b. Here,  $\hat{\sigma}_+ = |e\rangle\langle g|$  and  $\hat{\sigma}_- = |g\rangle\langle e|$  are the atomic raising and lowering operators, respectively, so that the interaction mediates an energy exchange between the atoms. If the atoms are in a statistical mixture, as described by the thermal density matrix

$$\rho = \frac{|g\rangle\langle g| + e^{-\beta\omega}|e\rangle\langle e|}{1 + e^{-\beta\omega}}, \quad (6.4)$$

then no energy will flow on *average*, as predicted by classical thermodynamics. If the atoms are returned to their reservoirs and the process is repeated then there will be no net energy exchanged between the reservoirs.

Now let us consider what happens if the atoms are instead in a coherent superposition. We replace the thermal mixture (equation 6.4) with the coherent quantum state

$$|\psi\rangle = \frac{|g\rangle + e^{-\beta\omega/2}|e\rangle}{\sqrt{1 + e^{-\beta\omega}}} \quad (6.5)$$

for each atom in both baths. This system has the same energy probability distribution as the classical thermal states. However, under time evolution of the interaction Hamiltonian  $\hat{V}$ , the two atoms in contact now perform coherent oscillations, so that the joint state of these atoms after time  $t$  is given by

$$|\psi(t)\rangle = \frac{|g\rangle|g\rangle + \sqrt{2}e^{-\beta\omega/2}\left(\cos(\lambda t - \frac{\pi}{4})|g\rangle|e\rangle - \sin(\lambda t - \frac{\pi}{4})|e\rangle|g\rangle\right) + e^{-\beta\omega}|e\rangle|e\rangle}{1 + e^{-\beta\omega}}. \quad (6.6)$$

Knowing the phase of the initial atoms, we can choose an interaction time  $\lambda t_{\max} = \frac{\pi}{4}$  to maximize the amplitude of  $|g\rangle|e\rangle$  compared to the state  $|e\rangle|g\rangle$ , producing the two-atom state

$$|\psi_{\max}\rangle = \frac{|g\rangle|g\rangle + \sqrt{2}e^{-\beta\omega/2}|g\rangle|e\rangle + e^{-\beta\omega}|e\rangle|e\rangle}{1 + e^{-\beta\omega}}. \quad (6.7)$$

Thus the second atom ends up with more energy than the first. When the atoms are returned to their respective reservoirs, the right reservoir gains energy on average (Figure 6.1c). As this process is repeated, energy is steadily extracted from the first reservoir and deposited in the second. Such a setup could then be used, for example, to drive a heat pump, and in this way, work is extracted from the system. This simple example illustrates that the presence of coherence enables operations that would otherwise be thermodynamically forbidden, so that coherence can be exploited as a source of work. In a sense, this is not surprising, as coherence is just another form of knowledge about the system which we can use to extract energy: although the coherent bath has the same energy probability distribution as the incoherent one, it has zero entropy.

As we have seen, coherence fundamentally changes how we have to think about thermodynamics. Its function as a thermodynamic resource from which one can extract work [81, 83, 93, 94] means it is of great importance to study how coherence can be distributed amongst systems, or generated under given constraints.

## 6.2 Catalytic Coherence: Åberg's proposal

In the following, we will briefly discuss the idea of catalytic coherence proposed by Åberg [84]. The original claim in this proposal was that a specific resource state could be used to build up coherence in an unlimited set of two-level atoms (or in general, qubits) in a catalytic manner, that is without degradation of the resource state. The resource state considered in [84] is an infinite-dimensional quantum system in an equally weighted superposition of  $L$  consecutive energy eigenstates

$$|\eta_{L,l_0}\rangle = \frac{1}{\sqrt{L}} \sum_{l=0}^{L-1} e^{il\theta} |l_0 + l\rangle, \quad (6.8)$$

which we will call a Ladder state. For simplicity and without loss of generality we can choose the relative phase  $\theta = 0$ . The interaction of an atom with this reservoir shall perform the operation

$$|e\rangle \rightarrow \hat{U} |e\rangle = \frac{1}{\sqrt{2}}(|e\rangle + |g\rangle) \quad (6.9)$$

on the atom at least approximately, thereby bringing it from an incoherent to a maximally coherent state. This can be realized by an interaction of the form

$$V(U) = \sum_{n,n'=0,1} |n\rangle \langle n| \hat{U} |n'\rangle \langle n'| \otimes \Delta^{n'-n} \quad (6.10)$$

where the first part acts on the Hilbert space of the atom and  $\Delta^k = \sum_j |j+k\rangle \langle j|$  is a shift operator of the reservoir. This interaction will leave the joint atom-reservoir system in the state

$$|\Psi_1\rangle = V(U) |e\rangle \otimes |\eta_{L,l_0}\rangle = \frac{1}{\sqrt{2}} (|g\rangle \otimes \Delta |\eta_{L,l_0}\rangle + |e\rangle \otimes |\eta_{L,l_0}\rangle). \quad (6.11)$$

At first glance this looks like a highly entangled state, however, the two states of the reservoir,  $\Delta |\eta_{L,l_0}\rangle = |\eta_{L,l_0+1}\rangle$  and  $|\eta_{L,l_0}\rangle$  have a large overlap given that the size of the "ladder"  $L$  is large and thus there is not much actual entanglement (i.e. dependence of the atomic state on the state of the cavity or vice versa) present. The reduced density matrix of the atom

$$\rho_A = \text{Tr}_B |\Psi\rangle \langle \Psi| \quad (6.12)$$

can now be described as a mixture of the states  $|+\rangle$  and  $|-\rangle$ ,

$$\rho_A = \left(1 - \frac{1}{2L}\right) |+\rangle \langle +| + \frac{1}{2L} |-\rangle \langle -|. \quad (6.13)$$

For large  $L$ , this is approximately describing the desired (pure) state  $|+\rangle$ : When measured, the atom will be found in  $|+\rangle$  with a probability of

$$P(+)= 1 - \frac{1}{2L} \quad (6.14)$$

Similarly, the reservoir is now described by a mixture of the initial state and another Ladder state with a shifted offset

$$\rho_R = \frac{1}{2} (|\eta_{L,l_0}\rangle \langle \eta_{L,l_0}| + \Delta |\eta_{L,l_0}\rangle \langle \eta_{L,l_0}| \Delta^{-1}). \quad (6.15)$$

The claims of [84] stating a catalytic process are based on the observation that although this is not the same as the initial state, both parts of this mixture work equally well for a subsequent interaction round with another atom, so no knowledge is required of which of the two states the reservoir is in. Thus, without needing to reset the reservoir into its initial state again, one can repeat the interaction with new atoms and thereby (approximately) transform an arbitrary number of them into the desired superposition state.

### 6.3 Correlations

It has been shown [85] that this argument does no longer hold when taking correlations into account. Considering only the reduced density matrices of the atom and the reservoir separately ignores a crucial piece of information: The reservoir after the first interaction is not randomly in one of two Ladder states but rather entangled with the atom. Let us have a closer look at this entanglement: Two physical systems are separable, i.e. without entanglement, if we can write their state vector as a product of the two subsystem state vectors

$$|\Psi_{tot}\rangle = |\psi_1\rangle |\psi_2\rangle, \quad (6.16)$$

and thus both systems have a clearly defined state, independent of each other. In terms of the density matrix this means that the reduced density matrix of each subsystem represents a pure state which can be written as a projector,

$$\rho_i = |\psi_i\rangle \langle \psi_i|. \quad (6.17)$$

After the interaction of the resource with the atom in the above protocol, the two systems are no longer separable. However, the entanglement is very weak which we

can see by writing

$$\begin{aligned} |\Psi\rangle &= \frac{1}{\sqrt{2}} (|g\rangle \otimes \Delta |\eta_{L,l_0}\rangle + |e\rangle \otimes |\eta_{L,l_0}\rangle) \\ &= \frac{1}{\sqrt{2}} \left( |g\rangle \otimes \frac{1}{\sqrt{L}} \sum_{l=0}^{L-1} |l_0 + l + 1\rangle + |e\rangle \otimes \frac{1}{\sqrt{L}} \sum_{l=0}^{L-1} |l_0 + l\rangle \right). \end{aligned}$$

All terms apart from the two edge contributions  $l = l_0$  and  $l = l_0 + L$  in the two sums are the same, so the corresponding part of the superposition can be written as a product,

$$|\Psi\rangle = \frac{1}{\sqrt{2}} \left( |g\rangle \otimes \frac{1}{\sqrt{L}} |l_0 + L\rangle + (|g\rangle + |e\rangle) \frac{1}{\sqrt{L}} \sum_{l=1}^{L-1} |l_0 + l\rangle + |e\rangle \otimes \frac{1}{\sqrt{L}} |l_0\rangle \right). \quad (6.18)$$

For large  $L$ , the sum in the second term is much larger than the two individual terms, which is the reason why in [84] the assumption is made that the state is indeed approximately separable with the atom approximately in the state  $\frac{1}{\sqrt{2}}(|g\rangle + |e\rangle)$ . However, it is exactly this non-separability which is important here. Even when taking into account the possibility for the atom to be not in the desired state as is done with the reduced density matrix in equation 6.13, one ignores the reason for this possibility and its connection to the resource state: Describing a quantum system as a mixed state usually is a means of describing the system despite some lack of information about it. Here, however we do have that information, it is the information about how the atom is entangled to the cavity. If the atom was later measured, this would also have an effect on the reservoir (and all atoms that have interacted with that reservoir afterwards). In particular, if the atom was found in the state  $|-\rangle$ , the reservoir would no longer be in a Ladder state at all but become projected to a simple superposition of two energy levels

$$\langle\Psi_-| = \frac{1}{\sqrt{2}} (|l_0\rangle - |l_0 + L + 1\rangle) \quad (6.19)$$

as all states which were overlapping between the initial and the shifted ladder cancel out now. Such a state has much less coherence left and can't be used for the protocol anymore. The probability for this to happen is very small for big enough

Ladder states but never zero. One further point to note is that our interpretation of the entanglement depends very much on the basis we choose. In equation 6.15 for example, the cavity state is described as a mixture between the cavity state if the atom was in the state  $|g\rangle$  and the cavity if the atom was in the state  $|e\rangle$ . In this basis, it indeed appears like it does not matter which state the cavity actually is in. In other words, if one were to measure the atomic state in its energy basis, the cavity would indeed not be degraded. However, we could just as easily describe the same mixed state as

$$\rho_{\text{R}} = \left(1 - \frac{1}{2L}\right) |\Psi_{+}\rangle \langle\Psi_{+}| + \frac{1}{2L} |\Psi_{-}\rangle \langle\Psi_{-}| \quad (6.20)$$

with  $|\Psi_{\pm}\rangle$  being the state the cavity would be projected to when measuring the atom in the basis of  $|\pm\rangle$ . And then we would see that, while  $|\Psi_{+}\rangle$  is still approximately a ladder state, the state  $\langle\Psi_{-}|$  is far from being a good resource.

It is important to note that it does not matter when the atoms are measured, or even if they are measured at all. Due to the entanglement between all atoms and the reservoir, measuring one of the atoms at any time in the wrong state will corrupt the whole system. And if they are not measured, they are still not in the exact individual superposition states we desired, but in a largely entangled system (the possibility of what would happen if one were to measure is enough to change the nature of the whole system).

If we calculate the coherence of the whole system we also note that the total coherence is not increasing, only the coherence of the subsystems is. We thus see that coherence is not additive between subsystems, at least not if they are entangled with each other. Therefore, the apparent paradox of catalytic coherence is no paradox at all but just a manifestation of this non-additiveness, i.e. Åberg has successfully shown that one can indeed create an arbitrary number of copies of states which exhibit a fixed amount of coherence from one single finite resource, but not that the total coherence of the whole system can be increased to arbitrary values.

Instead of using Ladder states and the idealized interaction described above, in the following we want to investigate the behaviour and robustness of coherent states in a Jaynes-Cummings interaction for the same task.

## 6.4 Variations to the initial protocol

### 6.4.1 Coherent states

Let us first recap the basic properties of coherent states, for more detail or proofs see for example Refs. [95,96].

A coherent state is defined as a superposition of the form

$$|\alpha\rangle = \frac{e^{-|\alpha|^2/2}}{\sqrt{2}} \sum_{n=0}^{\infty} \frac{\alpha^n}{\sqrt{n!}} |n\rangle \quad (6.21)$$

where  $\alpha$  can be any complex number and  $|n\rangle$  are the energy eigenstates of a harmonic oscillator. In the limit of large average photon number  $|\alpha| \rightarrow \infty$  such a state resembles a classical state, while for  $\alpha \rightarrow 0$  it becomes identical to the vacuum state. Any coherent state can be also created from the vacuum state with the displacement operator

$$\hat{D}(\alpha) = e^{\alpha\hat{a}^\dagger - \alpha^*\hat{a}} \quad (6.22)$$

as

$$|\alpha\rangle = \hat{D}(\alpha) |0\rangle. \quad (6.23)$$

It is easy to show that coherent states are eigenstates of the photonic annihilation operator,

$$\hat{a}|\alpha\rangle = \alpha|\alpha\rangle \quad (6.24)$$

which gives them some intrinsic robustness to photon losses. The average photon number of a state  $|\alpha\rangle$  is  $\bar{n} = |\alpha|^2$  and the photon number probability

$$P(n) = |\langle n|\alpha\rangle|^2 = \frac{|\alpha|^{2n} e^{-|\alpha|^2}}{n!} \quad (6.25)$$

follows a Poissonian distribution with width  $\Delta n = |\alpha| = \sqrt{\bar{n}}$ . Even though the set of all coherent states form a (over)complete basis, they are not mutually orthogonal, as

$$|\langle\beta|\alpha\rangle|^2 = e^{-|\alpha-\beta|^2} \quad (6.26)$$

vanishes only in the limit  $|\alpha - \beta| \gg 1$ .

**Coherent states in phase space** A good way of representing coherent states and getting an intuitive picture of them is by looking at quasi-probability distributions in phase space, a two-dimensional space where the two axes correspond to the two quadratures  $\hat{q} = \frac{1}{2}(\hat{a}^\dagger + \hat{a})$  and  $\hat{p} = \frac{1}{2}i(\hat{a}^\dagger - \hat{a})$ . For a coherent state, the expectation values of these quadratures are

$$\langle \alpha | \hat{q} | \alpha \rangle = \text{Im}(\alpha) \quad (6.27)$$

and

$$\langle \alpha | \hat{p} | \alpha \rangle = \text{Re}(\alpha), \quad (6.28)$$

and we will always find a coherent state to be centred around the position in phase space which corresponds to these coordinates, i.e. we can actually understand the two axes as giving the real and imaginary part of a coherent state. An example representation of a coherent state is shown in Figure 6.2.

As the two quadrature operators are not commuting, a proper probability distribution over both quadratures at the same time is impossible (just like it is impossible to measure both simultaneously with full accuracy). However, there are some distributions which at least give the right distribution of one quadrature when integrating over the other. One such distribution is the Husimi Q-function, which represents a quantum state  $\hat{\rho}$  at the phase-space position  $(q, p)$  by how much it overlaps to a coherent state of the corresponding quadratures  $|\alpha\rangle = |q + ip\rangle$ ,

$$Q(\alpha) = Q(q + ip) = \frac{1}{\pi} \langle \alpha | \hat{\rho} | \alpha \rangle \quad (6.29)$$

or purely in terms of the quadratures,

$$Q(q, p) = \frac{1}{\pi} \frac{e^{-(q^2+p^2)}}{2} \sum_{n,m} \frac{(q + ip)^{m-n}}{\sqrt{m!n!}} \langle m | \hat{\rho} | n \rangle. \quad (6.30)$$

Hence, instead of using the two coordinates  $q$  and  $p$  one can intuitively also use the complex coordinate  $\alpha = q + ip$  to denote a position in phase space. A density matrix describing a coherent state  $\hat{\rho} = |\beta\rangle \langle \beta|$  will have a Gaussian distribution

$$Q(\alpha) = \frac{1}{\pi} e^{-|\alpha - \beta|^2} \quad (6.31)$$

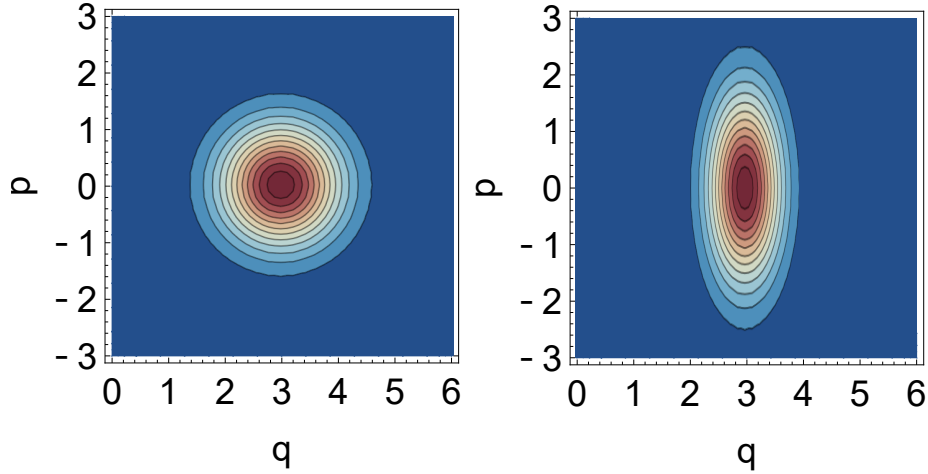


Figure 6.2: Phase space representation of a coherent state (left) and a squeezed state (right). The center of the coherent state distribution is at the phase-space coordinate  $p = 0$ ,  $q = 3$ , corresponding to a state  $|\alpha\rangle$  with  $\alpha = 3$ . The squeezed state has the same average quadratures, but a reduced variance in  $q$  at the cost of a higher variance in  $p$ .

centred around the point  $\alpha = \beta$ , or in terms of quadrature coordinates,  $p = \text{Re}\beta$  and  $q = \text{Im}\beta$ . Keep in mind that coherent states are not mutually orthogonal and hence even the distribution of a perfect coherent state has a finite width as it has non-vanishing overlap with other coherent states. In fact, coherent states are minimal uncertainty states and their uncertainty in both variances is

$$\Delta q = \Delta p = \frac{1}{2} \quad (6.32)$$

and therefore also all valid phase-space distributions must have finite width. A related class of states to coherent states are squeezed states, which can for example arise from coherent states after non-linear interactions. Squeezed states still have minimum uncertainty as well, but have it weighted differently between the two quadratures<sup>2</sup>. In phase space this literally looks like squeezing an initially round blob in one direction and thereby making it longer, as can be seen in Figure 6.2.

Using the number state decomposition, the coherence of a coherent state as de-

<sup>2</sup>It is also possible to squeeze a coherent state with respect to its photon number and phase distribution (leading for example to a banana-like shape in phase space), but for large photon numbers and weak squeezing this is almost identical to quadrature squeezing.

defined by the relative entropy can be calculated as [80]

$$C_{\text{ent}}(\hat{\rho}) = e^{-|\alpha|^2} \sum_{n=0}^{\infty} \frac{|\alpha|^{2n} \log n!}{n!} - |\alpha|^2 \log \frac{|\alpha|^2}{e}. \quad (6.33)$$

## 6.4.2 The Jaynes Cummings Model

The Jaynes-Cummings model [87–89,97] describes the interaction of a two-level system, such as two levels of an atom, resonantly coupled with a bosonic mode, for example the electromagnetic field inside a cavity. The interaction Hamiltonian is given by

$$\hat{H} = -i\hbar g (\hat{a}\hat{\sigma}_+ - \hat{a}^\dagger\hat{\sigma}_-), \quad (6.34)$$

where  $\hat{a}$  and  $\hat{a}^\dagger$  are the usual bosonic ladder operators of the field and  $\hat{\sigma}_\pm$  the atomic lowering and raising operators. If we bring the Hamiltonian of the dipole interaction, as introduced in equation 1.87 back to our mind, we see that the Jaynes-Cummings Hamiltonian indeed describes the same interaction in the rotating wave approximation, i.e. fast rotating terms like  $\hat{a}\hat{\sigma}_-e^{-i(\omega+\omega_A)t}$  and their complex conjugate are omitted due to their weak impact on measurable outcomes<sup>3</sup>. Furthermore we only take into account one discrete mode of the cavity and ignore all the details about the nature of the field or the two-level system, as we are only interested in the general dynamics. All underlying physical information are compacted within the coupling strength  $g$ . In the rotating wave approximation as we have it here, the total number of excitations is a constant of the motion, and the effect of the interaction is to induce a unitary operation within subspaces of constant total energy, giving an exactly solvable model for atom-light interaction. Note that as this is a strictly energy-conserving operation it is an incoherent operation in the context of coherence resource theory.

From solving the Schrödinger equation we find that a general atom-cavity state of the form

$$|\Psi\rangle = \sum_n G_n |g\rangle |n\rangle + E_n |e\rangle |n\rangle \quad (6.35)$$

---

<sup>3</sup>In the calculation of spontaneous emission rates with first order perturbation theory they also vanish as they correspond to the creation or annihilation of two excitations simultaneously (atomic and photonic) instead of an exchange of excitations.

whose time evolution is given by the Hamiltonian 6.34 satisfies

$$\dot{G}_n = gE_{n-1}\sqrt{n} \quad (6.36)$$

$$\dot{E}_n = -gG_{n+1}\sqrt{n+1}. \quad (6.37)$$

The evolution of an initially excited atom interacting with an arbitrary cavity state,  $|\Psi(0)\rangle = \sum_n c_n |n\rangle |e\rangle$ , is thus given by

$$|\Psi(t)\rangle = \sum_{n=0}^{\infty} c_n \left[ \cos(\sqrt{n+1}gt) |n\rangle |e\rangle + \sin(\sqrt{n+1}gt) |n+1\rangle |g\rangle \right]. \quad (6.38)$$

Note that the frequency of this oscillation is different in each constant energy subspace, and depends on the total excitation number  $n+1$ : thus as time progresses the oscillations for different total energy drift in and out of phase, giving rise to the famous collapses and revivals of the Jaynes-Cummings model [87, 89, 97, 98]. Our interest, however, is in interaction times that are much shorter than the collapse and revival times. A key feature of the evolution is that at any given time  $t > 0$  the atom and field mode will be in an entangled state and it is this entanglement that encapsulates the back action on the state of the field mode.

We will be primarily interested with the cavity mode being in a coherent state, which results in a time evolution of the joint state

$$|\Psi(t)\rangle = e^{-|\alpha|^2/2} \sum_{n=0}^{\infty} \frac{\alpha^n}{\sqrt{n!}} \left[ \cos(\sqrt{n+1}gt) |n\rangle |e\rangle + \sin(\sqrt{n+1}gt) |n+1\rangle |g\rangle \right]. \quad (6.39)$$

After a quarter rotation the atom can be found in a coherent superposition state with high probability and very weak entanglement to the cavity. Just like in Åberg's proposal we can thus approximately rotate an atom from an initially incoherent state into the desired coherent superposition. For simplicity and without loss of generality we restrict ourselves to real values of  $\alpha$  so that with the given interaction, we can indeed rotate the atomic state into the superposition  $|+\rangle = \frac{1}{\sqrt{2}}(|g\rangle + |e\rangle)$ , other values will only lead to different phases of the superposition state that can be reached.

In the following chapter we are going to explore the interaction of a sequence of

atoms with the same coherent state under such an operation and study the coherence transfer, the building up of correlations and the robustness of the resource state with repetitive interactions.

# Chapter 7

## Coherence catalysis in the Jaynes-Cummings model

As has been shown already [85], no process can create coherence fully catalytically, degradation is always hidden in the emerging correlations between subsystems. However, it is still important to know how much coherence can be practically extracted from a reservoir, and how many subsystems could in principle be put in a coherent superposition before the entanglement becomes too strong and the protocol too unreliable. In quantum computing applications, this is an important information as superpositions of computational states are usually created by exactly these coherence transferring interactions. In this chapter, we investigate in particular the catalyticity of a coherent state resource, and study the trade-off between the state's accuracy in preparing exact atomic superposition states and its ability in performing many interactions without degradation under the natural interaction between atoms and the electromagnetic field in the rotating-wave approximation, i.e. the interaction described by the Jaynes-Cummings model.

## 7.1 Successive interactions with the same cavity

We start by rewriting equation 6.39 in the basis of  $|\pm\rangle$  and shifting the second term in the sum to obtain

$$|\Psi(t)\rangle = \frac{e^{-|\alpha|^2/2}}{\sqrt{2}} \sum_{n=0}^{\infty} \frac{\alpha^n}{\sqrt{n!}} |n\rangle \left[ \left( \cos(\sqrt{n+1}gt) + \frac{\sqrt{n}}{\alpha} \sin(\sqrt{n}gt) \right) |+\rangle + \left( \cos(\sqrt{n+1}gt) - \frac{\sqrt{n}}{\alpha} \sin(\sqrt{n}gt) \right) |-\rangle \right].$$

We want to maximize the probability of the atom ending up in the state  $|+\rangle$ . A good approximation of the ideal interaction time for this is obtained by maximizing the probability for the centre of the photon number distribution, i.e. maximizing  $|\cos(\sqrt{\bar{n}+1}gt) + \sin(\sqrt{\bar{n}}gt)|^2$  with  $\bar{n} = \alpha^2$ . We choose an interaction time  $t_1$  defined by

$$\sqrt{\bar{n}+1}gt_1 = \frac{\pi}{4} \quad (7.1)$$

which is not the exact maximum but a good enough approximation for large photon numbers<sup>1</sup>. The probability of measuring the atom in the state  $|-\rangle$  for this choice is

$$P_- = \frac{e^{-|\alpha|^2}}{2} \sum_n \frac{\alpha^{2n}}{n!} \left| \cos(\sqrt{n+1}gt_1) - \frac{\sqrt{n}}{\alpha} \sin(\sqrt{n}gt_1) \right|^2 \quad (7.2)$$

$$\simeq \frac{(\pi+2)^2}{64\bar{n}} + \mathcal{O}\left(\frac{1}{\bar{n}^2}\right) \quad (7.3)$$

which tends to zero in the limit of large  $\bar{n}$ . A detailed derivation of this approximation can be found in Appendix B. There are two main conditions that determine how well our protocol will work. The first is that the spread in Rabi frequencies  $\sqrt{n+1}g$  is small compared to the central frequency, or in other words, the spread in photon number is small compared to the mean photon number, so that it is possible to choose  $t_1$  satisfying  $\sqrt{n+1}gt_1 \simeq \pi/4$  for all  $n$  with appreciable amplitude in the superposition. The second condition is that the distribution  $c_n = \frac{\alpha^n}{\sqrt{n!}}$  is such that the shifted state, with one additional photon in the field, has large overlap with the

---

<sup>1</sup>One could choose  $\sqrt{\bar{n}}gt_1 = \frac{\pi}{4}$  or  $\sqrt{\bar{n} + \frac{1}{2}}gt_1 = \frac{\pi}{4}$  instead for similar arguments without changing the probabilities in first order approximation. The exact interaction time minimizing the failing probability for  $\alpha = 10$  was found numerically as  $\sqrt{\bar{n} + 1.5726}gt_1 = \frac{\pi}{4}$ .

initial state so that the atom and the cavity are not too entangled after the process<sup>2</sup>. There is a tension or complementarity between these two conditions: a narrower distribution means the former condition is readily satisfied, but requires a sharper change in the coefficients  $c_n$ , making the second more difficult to meet.

Comparing this interaction to the one described in section 6.2 we note two main differences: First, the operation  $V(U)$  did not make a distinction between the energy levels of the reservoir. The atom would lose half a quantum of energy no matter which state the reservoir is in. In the Jaynes-Cummings interaction on the other hand, each energy level of the cavity causes a different strength of rotation of the atomic state and the interaction time needs to be chosen according to the mean photon number in the cavity. Secondly, as a consequence of this, the success probability does not only depend on the size of the resource state as was the case in Åberg's proposal [84] but also on the offset, i.e. the mean photon number. For a coherent state these two are linked together as there is only one parameter  $\alpha$ . However, for a more general case like squeezed states this indeed makes a difference.

After having measured the atom in the state  $|+\rangle$  or  $|-\rangle$ , the cavity is projected to the state

$$|\Psi_{\text{cav}}\rangle_{\pm} = \frac{e^{-|\alpha|^2/2}}{\sqrt{2P_{\pm}}} \sum_{n=0}^{\infty} \frac{\alpha^n}{\sqrt{n!}} \left( \cos(\sqrt{n+1}gt_1) \pm \frac{\sqrt{n}}{\alpha} \sin(\sqrt{n}gt_1) \right) |n\rangle. \quad (7.4)$$

Without information on the atomic state, the cavity must be described as a mixed state with the density matrix

$$\rho = P_+ |\Psi_{\text{cav}}\rangle_+ \langle\Psi_{\text{cav}}|_+ + P_- |\Psi_{\text{cav}}\rangle_- \langle\Psi_{\text{cav}}|_- \quad (7.5)$$

where  $P_{\pm} = {}_{\pm} \langle\Psi_{\text{cav}}|\Psi_{\text{cav}}\rangle_{\pm}$  is the probability of the respective measurement outcome (if it were measured).

For large  $\alpha$ , as  $P_+ \rightarrow 1$ , the system can be understood as approximately in the state  $|\Psi_{\text{cav}}\rangle_+ |+\rangle$ , where the states of the field at the atom are independent of each other.

This cavity state shall now be used again to bring another initially excited atom

---

<sup>2</sup>To help picture this reasoning, consider a general state  $|\Psi\rangle_A |e\rangle + |\Psi\rangle_B |g\rangle$ . If  $\langle\Psi_A|\Psi_B\rangle = 1$  the two systems are not entangled at all as we can just write  $|\Psi\rangle_A (|e\rangle + |g\rangle)$  instead. If  $\langle\Psi_A|\Psi_B\rangle = 0$  then the system is maximally entangled.

to a coherent superposition, i.e. we now start with the state  $|\Psi^{(2)}(0)\rangle = |\Psi_{\text{cav}}\rangle_{\pm} |e\rangle$  and use equations (6.35)-(6.37) to find the corresponding time evolution

$$|\Psi^{(2)}(t)\rangle = \frac{e^{-\frac{|\alpha|^2}{2}}}{\sqrt{2P_{\pm}}} \sum_n \frac{\alpha^n}{\sqrt{n!}} \left[ \left( \frac{\sqrt{n-1}}{\alpha} \sin(\sqrt{n-1}gt_1) \pm \cos(\sqrt{n}gt_1) \right) \frac{\sqrt{n}}{\alpha} \sin(\sqrt{n}gt) |g, n\rangle \right. \\ \left. + \left( \frac{\sqrt{n}}{\alpha} \sin(\sqrt{n}gt_1) \pm \cos(\sqrt{n+1}gt_1) \right) \cos(\sqrt{n+1}gt) |e, n\rangle \right].$$

As the cavity is not in the exact same state as in the first round, an adjustment of the interaction time might be necessary according to the new mean photon number. This process can be arbitrarily repeated and the evolution of the cavity state after  $N$  rounds can be found iteratively. The coefficients of the joint state  $\langle \Psi_N |$ , as defined by

$$\langle n | \langle \pm |^{\otimes N} | \Psi_N \rangle \equiv e^{-\frac{|\alpha|^2}{2}} \frac{\alpha^n}{\sqrt{n!}} f_{N, \{\pm\}}(n) \quad (7.6)$$

can be obtained from the previous coefficients

$$f_{N, \{\pm\}}(n) = \frac{1}{\sqrt{2}} \left( f_{N-1, \{\pm\}}(n-1) \frac{\sqrt{n}}{\alpha} \sin(\sqrt{n}gt_N) \pm f_{N-1, \{\pm\}}(n) \cos(\sqrt{n+1}gt_N) \right) \quad (7.7)$$

with  $f_0(n) = 1$  and  $t_N$  being the interaction time chosen for the corresponding round. This can be calculated for any combination of atomic states  $\{\pm\} = \{\pm_1, \pm_2, \dots\}$ , the sign determining  $f_{N, \{\pm\}}$  is always defined by the state of the last atom the cavity interacted with,  $\pm_N$ .

The state of the cavity depends on the measurement outcome of all the atoms it interacted with and therefore we expect the success probability of following rounds to depend on these, too. In the case of not measuring the atoms, we thus expect the atoms to be correlated both with each other and with the cavity after the interaction. For all theoretical considerations it is sufficient to calculate the dynamics separately for an outcome  $|\Psi_{\text{cav}}\rangle_+$  and  $|\Psi_{\text{cav}}\rangle_-$  after each round (and therefore to calculate  $2^N$  possible cavity states) as if we always measured the atomic state. Even if the atoms are not actually measured, the true state of the joint system can always be obtained

by simply taking the corresponding superposition of all possible outcomes,

$$|\Psi_N\rangle = \sum_n e^{-\frac{|\alpha|^2}{2}} \frac{\alpha^n}{\sqrt{n!}} |n\rangle (f_{N,\{+,+, \dots\}}(n) |+\rangle |+\rangle |\dots\rangle + f_{N,\{-,+, \dots\}}(n) |-\rangle |+\rangle |\dots\rangle + \dots). \quad (7.8)$$

In any practical application, one would probably not directly measure the atoms after the protocol (if we could measure them in the basis of  $|\pm\rangle$ , we wouldn't need the protocol in the first place)<sup>3</sup>. However, as analyzing the complete state of the increasingly large quantum system does not reveal very much insight, we instead focus on the special cases of having measured something particular, which is nothing but an analysis of the corresponding parts of the superposition we are interested in.

## 7.2 Evolution of the cavity field

In each round, one atom is brought from the excited state to approximately the state  $|+\rangle$ , we therefore expect the mean photon number in the cavity to increase by half a photon per round. Numerical results obtained for an initial coherent state of  $\alpha = 10$  confirm that the mean photon number after a successful interaction is indeed increased to  $\bar{n}_+ = 100.502$ . However, after an unsuccessful round in which the atom was measured in the state  $|-\rangle$ , the mean photon number in the cavity decreases to  $\bar{n}_- = 99.812$ . This is not in contradiction with energy conservation as a measurement in the  $\{|+\rangle, |-\rangle\}$ -basis can change the energy of the system. As the original goal of the protocol is to use coherence of the resource state to create coherent atomic states we want to avoid the necessity of measurement during the protocol. For this reason, we seek to adjust the interaction times of future rounds only according to an assumed increase of half a photon per round in all numeric calculations throughout this work instead of using the actual number obtained from measuring the atom.

Figure 7.1 shows the photon number distribution of the cavity field after the atom

---

<sup>3</sup>A measurement is a not an incoherent operation. Take for example a measurement in the  $|\pm\rangle$  basis of an atom in an energy eigenstate. After the measurement the atom will be in a maximally coherent state. The coherence in this case comes from the measurement device itself which needs to use a coherent reference to determine the measurement outcome. In fact, in most cases such a measurement is actually performed by rotating the atom first and then measuring in the computational basis, i.e. coherence is actively created in the atom by interaction with another coherence reservoir.

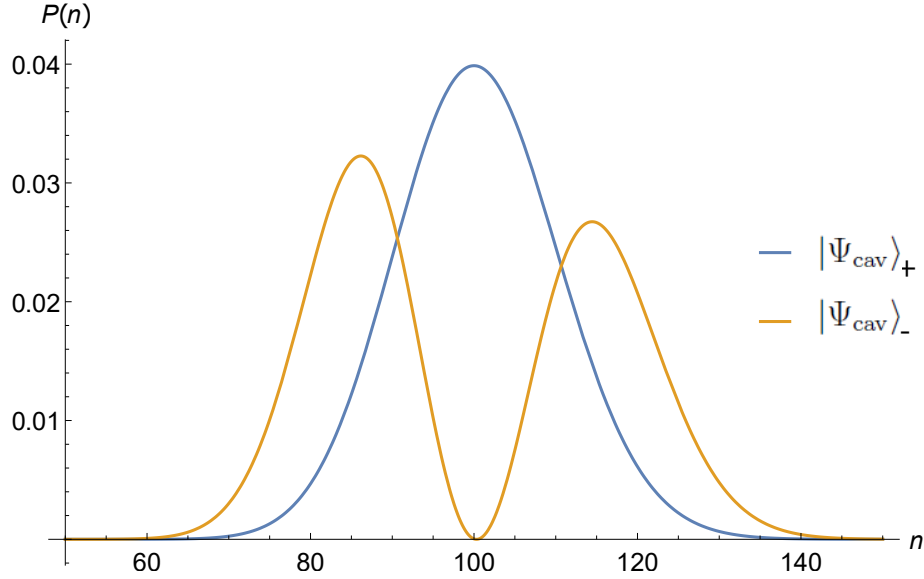


Figure 7.1: Photon number distribution of the cavity field after one successful (blue) or failed (orange) interaction.

has been measured in the state  $|+\rangle$  or  $|-\rangle$  after the first round. It appears that the atomic state  $|-\rangle$  is mostly correlated with the low and high photon number sides of the distribution after interaction. Thus, the possibility of ending up in  $|-\rangle$  removes the “wings” of the distribution from the cavity state  $|\Psi_{\text{cav}}\rangle_+$ , suggesting that success in producing the desired state  $|+\rangle$  acts to reduce the amplitude uncertainty in the cavity, i.e. squeeze the state of the field. This is confirmed in our numerical example of  $\alpha = 10$ . The variance of the photon number distribution  $P_+(n)$  is given by

$$(\Delta n_+)^2 = \langle \hat{n}_+^2 \rangle - \langle \hat{n}_+ \rangle^2 = 100.211. \quad (7.9)$$

The width of the distribution is increased with respect to the initial coherent state with average photon number  $\bar{n}_0 = 100$ , but is smaller than that of the coherent state with average photon number  $\bar{n}_0 + 1/2$ .

The variance of the phase distribution [99]

$$P(\phi) = \frac{1}{2\pi} \sum_{n,m=0}^{\infty} e^{i(m-n)\phi} \langle n|\psi\rangle \langle \psi|m\rangle \quad (7.10)$$

increases similar to the decrease of the number variance, leaving the product un-

changed. Only when considering the mixed cavity state without measurement of the atom, both the phase and number variances increase and the total uncertainty  $(\Delta n_{\text{tot}})^2(\Delta \phi_{\text{tot}})^2$  increases by around 2% in our example.

We further note that the photon number distribution of the cavity after a failed round is very different from the corresponding cavity state in [84]: While in the ladder state, all terms in the superposition have equal probability amplitudes, and therefore in the failed cavity state  $\langle \Psi_- |$ , most of the terms exactly cancel out and leave the cavity in a state of very low coherence, when using coherent states this does not happen. Here, the poissonian photon number distribution of the initial state makes sure that in a superposition of that state with a shifted-photon-number version of it, no term cancels out completely, so we are still left with a large superposition of states and therefore with a significant amount of coherence.

The evolution of the number and phase uncertainty during the first three rounds of interactions can be seen in Figure 7.2. The photon number variance seems to increase linearly with the number of rounds by the same amount the phase uncertainty decreases when taking into account only successful rounds. Without the information of the atomic states after interaction, both phase and number uncertainties increase, there is no squeezing present in that case, as the uncertainty due to entanglement apparently overweights the effects of the squeezing.

To help intuition about what is happening to the resource state, Figures 7.4-7.6 show the Husimi Q-function in phase-space for successful and unsuccessful interactions. Each failing round pushes the cavity state further towards a (squeezed) vacuum. Furthermore, we see that successful rounds can still somewhat compensate for unsuccessful rounds as they bring the cavity closer to a coherent state and further push up the photon number. If we omit knowledge of the outcomes, the mixed cavity state does not exhibit any squeezing below the original width.

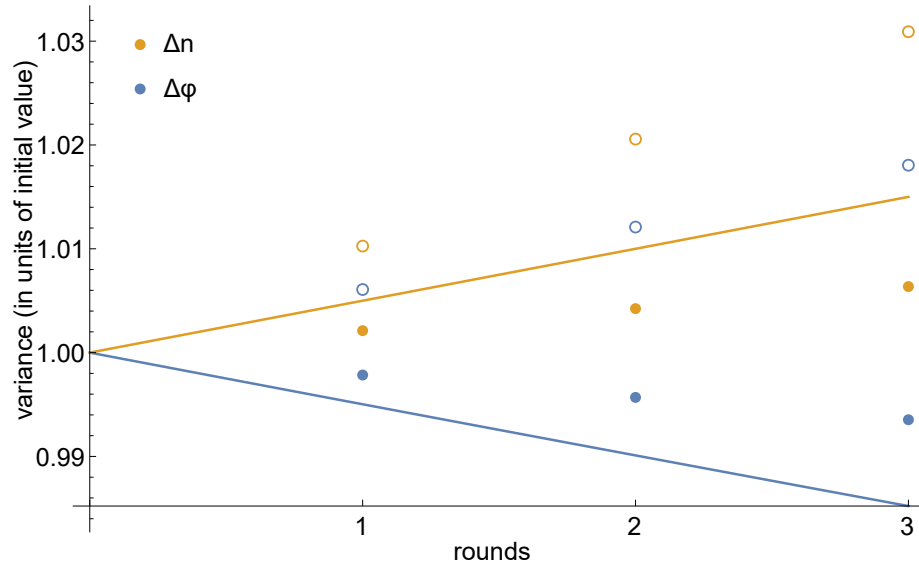


Figure 7.2: Evolution of the number (orange) and phase (blue) uncertainties of the cavity state after several iterations. The lines show the variance of exact coherent states when assuming an increase of half a photon per round, filled circles show the variance of the cavity state after all atoms have been found in  $|+\rangle$ , empty circles show the variance of the mixed cavity state without any information on the atomic states.

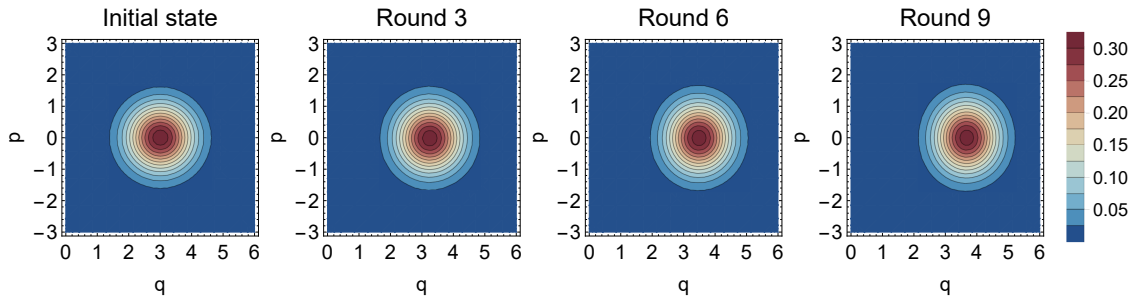


Figure 7.3: Q-function of the cavity state before the interactions and after 3, 6 and 9 rounds of interactions in the case of all atoms being found in the intended state.

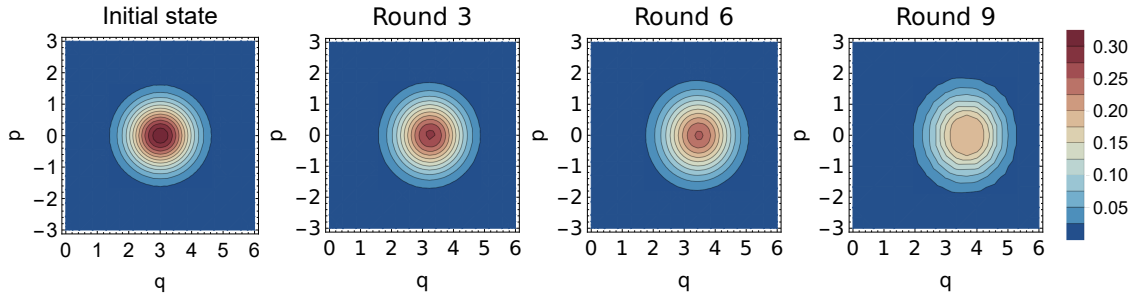


Figure 7.6: Q-function of the (mixed) cavity state before the interactions and after 3,6 and 9 rounds of interactions without knowledge of the atomic state.

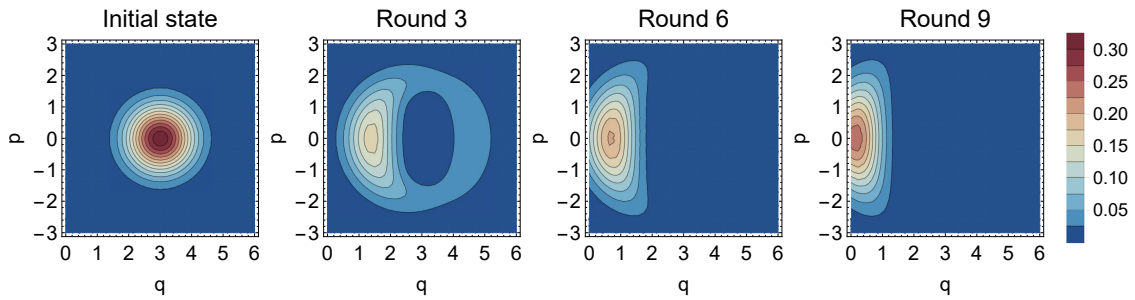


Figure 7.4: Q-function of the cavity state before the interactions and after 3,6 and 9 rounds of interactions in the case of all atoms being found in the undesired state.

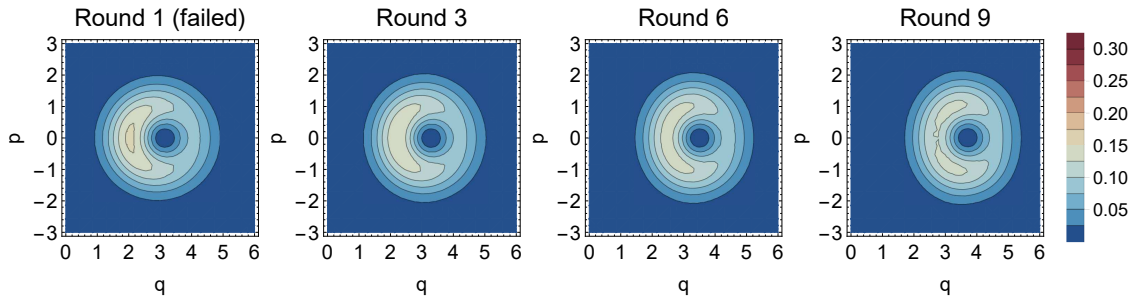


Figure 7.5: Q-function of the cavity state after 1,3,6 and 9 rounds of interactions in a mixed sequence with the first atom being found in the undesired state but all following rounds being successful.

### 7.3 Catalyticity and Robustness

In the following we want to investigate the performance of coherent states in the presented scheme. As the nature of the cavity field changes with each round we expect the success probabilities to change, too.

Figure 7.7 shows the conditional success probabilities in the  $r$ -th round after  $r - 1$  consequent successful or unsuccessful rounds. For the first case we see an increase of the success probability with rounds that goes even beyond what can be expected due to the increase of the mean photon number in the cavity. This suggests that the deformation or squeezing of the coherent state must have a further positive effect on the success. We therefore want to know if a squeezed coherent state has any advantage to a regular coherent state in the given interaction.

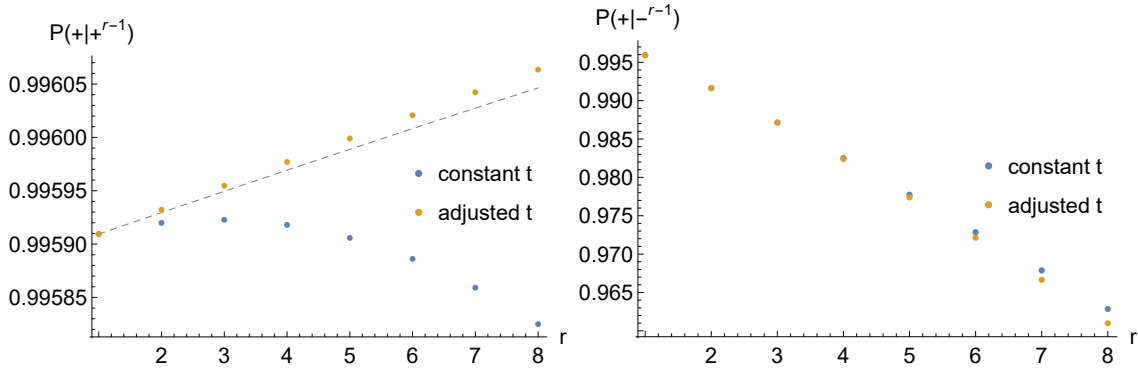


Figure 7.7: Left: Probability for the last ( $r$ -th) qubit to be found in the  $|+\rangle$  state after all previous were measured in  $|+\rangle$  with (orange) or without (blue) adjustment of interaction times according to an increase of half a photon in the cavity per round. The dashed line shows the probability for obtaining the state  $|+\rangle$  when the cavity field starts in a new coherent state with an increased photon number of  $1/2$  per each step. Right: Probability for the  $r$ -th qubit to end up in the state  $|+\rangle$  after all previous were measured in  $|-\rangle$ .

### 7.3.1 The effect of squeezing

An analysis of the success probabilities for squeezed initial states shows that reducing the variance of the number distribution can indeed lead to higher success probabilities up to a certain squeezing strength. Figure 7.8 shows the probability of the atom ending in the state  $|+\rangle$  when the cavity is in a quadrature-squeezed state<sup>4</sup>

$$|\alpha, \zeta\rangle = D(\alpha)S(\zeta)|0\rangle \quad (7.11)$$

with  $D(\alpha) = e^{\alpha\hat{a}^\dagger - \alpha^*\hat{a}}$  being the displacement operator and  $S(\zeta) = e^{\frac{\zeta}{2}(\hat{a}^2 - \hat{a}^{\dagger 2})}$  a squeezing operator. For a mean photon number of 100.5, the maximal success prob-

<sup>4</sup>For high photon numbers and weak squeezing, this is approximately equivalent to squeezing in the photon number.

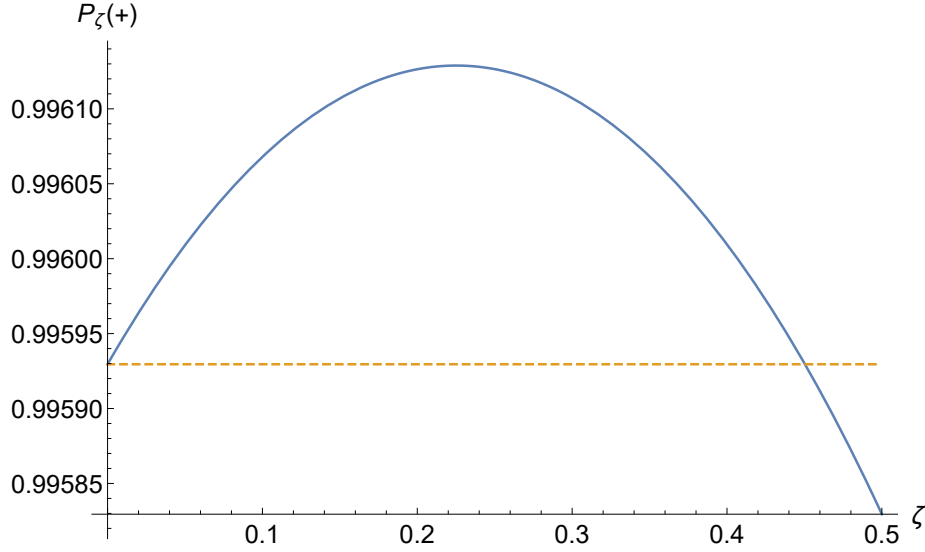


Figure 7.8: Probability of measuring the qubit in the state  $|+\rangle$  after one round with the cavity initially being in a q-quadrature squeezed state with mean photon number  $\bar{n} = 100.5$ , as a function of the squeezing parameter  $\zeta$ . The dashed line shows the probability without squeezing.

ability with such a squeezed state is  $P_{+, \max} = 0.99613$ : This is far above the value obtained when the the cavity field is re-used in the second interaction step. The effect of squeezing, together with growing photon numbers, would therefore suffice to explain the observed increase of success probabilities as discussed in 7.3. However, we can also observe something else: After reaching its maximum at a certain squeezing strength  $\zeta$ , the success probability rapidly starts decreasing again and we expect the same to happen for the evolved cavity state once it reaches a certain level of squeezing. Due to the increasing complexity of the system, this point has not been reached in the numeric simulations. At the limit of small squeezing parameter  $\zeta$ , we can approximate the photon distribution of an amplitude squeezed state by a Gaussian number distribution with reduced width:

$$\frac{1}{\sqrt{2\pi\bar{n}}} \exp\left[-\frac{(n - \bar{n})^2}{2\bar{n}}\right] \rightarrow \frac{1}{\sqrt{2\pi\bar{n}e^{-2\zeta}}} \exp\left[-\frac{(n - \bar{n})^2}{2\bar{n}e^{-2\zeta}}\right]. \quad (7.12)$$

Following this, the analytic approximation of the success probability using this squeezed state is given by

$$P(+)\simeq 1 - \frac{(e^{-2\zeta}\pi + 2)^2}{64\bar{n}e^{-2\zeta}} + \mathcal{O}\left(\frac{1}{\bar{n}^2}\right), \quad (7.13)$$

which has a maximum of  $1 - \frac{\pi}{8n}$  at a squeezing strength of  $e^{-2\zeta} = \frac{2}{\pi}$  when omitting higher order terms.

This study of squeezed states is a clear manifestation of the trade-off between the width of the distribution and the overlap with the shifted state we mentioned earlier. If the state is squeezed too much, the distribution of the photon number is very narrow and thus the interaction time chosen will lead to a very exact rotation for the biggest part of the superposition and only to small errors overall. However, the overlap of such a strongly squeezed state with the state shifted in photon number (that is, the overlap between the two possible cavity states after interaction), will be smaller than for a wider distribution and therefore the approximation of the atomic state being separable from the cavity starts to fail. On the other hand, if the state is not squeezed enough, the distribution is wide enough to ensure a good separation between atom and cavity but the rotation of the atom is less exact. This is why we see the success probability decreasing in both directions of the squeezing strength in figure 7.8.

### 7.3.2 Correlations

The second graph in figure 7.7 shows that after failure the success probability for the next round is only slightly reduced which is in contrast to the abrupt breakdown of the performance when using ladder states in the scheme proposed by [84].<sup>5</sup> This effect does not change significantly when more unsuccessful rounds occur. However, we see that there must still be correlations between the operation performed by the resource and the state of the atoms from previous interactions.

Comparing conditional probabilities after two rounds, we see that the probabilities after the second round of interaction strongly depend on the outcome of the first round: The failing probability given that the first atom ended up in the state  $|-\rangle$  is more than twice as large as after a successful first round. However, as it is very unlikely to actually find the first atom in the state  $|-\rangle$ , the overall probability of success in the second round  $P(+_2)$  (without any information on the first round) is

---

<sup>5</sup>One has to be careful here: This is a feature of the interaction used in [84] and not of the Ladder states per se. When using Ladder states in a Jaynes-Cummings interaction, they show similar behaviour as coherent states: After a failed round, the photon numbers are distributed on two peaks around the ladder boundaries and the remaining coherence can be used for another round.

still higher than that of the first round. A comparison of probabilities can be found in Table 7.1.

Table 7.1: Probability amplitudes after two rounds for  $|\alpha| = 10$  with adjustment of interaction times after the first cycle. Bold ciphers show the deviation from the corresponding single-atom probabilities for easier comparison.

$P(+_1)$	$P(+_2)$	$P(+_2 +_1)$	$P(+_2)P(+_1)$	$P(+_2 \cap +_1)$
0.9959 <b>09</b>	0.9959 <b>15</b>	0.9959 <b>32</b>	0.9918 <b>41</b>	0.9918 <b>58</b>
$P(-_1)$	$P(-_2)$	$P(+_2 -_1)$	$P(+_2)P(-_1)$	$P(+_2 \cap -_1)$
0.0040 <b>91</b>	0.0040 <b>85</b>	0.99 <b>1631</b>	0.0040 <b>74</b>	0.0040 <b>56</b>

Analytical expressions for the joint probabilities in terms of the “scaling parameter” of our problem,  $1/\bar{n}$ , up to second order, are given in Table 7.2. Again, we see that the state of the two atomic qubits after the interaction is non-separable, since the joint probabilities show (weak) correlations. This correlation is not evident if we consider only the first order of the approximation. Comparing our results to the scheme proposed by Åberg [84] we see that although the single-atom probabilities in both models scale linearly with the inverse size of the state, i.e.  $\frac{1}{\bar{n}}$  and  $\frac{1}{L}$ , the Jaynes-Cummings model using coherent states is much more robust against multiple failures: The probability for ending up in the state  $|-\rangle$  for two consecutive atoms in this case scales as  $\frac{1}{\bar{n}^2}$  compared to being still  $\frac{1}{L}$  in Åberg’s scheme.

To allow for comparison of the scaling with the number of rounds, a plot of the failure probability as a function of  $\alpha$  is shown in Figure 7.9, for the first five rounds of ending up in the state  $|-\rangle$ . Alongside these plots are shown trend lines, which allow us to roughly estimate the dependence of the worst-case probability  $P(-^r)$  on  $\bar{n}$  as

$$P(-^r) = P(-_r \cap -_{(r-1)} \cap \dots \cap -_1) \sim \frac{1}{\bar{n}^r}. \quad (7.14)$$

This  $\sim 1/\bar{n}^r$  dependence on  $\bar{n}$  confirms the analytical results and reinforces our suspicion that coherent states are indeed more robust to the extraction of coherence than Ladder states in Åberg’s scheme [85], as the probability of failure in all rounds decreases exponentially with the number of rounds  $r$ .

Table 7.2: Comparison of probabilities and joint probabilities obtained from using coherent states in a Jaynes-Cummings interaction and using Ladder states in the scheme proposed by Åberg [84]. The product of single-atom probabilities are calculated from first-round probabilities only. Using the total probability after the second round  $P(\pm_2) = P(\pm \cap +) + P(\pm \cap -)$  would only lead to changes in higher orders,  $P(\pm_2) = P(\pm) + \mathcal{O}\left(\frac{1}{\bar{n}^3}\right)$ . Interaction times are kept constant for simplicity, giving a lower bound to success probabilities. In this table, we set the interaction time such that  $gt\sqrt{\bar{n} + \mu} = \pi/4$ , when  $\mu$  is an arbitrary real number and  $\mu \ll \bar{n}$ . These expressions were derived by Atirach Ritboon.

	Jaynes-Cummings	Åberg's scheme
$P(+)$	$1 - \frac{(\pi+2)^2}{64\bar{n}} + \frac{\pi^4 - 4(5 - 40\mu + 16\mu^2)\pi^2 + 64(1+2\mu)\pi + 16}{4096\bar{n}^2}$	$1 - \frac{1}{2L}$
$P(-)$	$\frac{(\pi+2)^2}{64\bar{n}} - \frac{\pi^4 - 4(5 - 40\mu + 16\mu^2)\pi^2 + 64(1+2\mu)\pi + 16}{4096\bar{n}^2}$	$\frac{1}{2L}$
$P(-) \times P(-)$	$\frac{(\pi+2)^4}{4096\bar{n}^2}$	$\frac{1}{4L^2}$
$P(- \cap -)$	$\frac{(\pi+2)^2(3\pi^2 + 4\pi + 12)}{4096\bar{n}^2}$	$\frac{1}{4L}$

## 7.4 Discussion

As was shown in [85], the scheme proposed by Åberg does not describe a catalytic process, i.e. coherent superpositions can not be created an arbitrary amount of times with constant efficiency. The reason for this is the fact that the possibility of ending up in the wrong state, no matter how small it may be, has an effect on the resource state. This effect is strong enough to lead to an effective breakdown of the protocol once an atom is found in that state. Consequently, probabilities of multiple failed rounds don't scale like the the product of single-round probabilities and therefore exponential with rounds but rather similar to the probability of one single failure. This can be understood intuitively: If one qubit is measured in the undesired state  $|-\rangle$ , the probability of measuring the next qubit in  $|-\rangle$  as well is in the order of  $\mathcal{O}(1)$  and does not depend on the original size of the resource state anymore. Therefore, also the probability of multiple failures does not scale any better (qualitatively) than the single-failure probability,  $P(-^r) = P(-|^{-r-1})P(-|^{-r-2})\dots P(-) \sim \mathcal{O}\left(\frac{1}{L}\right)$ .

For the Jaynes-Cummings interaction proposed in this work we have seen that, even though we still find correlation between the atoms and a decrease of efficiency

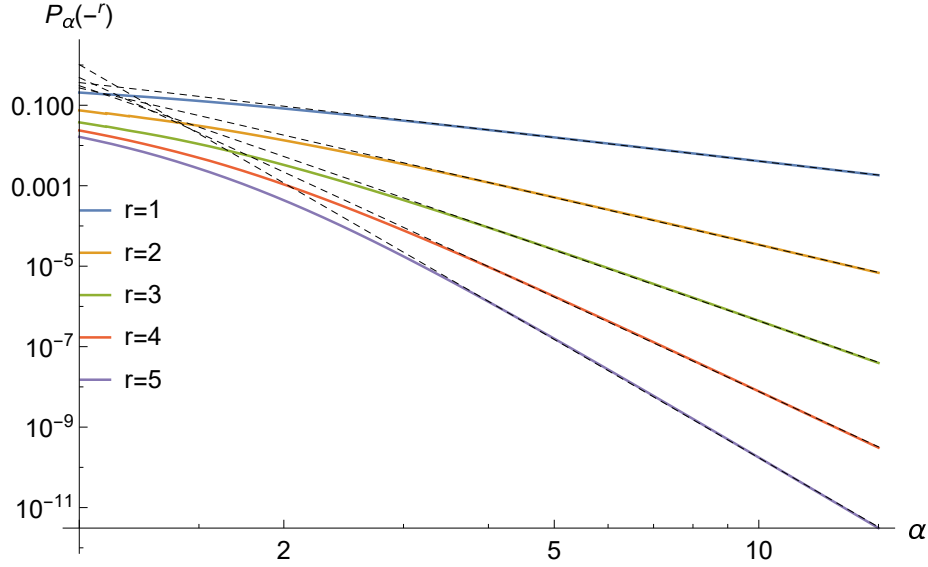


Figure 7.9: Double-logarithmic plot of the probability for all atoms to end up in the state  $|-\rangle$  during one to five rounds as a function of  $\alpha$ . The graphs were obtained from numeric calculations with adjustment of interaction times. The dotted lines show power series  $0.3667\alpha^{-1.954}$ ,  $0.2693\alpha^{-3.899}$ ,  $0.3064\alpha^{-5.847}$ ,  $0.4884\alpha^{-7.805}$  and  $1.0225\alpha^{-9.772}$  (top to bottom) obtained from fitting the numerical data for  $\alpha > 3$ .

after failure, the interaction is much more robust against multiple failure. In particular, both numerical and analytical estimations suggest that the failure probability indeed is exponential in the number of (unsuccessful) rounds. This is due to the fact that even after measuring an atom in the state  $|-\rangle$ , the cavity does not instantaneously lose all its coherence but is transformed to a different state which still has a high degree of coherence and can still be used for the interaction to some degree. It can be shown [86] that a coherent state  $|\alpha\rangle$  can produce approximately  $\mathcal{O}(\alpha^2)$  copies of coherent atoms before the resource is degraded too much. If one compares the coherence contained in such an amount of atoms with the coherence of the resource, this suggests that the extraction of coherence through the Jaynes-Cummings interaction is in fact close to optimal.

On the other hand, it should be noted that even in the case of success, the cavity undergoes a slight change of its state. For the repetition rates that were investigated in this work we only saw an improvement due to these cavity changes. Nevertheless, we have to assume that this improvement will not last for an infinite amount of repetitions and at some point will turn into a decrease of success probabilities, espe-

cially if we explain the improvement with the squeezing of the cavity state. So, even though coherent states in a Jaynes-Cummings interaction show more robust features with regard to failure, they have a trade-off in terms of stability in the successful case when compared to Ladder states in Åberg's scheme.

# Chapter 8

## Conclusion

In the second part of this work, we have investigated the nature of coherence as a resource within the coherent state Jaynes–Cummings model. We have explored the extent to which a sequence of atoms, prepared initially in their excited state, could be prepared in a state close to a desired coherent superposition by interacting with a single cavity mode which is initially in a coherent state. We have shown that in such a protocol, the probability with which the atoms are transformed to the desired superposition state scales linearly with the inverse mean photon number of the cavity and that in repeated interactions, the probability of finding  $r$  atoms in the undesired, orthogonal state scales exponentially with the number of failed rounds  $r$ . We have compared our results with the original proposal of [84] and concluded that, in contrast to the strong correlations that build up between the ladder states, in the implementation presented here, subsequent atoms are almost independent after interacting with the resource state. We have furthermore studied the phase and photon number statistics of the cavity state and the changes thereof associated with the repeated interactions. We have found that, even though a successful interaction has some effect of degrading the cavity state, for the same reason an unsuccessful interaction does not destroy all coherence and therefore does not lead to an instantaneous breakdown of the efficiency. We have studied the relation between the cavity statistics and the efficiency of the protocol and found that slightly squeezed coherent states indeed have the highest probability in obtaining the desired atomic states after interaction.

Our results are reassuring in light of the extensive use of coherent states in the-

oretical and experimental quantum optics, and also illustrative of the limitations of using coherence as a thermodynamic resource.

# Appendix A

## Green's functions derived from the vector potential

The Green's function for the vector potential can be derived in exact analogy to the electric field Green's function as derived in chapter 4 by comparing the differential equations that determine the Green's functions: For the transverse electric field we have

$$(\nabla^2 + \omega^2 \mu \epsilon) \mathbf{E}^T = \mu \omega^2 \mathbf{P}_N^T \quad (\text{A.1})$$

whereas for the vector potential the equations read

$$(\nabla^2 + \omega^2 \mu \epsilon) \mathbf{A} = -\mu \mathbf{J}^T \quad (\text{A.2})$$

where  $\mathbf{P}_N^T$  and  $\mathbf{J}^T$  are the respective sources of the field according to choices of writing the Hamiltonian as  $H = \mathbf{d} \cdot \mathbf{E}$  or  $H = \mathbf{J} \cdot \mathbf{A}$ . Hence, the only difference between the Green's function of the electric field and that of the vector potential are a factor of  $-\omega^2$ . The Green's function of the vector potential  $G_{ij}^{(A)}$  can be written as

$$G_{ij}^{(A)}(\omega, \mathbf{k}) = \mu \frac{\delta_{ij} - \frac{k_i k_j}{k^2}}{\omega^2 \mu \epsilon - k^2} \quad (\text{A.3})$$

in Fourier space, or

$$G_{ij}^{(A)}(\omega, \mathbf{R}) = -\frac{1}{4\pi\varepsilon} (\partial_i \partial_j - \delta_{ij} \nabla^2) \frac{1}{R} (e^{i\sqrt{\varepsilon\mu}\omega R} - 1) \quad (\text{A.4})$$

$$= \frac{1}{4\pi\varepsilon\omega^2} \left( \frac{2}{3} i(\sqrt{\varepsilon\mu}\omega)^3 \delta_{ij} + \frac{1}{2} \varepsilon\mu\omega^2 \left( \frac{\delta_{ij}}{R} + \frac{R_i R_j}{R^3} \right) + \mathcal{O}(R) \right) \quad (\text{A.5})$$

with the same Gaussian averaging to be performed for absorbing magnetic media. As shown in equation 1.136, the spontaneous emission rate is calculated from this Green's function as

$$\gamma = \frac{2\omega_A^2 d_i d_j}{\hbar} \text{Im} G_{ij}^{(A)}(\omega_A, \mathbf{r}, \mathbf{r}). \quad (\text{A.6})$$

Now, just like the Green's function for the electric field  $\mathbf{E}$  can be obtained from  $G_{ij}^{(A)}$  by multiplying  $-\omega^2$  as  $\mathbf{E} = i\omega\mathbf{A}$ , we can also obtain a Green's function for the magnetic field  $\mathbf{B}$  using  $\mathbf{B} = \nabla \times \mathbf{A}$ . From

$$\langle \hat{B}_i(\mathbf{r}) \hat{B}_j(\mathbf{r}') \rangle = \left\langle \left( \nabla \times \hat{A}(\mathbf{r}) \right)_i \left( \nabla' \times \hat{A}(\mathbf{r}') \right)_j \right\rangle \quad (\text{A.7})$$

we know that the Green's functions must fulfil

$$G_{ij}^{(B)}(\omega, \mathbf{r}, \mathbf{r}') = \varepsilon_{ikl} \partial_k \varepsilon_{jmn} \partial'_m G_{ln}^{(A)}(\omega, \mathbf{r}, \mathbf{r}') \quad (\text{A.8})$$

with  $\varepsilon_{ijk}$  being the Levi-Civita tensor and  $\partial'_m$  being the derivative with respect to  $\mathbf{r}'$ . As we already know  $G_{ln}(\omega, \mathbf{r}, \mathbf{r}') = G_{ln}(\omega, \mathbf{r} - \mathbf{r}')$ , we can replace the second differential operator  $\partial'_m$  by  $-\partial_m$  and rewrite equation A.8 in terms of the relative coordinate  $\mathbf{R} = \mathbf{r} - \mathbf{r}'$ ,

$$G_{ij}^{(B)}(\omega, \mathbf{R}) = -\varepsilon_{ikl} \partial_k \varepsilon_{jmn} \partial_m G_{ln}(\omega, \mathbf{R}). \quad (\text{A.9})$$

We start with the vector potential Green's function as expressed in equation A.4 and rearrange the derivatives according to

$$\varepsilon_{ikl} \partial_k \varepsilon_{jmn} \partial_m (\partial_l \partial_m - \delta_{lm} \nabla^2) = (\partial_i \partial_j - \delta_{ij} \nabla^2) \nabla^2 \quad (\text{A.10})$$

so that the magnetic Green's function takes the form

$$G_{ij}^{(B)}(\omega, \mathbf{R}) = -\frac{1}{4\pi\varepsilon} (\partial_i\partial_j - \delta_{ij}\nabla^2) \nabla^2 \frac{1}{R} (e^{i\sqrt{\varepsilon\mu}\omega R} - 1). \quad (\text{A.11})$$

These derivatives are not well defined in the limit  $R \rightarrow 0$  and lead to singularities in the form of Dirac delta-functions. However, for real values of  $\varepsilon$  and  $\mu$ , the imaginary part remains well defined,

$$\begin{aligned} \text{Im}G_{ij}^{(B)}(\omega, \mathbf{R}) &= \text{Im} \left( \frac{-\mu}{4\pi R^2} e^{iqR} [R_i R_j (q^2 R^2 + 3iqR - 3) - \delta_{ij} R^2 (q^2 R^2 - 1)] \right) \\ &= \delta_{ij} \frac{\mu q^3}{6\pi} + \mathcal{O}(R) \end{aligned}$$

with  $q = \sqrt{\varepsilon\mu}\omega$ .

If we want to consider absorbing media we can use a similar Gaussian averaging method as in section 3.3.3. For this we first have to take one step back and write equation A.11 as a Fourier decomposition again,

$$\begin{aligned} G_{ij}^{(B)}(\omega, \mathbf{R}) &= -\frac{1}{4\pi\varepsilon\omega^2} (\partial_i\partial_j - \delta_{ij}\nabla^2) \nabla^2 \frac{1}{R} (e^{i\sqrt{\varepsilon\mu}\omega R} - 1) \\ &= -\frac{\mu}{(2\pi)^3} (\partial_i\partial_j - \delta_{ij}\nabla^2) \nabla^2 \int d^3k \frac{e^{i\mathbf{k}\mathbf{R}}}{k^2(k^2 - \varepsilon\mu\omega^2)} \\ &= \frac{\mu}{(2\pi)^3} \int d^3k \frac{k^2 \left( \delta_{ij} - \frac{k_i k_j}{k^2} \right)}{k^2 - \varepsilon\mu\omega^2} e^{i\mathbf{k}\mathbf{R}}. \end{aligned}$$

We can now use this expression to calculate the smoothed version of the magnetic Green's function

$$\begin{aligned} \tilde{G}_{ij}^{(B)}(\omega, 0) &= \frac{\mu}{(2\pi)^3} \int dV \int dV' \left( \frac{2}{\rho} \right)^3 e^{-\frac{2\pi}{\rho^2}(r^2+r'^2)} \int d^3k \frac{k^2 \left( \delta_{ij} - \frac{k_i k_j}{k^2} \right)}{k^2 - \varepsilon\mu\omega^2} e^{i\mathbf{k}(\mathbf{r}-\mathbf{r}')} \\ &= \frac{\mu\delta_{ij}}{3\pi^2} \int dk e^{-\frac{k^2\rho^2}{4\pi}} \frac{k^4}{k^2 - \varepsilon\mu\omega^2} \\ &\stackrel{\varepsilon\mu\omega^2\rho^2 \ll 1}{\approx} \frac{\mu\delta_{ij}}{6\pi} \left( \frac{4\pi}{\rho^3} + \frac{2(\sqrt{\varepsilon\mu}\omega)^2}{\rho} + \frac{(\sqrt{\varepsilon\mu}\omega)^4}{\sqrt{-(\sqrt{\varepsilon\mu}\omega)^2}} \right). \end{aligned}$$

Let us see what happens if we wanted to use this Green's function to calculate the spontaneous emission rate of a magnetic dipole. We still assume a coupling of the form  $\mathbf{m} \cdot \mathbf{H} = \mathbf{m} \cdot \mu^{-1} \mathbf{B}$ , so from

$$\begin{aligned} \gamma &= \sum_{\mathbf{k}\lambda} \frac{2\pi}{\hbar} |\langle \mathbf{k}\lambda | \mu_0 \mathbf{m} \cdot \mu^{-1} \hat{\mathbf{B}} | 0 \rangle|^2 \delta(\omega_k - \omega_A) \\ &= \frac{2\pi \mu_0^2 m_i m_j}{\hbar |\mu|^2} \langle 0 | \hat{B}_i \hat{B}_j | 0 \rangle \delta(\omega - \omega_A) \end{aligned}$$

the emission rate follows as

$$\gamma^{(B)} = \frac{\omega^3 m^2 \mu_0}{3\pi \hbar c^3 |\mu_r|^2} \left( 2 \frac{c}{\rho \omega} \text{Im}(n^2 \mu_r) + \text{Re}(n^3 \mu_r) + 4\pi \left( \frac{c}{\rho \omega} \right)^3 \text{Im}(\mu_r) \right) \quad (\text{A.12})$$

where now indeed the full rate is included, not only the transverse part (the longitudinal part is the term proportional to  $1/\rho^3$ ). This is not the same rate as the one calculated in section 3.3.4 with the Green's function of the field  $\mathbf{H}$ , and only coincides in the case of  $\mu = |\mu|$ , i.e. a medium without magnetic losses. In fact, this result could be obtained from that in section 3.3.4 by multiplying the argument of the real and imaginary parts with  $\frac{\mu^2}{|\mu|^2}$ . The reason for the differences lies in the choice of the sources and corresponding fields: In this calculation, the final result has a pre-factor of  $\frac{1}{|\mu_r|^2}$  because the  $\mathbf{H}$  field is rewritten in terms of  $\mathbf{B}$  in the commutator and hence only the absolute value of the permittivity comes into play. In the other case one has a pre-factor of  $\frac{1}{\mu_r^2}$  inside the Green's function as the Green's function itself is that of the  $\mathbf{H}$  field. It is still not entirely clear how to fully justify a certain approach over another, which is the topic of ongoing research, however, the choice as described in the main body appears to be the more reasonable, especially due to its agreement with duality. We furthermore note that the general technique of retrieving the Greens function from the vector potential is still valid, we could for example obtain the Green's function of the  $\mathbf{H}$  field from

$$G_{ij}^{(H)}(\omega, \mathbf{R}) = \frac{1}{\mu^2} G_{ij}^{(B)}(\omega, \mathbf{R}) \quad (\text{A.13})$$

which gives the same Green's function as derived in section 4.2.

## Appendix B

# Approximation of success probabilities in the Jaynes-Cummings interaction

We evaluate the analytical expressions of the probability  $P(-)$  up to the order of  $\mathcal{O}(1/\bar{n}^2)$ , setting the optimal interaction time to satisfy  $gt_1\sqrt{\bar{n} + \mu} = \pi/4$ . We approximate the Poisson distribution of a coherent state with a Gaussian [4]

$$\exp[-\bar{n}] \frac{\bar{n}^n}{n!} \simeq \frac{1}{\sqrt{2\pi\bar{n}}} \exp\left[-\frac{(n - \bar{n})^2}{2\bar{n}}\right], \quad (\text{B.1})$$

and replace the summation in (7.2) by an integration  $\sum_{n=0}^{\infty} \rightarrow \int_0^{\infty} dn$ . As the centre of the Gaussian is far away from the origin, the integration limit can be extended from  $0 \rightarrow \infty$  to  $-\infty \rightarrow \infty$  without effecting the result. Following this, the probability

of obtaining the state  $|-\rangle$  in the first round is calculated as

$$\begin{aligned}
P(-) &\simeq \int_{-\infty}^{\infty} \frac{dn}{\sqrt{8\pi\bar{n}}} \left| e^{-(n-\bar{n})^2/4\bar{n}} \cos\left(\frac{\pi}{4} \sqrt{1 + \frac{(n-\bar{n}+1-\mu)}{\bar{n}+\mu}}\right) \right. \\
&\quad \left. - e^{-(n-\bar{n}-1)^2/4\bar{n}} \sin\left(\frac{\pi}{4} \sqrt{1 + \frac{(n-\bar{n}-\mu)}{\bar{n}+\mu}}\right) \right|^2 \\
&= \frac{1}{2} - \frac{e^{-1/8\bar{n}}}{\sqrt{2\pi\bar{n}}} \int_{-\infty}^{\infty} d\xi e^{-\xi^2/2\bar{n}} \cos\left(\frac{\pi}{4} \sqrt{1 + \frac{(\xi-\mu+3/2)}{\bar{n}+\mu}}\right) \\
&\quad \times \sin\left(\frac{\pi}{4} \sqrt{1 + \frac{(\xi-\mu+1/2)}{\bar{n}+\mu}}\right),
\end{aligned}$$

where  $\xi = n - \bar{n} - 1/2$ . The second term can be approximated by Taylor expansion of the trigonometric functions and

$$\int_{-\infty}^{\infty} x^n e^{-\alpha x^2} dx = \frac{(1 + (-1)^n)}{2} \frac{1 \cdot 3 \cdot 5 \dots (n-1) \sqrt{\pi}}{2^{n/2} \alpha^{(n+1)/2}}; \quad n > 0, \quad (\text{B.2})$$

leading to

$$P(-) \simeq \frac{(\pi+2)^2}{64\bar{n}} - \frac{\pi^4 - 4(5 - 40\mu + 16\mu^2)\pi^2 + 64(1+2\mu)\pi + 16}{4096\bar{n}^2} + \mathcal{O}\left(\frac{1}{\bar{n}^3}\right). \quad (\text{B.3})$$

# Bibliography

- [1] J. D. Jackson, *Classical Electrodynamics*. John Wiley & Sons, 1999.
- [2] C. Cohen-Tannoudji, J. Dupont-Roc, and G. Grynberg, *Photons and Atoms*. Wiley-VCH, 1989.
- [3] D. P. Craig and T. Thirunamachandran, *Molecular quantum electrodynamics: an introduction to radiation-molecule interactions*. Courier Corporation, 1998.
- [4] R. Loudon, *The quantum theory of light*. OUP Press, 2003.
- [5] L. D. Landau and E. M. Lifshitz, *Quantum Mechanics*, vol. 3 of *Course of Theoretical Physics*. Pergamon Press, 1958.
- [6] C. Cohen-Tannoudji, B. Diu, and F. Laloe, *Quantum Mechanics 2*, vol. II. Wiley-VCH, 2 ed., 2019.
- [7] E. Fermi, *Nuclear Physics*. University of Chicago Press, 1950.
- [8] E. M. Purcell, “Spontaneous emission probabilities at radio frequencies,” *Phys. Rev.*, vol. 69, no. 681, 1946.
- [9] R. Kubo, “The fluctuation-dissipation theorem,” *Reports on Progress in Physics*, vol. 29, no. 1, p. 255, 1966.
- [10] E. M. Lifshitz and L. P. Pitaevskii, *Statistical Physics Part 2*, vol. 9. Butterworth-Heinemann, 1996.
- [11] O. F. Mossotti, “Discussione analitica sull’influenza che l’azione di un mezzo dielettrico ha sulla distribuzione dell’elettricità alla superficie di più corpi elettrici disseminati in esso,” *Mem. Soc. Ital.*, vol. 24, p. 49, 1850.

- [12] R. Clausius, *Die Mechanische Behandlung der Electricität*. Wiesbaden: Vieweg+Teubner Verlag, 1879.
- [13] P. Debye, *Polar Molecules*. Dover Publications, New York, 1945.
- [14] D. E. Aspnes, "Local-field effects and effective-medium theory: A microscopic perspective," *American Journal of Physics*, vol. 50, no. 8, pp. 704–709, 1982.
- [15] A. R. von Hippel, *Dielectrics and Waves*. John Wiley and Sons, New York, 1954. chapter 3.
- [16] A. Aubret, M. Orrit, and F. Kulzer, "Understanding local-field correction factors in the framework of the onsager-böttcher model," *ChemPhysChem*, vol. 20, no. 3, pp. 345–355, 2019.
- [17] L. Onsager, "Electric moments of molecules in liquids," *Journal of the American Chemical Society*, vol. 58, pp. 1486–1493, Aug 1936.
- [18] P. de Vries and A. Legendijk, "Resonant scattering and spontaneous emission in dielectrics: microscopic derivation of local-field effects," *Physical review letters*, vol. 81, no. 7, p. 1381, 1998.
- [19] I. Rebane, "Spontaneous emission rates of a single impurity molecule in a uniaxial host crystal," *Optics Communications*, vol. 217, no. 1, pp. 265 – 268, 2003.
- [20] R. A. Vallée, M. Van Der Auweraer, F. C. De Schryver, D. Beljonne, and M. Orrit, "A microscopic model for the fluctuations of local field and spontaneous emission of single molecules in disordered media," *ChemPhysChem*, vol. 6, no. 1, pp. 81–91, 2005.
- [21] C. Lo, J. Wan, and K. W. Yu, "Geometric anisotropic effects on local field distribution: Generalized clausius-mossotti relation," *Computer Physics Communications*, vol. 142, pp. 453–456, 12 2001.
- [22] A. H. Sihvola, "On the dielectric problem of isotropic sphere in anisotropic medium," *Electromagnetics*, vol. 17, no. 1, pp. 69–74, 1997.

- [23] S. Scheel, L. Knöll, D.-G. Welsch, and S. M. Barnett, “Quantum local-field corrections and spontaneous decay,” *Physical Review A*, vol. 60, no. 2, p. 1590, 1999.
- [24] M. E. Crenshaw, “Comparison of quantum and classical local-field effects on two-level atoms in a dielectric,” *Physical Review A*, vol. 78, no. 5, p. 053827, 2008.
- [25] D. R. Smith, W. J. Padilla, D. C. Vier, S. C. Nemat-Nasser, and S. Schultz, “Composite medium with simultaneously negative permeability and permittivity,” *Phys. Rev. Lett.*, vol. 84, pp. 4184–4187, May 2000.
- [26] R. A. Shelby, D. R. Smith, and S. Schultz, “Experimental verification of a negative index of refraction,” *Science*, vol. 292, no. 5514, pp. 77–79, 2001.
- [27] A. Alù, M. G. Silveirinha, A. Salandrino, and N. Engheta, “Epsilon-near-zero metamaterials and electromagnetic sources: Tailoring the radiation phase pattern,” *Phys. Rev. B*, vol. 75, p. 155410, Apr 2007.
- [28] G. Dolling, C. Enkrich, M. Wegener, C. M. Soukoulis, and S. Linden, “Simultaneous negative phase and group velocity of light in a metamaterial,” *Science*, vol. 312, no. 5775, pp. 892–894, 2006.
- [29] M. C. K. Wiltshire, “Bending light the wrong way,” *Science*, vol. 292, no. 5514, pp. 60–61, 2001.
- [30] N. Litchinitser and V. Shalaev, “Photonic metamaterials,” *Laser Phys. Lett.*, vol. 5, pp. 411–420, 2008.
- [31] N. Engheta and R. W. Ziolkowski, *Metamaterials: physics and engineering explorations*. New York: John Wiley & Sons, 2006.
- [32] L. Solymar and E. Shamonia, *Waves in Metamaterials*. Oxford University Press, 2009.
- [33] G. Duan, X. Zhao, S. W. Anderson, and X. Zhang, “Boosting magnetic resonance imaging signal-to-noise ratio using magnetic metamaterials,” *Communications Physics*, vol. 2, Mar. 2019.

- [34] M. J. Freire, L. Jelinek, R. Marques, and M. Lapine, “On the applications of  $\mu r = -1$  metamaterial lenses for magnetic resonance imaging,” *Journal of Magnetic Resonance*, vol. 203, no. 1, pp. 81–90, 2010.
- [35] J. B. Pendry, A. J. Holden, D. J. Robbins, and W. J. Stewart, “Magnetism from conductors and enhanced nonlinear phenomena,” *IEEE Transactions on Microwave Theory and Techniques*, vol. 47, no. 11, pp. 2075–2084, 1999.
- [36] V. G. Veselago, “Properties of materials having simultaneously negative values of the dielectric ( $\epsilon$ ) and magnetic ( $\mu$ ) susceptibilities,” *Sov. Phys. Solid State*, vol. 8, p. 2854, 1967.
- [37] V. G. Veselago, “The electrodynamics of substances with simultaneously negative values of  $\epsilon$  and  $\mu$ ,” *Soviet Physics Uspekhi*, vol. 10, no. 4, p. 509, 1968.
- [38] J. B. Pendry, “Negative refraction makes a perfect lens,” *Phys. Rev. Lett.*, vol. 85, pp. 3966–3969, Oct 2000.
- [39] S. M. Barnett, B. Huttner, and R. Loudon, “Spontaneous emission in absorbing dielectric media,” *Phys. Rev. Lett.*, vol. 68, pp. 3698–3701, Jun 1992.
- [40] P. W. Milonni and G. Maclay, “Quantized-field description of light in negative-index media,” *Optics Communications*, vol. 228, no. 1, pp. 161 – 165, 2003.
- [41] P. W. Milonni, *Fast Light, Slow Light and Left-Handed Light*. Series in Optics and Optoelectronics, Taylor & Francis Group, LCC, 2005.
- [42] D. Wang, H. Kelkar, D. Martin-Cano, D. Rattenbacher, A. Shkarin, T. Utikal, S. Götzinger, and V. Sandoghdar, “Turning a molecule into a coherent two-level quantum system,” *Nature Physics*, vol. 15, pp. 483–489, Feb. 2019.
- [43] D. Wang, H. Kelkar, D. Martin-Cano, T. Utikal, S. Götzinger, and V. Sandoghdar, “Coherent coupling of a single molecule to a scanning fabry-perot microcavity,” *Phys. Rev. X*, vol. 7, p. 021014, Apr 2017.
- [44] R. Bartholin, “Experimenta crystalli islandici disdiaclastici quibus mira & in-folita refractio detegitur,” 1669.

- [45] G. H. C. New, “Biaxial media revisited,” *European Journal of Physics*, vol. 34, pp. 1263–1276, jul 2013.
- [46] M. V. Fedorov, M. A. Efremov, P. A. Volkov, E. V. Moreva, S. S. Straupe, and S. P. Kulik, “Anisotropically and high entanglement of biphoton states generated in spontaneous parametric down-conversion,” *Phys. Rev. Lett.*, vol. 99, p. 063901, Aug 2007.
- [47] A. Fiore, S. Janz, L. Delobel, P. van der Meer, P. Bravetti, V. Berger, E. Rosencher, and J. Nagle, “Second-harmonic generation at  $\hat{\Gamma}$ =1.6  $\hat{\Gamma}$ Em in algaas/al2o3 waveguides using birefringence phase matching,” *Applied Physics Letters*, vol. 72, no. 23, pp. 2942–2944, 1998.
- [48] D. J. Griffiths, *Introduction to electrodynamics*. Cambridge University Press, 4th edition ed., 2017.
- [49] K. K. Pukhov, “Radiative characteristics of the doped nanocrystals,” *Optical Materials*, vol. 35, no. 10, pp. 1762 – 1764, 2013. 3rd International Conference on the Physics of Optical Materials and Devices.
- [50] A. Rahmani, P. C. Chaumet, and G. W. Bryant, “Discrete dipole approximation for the study of radiation dynamics in a magnetodielectric environment,” *Optics express*, vol. 18, no. 8, pp. 8499–8504, 2010.
- [51] J. R. Ackerhalt and P. W. Milonni, “Interaction hamiltonian of quantum optics,” *JOSA B*, vol. 1, no. 1, pp. 116–120, 1984.
- [52] O. Heaviside, “Xi. on the forces, stresses, and fluxes of energy in the electromagnetic field,” *Philosophical Transactions of the Royal Society of London.(A.)*, no. 183, pp. 423–480, 1892.
- [53] J. Larmor, “Ix. a dynamical theory of the electric and luminiferous medium,” *Philosophical Transactions of the Royal Society of London. Series A, Containing Papers of a Mathematical or Physical Character*, no. 190, pp. 205–300, 1897.
- [54] J. A. Stratton, “Electromagnetic theory,” 1941.

- [55] A. Einstein and J. Laub, “über die im elektromagnetischen feld auf ruhende körper ausgeübten ponderomotorischen kräfte,” *Annalen der Physik*, vol. 26, p. 541, 1908.
- [56] S. M. Barnett and R. Loudon, “Theory of radiation pressure on mag-neto–dielectric materials,” *New Journal of Physics*, vol. 17, p. 063027, jun 2015.
- [57] S. Scheel and S. Y. Buhmann, “Macroscopic qed-concepts and applications,” *Acta Physica Slovaca*, vol. 58, pp. 675–809, 2008.
- [58] M. Born and E. Wolf, *Principles of optics: electromagnetic theory of propaga-tion, interference and diffraction of light*. Elsevier, 2013.
- [59] G. New, *Introduction to nonlinear optics*. Cambridge University Press, 2011.
- [60] J. Braat and P. Török, *Imaging Optics*. Cambridge University Press, 2019.
- [61] B. E. Saleh and M. C. Teich, *Fundamentals of photonics*. john Wiley & sons, 2019.
- [62] L. D. Landau, J. Bell, M. Kearsley, L. Pitaevskii, E. Lifshitz, and J. Sykes, *Electrodynamics of continuous media*, vol. 8. elsevier, 2013.
- [63] H. C. Chen, “Dyadic green’s function and radiation in a uniaxially anisotropic medium,” *International Journal of Electronics*, vol. 35, p. 633, 1973.
- [64] W. S. Weiglhofer, “Dyadic green’s functions for general uniaxial media,” *IEE Proceedings H - Microwaves, Antennas and Propagation*, vol. 137, pp. 5–10, Feb 1990.
- [65] W. S. Weiglhofer, “Analytic methods and free-space dyadic green’s functions,” *Radio Science*, vol. 28, no. 5, pp. 847–857, 1993.
- [66] A. Yariv and P. Yeh, *Optical Waves in Crystals*. New York: Wiley, 1983.
- [67] F. A. Jenkins and H. E. White, *Fundamentals of Optics*. New York: McGraw-Hill, 1965.
- [68] D. R. Lovett, *Tensor Properties of Crystals*. Philadelphia: Adam Hilger, 1989.

- [69] R. R. Chance, A. Prock, and R. Silbey, *Molecular Fluorescence and Energy Transfer Near Interfaces*, pp. 1–65. John Wiley & Sons, Ltd, 2007.
- [70] A. Messinger, N. Westerberg, and S. M. Barnett, “Spontaneous emission in anisotropic dielectrics,” *Phys. Rev. A*, vol. 102, p. 013721, Jul 2020.
- [71] A. Sihvola, *Homogenization of a dielectric mixture with anisotropic spheres in anisotropic background*, vol. TEAT-7050 of *Technical Report LUTEDX/(TEAT-7050)/1-15/(1996)*. [Publisher information missing], 1996. Published version: *Electromagnetics*, 17(3), 269–286, 1997.
- [72] B. Huttner and S. M. Barnett, “Quantization of the electromagnetic field in dielectrics,” *Phys. Rev. A*, vol. 46, pp. 4306–4322, Oct 1992.
- [73] S. M. Barnett, B. Huttner, R. Loudon, and R. Matloob, “Decay of excited atoms in absorbing dielectrics,” *Journal of Physics B: Atomic, Molecular and Optical Physics*, vol. 29, pp. 3763–3781, aug 1996.
- [74] S. M. Barnett and R. Loudon, “Sum rule for environmentally modified spontaneous emission rates,” *Quantum and Semiclassical Optics: Journal of the European Optical Society Part B*, vol. 10, no. 4, p. 591, 1998.
- [75] R. J. Glauber, “The quantum theory of optical coherence,” *Physical Review*, vol. 130, no. 6, p. 2529, 1963.
- [76] L. Mandel and E. Wolf, *Optical coherence and quantum optics*. Cambridge university press, 1995.
- [77] J. Gemmer, M. Michel, and G. Mahler, *Quantum thermodynamics: Emergence of thermodynamic behavior within composite quantum systems*, vol. 784. Springer, 2009.
- [78] J. Goold, M. Huber, A. Riera, L. Del Rio, and P. Skrzypczyk, “The role of quantum information in thermodynamics - a topical review,” *Journal of Physics A: Mathematical and Theoretical*, vol. 49, no. 14, p. 143001, 2016.
- [79] T. Baumgratz, M. Cramer, and M. B. Plenio, “Quantifying coherence,” *Phys. Rev. Lett.*, vol. 113, p. 140401, Sep 2014.

- [80] Y.-R. Zhang, L.-H. Shao, Y. Li, and H. Fan, “Quantifying coherence in infinite-dimensional systems,” *Phys. Rev. A*, vol. 93, p. 012334, Jan 2016.
- [81] J. A. Vaccaro, F. Anselmi, H. M. Wiseman, and K. Jacobs, “Tradeoff between extractable mechanical work, accessible entanglement, and ability to act as a reference system, under arbitrary superselection rules,” *Physical Review A*, vol. 77, no. 3, p. 032114, 2008.
- [82] G. Gour, M. P. Müller, V. Narasimhachar, R. W. Spekkens, and N. Y. Halpern, “The resource theory of informational nonequilibrium in thermodynamics,” *Physics Reports*, vol. 583, pp. 1–58, 2015.
- [83] K. Korzekwa, M. Lostaglio, J. Oppenheim, and D. Jennings, “The extraction of work from quantum coherence,” *New Journal of Physics*, vol. 18, p. 023045, feb 2016.
- [84] J. Åberg, “Catalytic coherence,” *Physical Review Letters*, vol. 113, no. 15, p. 150402, 2014.
- [85] J. A. Vaccaro, S. Croke, and S. M. Barnett, “Is coherence catalytic?,” *Journal of Physics A: Mathematical and Theoretical*, vol. 51, p. 414008, 2018.
- [86] A. Messinger, A. Ritboon, F. Crimin, S. Croke, and S. M. Barnett, “Coherence and catalysis in the jaynes–cummings model,” *New Journal of Physics*, vol. 22, no. 4, p. 043008, 2020.
- [87] B. W. Shore and P. L. Knight, “The jaynes-cummings model,” *Journal of Modern Optics*, vol. 40, no. 7, pp. 1195–1238, 1993.
- [88] E. T. Jaynes and F. W. Cummings, “Comparison of quantum and semiclassical radiation theories with application to the beam maser,” *Proceedings of the IEEE*, vol. 51, pp. 89–109, Jan 1963.
- [89] N. B. Narozhny, J. J. Sanchez-Mondragon, and J. H. Eberly, “Coherence versus incoherence: Collapse and revival in a simple quantum model,” *Phys. Rev. A*, vol. 23, pp. 236–247, Jan 1981.

- [90] J.-M. Raimond and S. Haroche, “Exploring the quantum,” *Oxford University Press*, vol. 82, p. 86, 2006.
- [91] A. Ashkin, *Optical trapping and manipulation of neutral particles using lasers: a reprint volume with commentaries*. World Scientific, 2006.
- [92] S. Vinjanampathy and J. Anders, “Quantum thermodynamics,” *Contemporary Physics*, vol. 57, no. 4, pp. 545–579, 2016.
- [93] P. Solinas, H. J. D. Miller, and J. Anders, “Measurement-dependent corrections to work distributions arising from quantum coherences,” *Phys. Rev. A*, vol. 96, p. 052115, 2017.
- [94] P. Kammerlander and J. Anders, “Coherence and measurement in quantum thermodynamics,” *Scientific Reports*, vol. 6, p. 22174, 2016.
- [95] D. F. Walls and G. J. Milburn, *Quantum Optics*. Springer, 1994.
- [96] M. Fox, *Quantum Optics*. Oxford Master Series in Physics, Oxford University Press, 2006.
- [97] S. M. Barnett and P. M. Radmore, *Methods in Theoretical Quantum Optics*. Oxford University Press, 1997.
- [98] S. Haroche and J.-M. Raimond, *Exploring the Quantum*. Oxford University Press, 2006.
- [99] S. M. Barnett and J. A. Vaccaro, *The Quantum Phase Operator: A Review*. CRC Press, 2007.